

News on Right Handed Neutrinos

TUM-HEP-881/13

Marco Drewes

Physik Department T70, Technische Universität München,
James Franck Straße 1, D-85748 Garching, Germany

Abstract

Neutrinos are the only particles in the Standard Model of particle physics that have only been observed with left handed chirality to date. If right handed neutrinos exist, they could be responsible for several phenomena that have no explanation within the Standard Model, including neutrino oscillations, the baryon asymmetry of the universe, dark matter and dark radiation. After a pedagogical introduction, we review recent progress in the phenomenology of right handed neutrinos. We in particular discuss the mass ranges suggested by hints for neutrino oscillation anomalies and dark radiation (eV), sterile neutrino dark matter scenarios (keV) and experimentally testable theories of baryogenesis (GeV to TeV). We summarize constraints from theoretical considerations, laboratory experiments, astrophysics and cosmology for each of these.

Contents

1	Introduction	2
1.1	The missing piece?	4
1.2	The range of RH neutrino masses	5
2	Neutrino oscillations	6
2.1	The standard scenario of massive neutrinos	7
2.2	Neutrino masses from RH neutrinos	8
2.3	The seesaw mechanism	9
3	Other laboratory experiments	11
3.1	Neutrino oscillation anomalies	12
3.2	Lepton flavour violation	13
3.3	Neutrinoless double β -decay	13
3.4	Collider searches	14
3.5	Direct DM searches	15
3.6	Other constraints	16
4	Thermal history of the universe	16
4.1	A brief history of the universe	17
4.2	Sterile neutrinos as dark radiation	24
4.3	Sterile neutrinos in astrophysics	25
5	Baryogenesis via leptogenesis	26
5.1	Leptogenesis from N_I freezeout and decay	27
5.2	Leptogenesis during N_I production	29
5.3	Towards a quantitative treatment	31
6	RH Neutrinos as dark matter	34
7	A theory of almost everything	39
8	Conclusions	41

1 Introduction

This review is intended to give a comprehensive overview of what we know (more precisely: what I know) about the phenomenology of right handed neutrinos. Faced with the difficulty to write a text that is readable within reasonable time, and at the same time is as precise as possible, I provide extra details, explanations and comments for the interested reader in extensive footnotes. For a quick read, you may essentially ignore all of them. A very quick summary is given in appendix A.

The Standard Model of particle physics (SM) and theory of General Relativity (GR) form the basic pillars of modern physics. Together they can describe almost all phenomena observed in nature¹ in terms of a small number of underlying principles - general covariance, gauge invariance and quantum mechanics - and a handful of numbers² [1]. All elementary particles we have observed to date can be understood as fundamental excitations of a few quantum fields, the properties of which are constrained by the local structure of space and time³. Interactions between them are the result of (gauge) symmetries of the Lagrangian.

In spite of its enormous success, this cannot be a complete theory of nature for two reasons. On one hand, it treats gravitational fields as a classical background, while matter and other interactions are described by quantum field theory in the SM. This approximation certainly becomes invalid and has to be extended to a theory of quantum gravity at energies near the Planck scale⁴ $M_P = 1.22 \times 10^{19}$ GeV. We do not address this problem in the following because it is of little relevance for experiments in foreseeable time. On the other hand, there are four experimental and observational facts which cannot be understood in the framework SM+GR. Three of them are widely believed to be related to particle physics,

- (I) flavour violation in neutrino experiments, section 2,
- (II) the cosmological origin of the baryonic matter in the universe, section 5,
- (III) the composition and origin of the observed dark matter (DM), section 6.

In addition to the above *evidence* for the existence of “new physics”, there are a number of *hints* in experimental data that may point towards the existence of physics beyond the SM; these have not (yet?) led to a claim of discovery and may also be explained by systematics. Of these, we will only discuss two in this article,

¹The basic laws of other areas of natural science and technology can be understood as effective theories, which in principle can be derived from the SM and GR. Though there exist many complex phenomena that we do not understand or cannot predict in detail, this lack of predictivity is almost certainly related to the complexity of the system rather than a lack of understanding of its basic components, the elementary quantum fields.

²There are 19 free parameters in the SM; these are usually chosen as six quark masses, three mixing angles and one CP violating phase for the quarks, three charged lepton masses, three gauge couplings, two parameters in the Higgs potential and a QCD vacuum angle. The neutrinos are massless in the SM. GR adds two additional parameters to this barcode of nature, the Planck mass and the cosmological constant.

³All known elementary particles transform under irreducible representations of the Poincaré group.

⁴We use natural units $c = \hbar = 1$.

- (i) the statistical preference for additional relativistic particles dubbed “dark radiation” (DR)⁵ in fits to cosmological data, section 4,
- (ii) the anomalies seen in some short baseline and reactor neutrino experiments, section 3.

All of the above phenomena may be related to *right handed (RH) neutrinos* with different masses. It is the purpose of this article to summarize how they can be connected to these hypothetical particles and review bounds from theoretical considerations, laboratory experiments and cosmology on RH neutrino properties.

To complete the list, we briefly list the fourth piece of evidence for physics beyond SM+GR, which is related to gravitation of cosmology,

- (IV) the overall geometry of the universe (isotropy, homogeneity and spatial flatness), as e.g. seen in the cosmic microwave background (CMB).

We do not address (IV) here, as it is not related to RH neutrinos (or particle physics in general) in an obvious way⁶. An intuitive explanation is given by cosmic inflation, see section 4.1. Finally, the observed acceleration of the universe’s expansion is often included in this list. However, all current data can currently be explained in terms of a cosmological constant Λ , which is simply a free parameter in GR. Hence, it can formally be explained within the framework of SM+GR. The question of the microphysical “origin” of Λ (and its smallness) only arises when the SM and GR are interpreted as low energy limits of a more general theory, including a complete description of quantum gravity. To date, (I)-(III) and (IV) are the only confirmed empirical proofs of physics beyond the SM⁷.

In the remainder of this section we introduce the concept of RH neutrinos and define our notation. In section 2 we review how they can generate masses for the known neutrinos. In section 3 we summarize bounds from past laboratory experiments on RH neutrino properties, discuss the interpretation of the observed neutrino oscillation anomalies (ii) in terms of RH neutrinos and comment on possible future searches. In sections 4-6 we discuss various cosmological constraints; after a general summary in section 4.1, the perspectives to interpret the hints for “dark radiation” (i) in terms of RH neutrinos and reconcile them with the oscillation anomalies (ii) are addressed in section 4.2. Section 5 is devoted to the idea that RH neutrinos are the origin of the baryonic matter in the universe (leptogenesis) and possible implications for their properties. Section 6 discusses RH neutrinos as DM candidates. In section 7 we address the question how many of these phenomena can be explained *simultaneously* by RH neutrinos *alone*. We conclude in section 8 and give a tabular summary of possible RH neutrino mass scales and their implications for known and future observations in appendix A.

⁵The term “dark radiation” refers to relativistic particles in the early universe whose interactions with SM particles except gravity are negligible at temperatures $T \lesssim 2$ MeV. It is in contrast to the nonrelativistic dark matter.

⁶It has been speculated that this point may be related to the RH neutrinos’ superpartners [2].

⁷There are various aspects of the SM that may be considered “problems” from an aesthetic viewpoint or physical intuition, such as the hierarchy between the electroweak and Planck scale, the strong CP problem, the factorization of the gauge group and the flavour structure. We do not discuss these here. We also do not discuss the issue of vacuum stability, which seems inconclusive at this stage due to uncertainties in the top mass [3–7].

1.1 The missing piece?

All matter we know is composed of elementary fermions with spin $\frac{1}{2}$. These can be described by Weyl spinors, which transform under irreducible representations of the Poncaré group, and combinations thereof. There are two such representations, known as “left chiral” and “right chiral” spinors. Remarkably, all known elementary fermions except neutrinos come in pairs of opposite chirality, i.e. have been observed as “left handed” (LH) and “right handed” (RH) particles⁸, see figure 1. For unknown reasons the interactions of the SM are such that both can be combined into a Dirac spinor, see appendix B. Neutrinos, however, so far have only been observed as LH particles. One conclusion that could be derived from this is that no right chiral “partner” for the observed LH neutrinos exists in nature. Another possible conclusion is that we have not seen RH neutrinos just because their interaction with other matter is too weak. Indeed LH neutrinos are electrically and colour neutral; in the SM they only participate in the weak interaction, which does not couple to RH fields. This suggests that their RH partners are singlet under all gauge interactions⁹. Such particles are referred to as “sterile neutrinos”.

Let us add n RH fermions $\nu_{R,i}$ to the SM that are singlet under all gauge interactions and couple to LH neutrinos in same way as RH charged leptons couple to LH charged leptons, i.e. via Yukawa interactions. We will refer to these fields as *RH neutrinos* and to the index i that labels them as *flavour index*. Then the most general renormalizable Lagrangian in Minkowski space that only contains SM fields and ν_R reads

$$\mathcal{L} = \mathcal{L}_{SM} + i\overline{\nu_R}\not{\partial}\nu_R - \overline{l_L}F\nu_R\tilde{\Phi} - \overline{\nu_R}F^\dagger l_L\tilde{\Phi}^\dagger - \frac{1}{2}(\overline{\nu_R^c}M_M\nu_R + \overline{\nu_R}M_M^\dagger\nu_R^c). \quad (1)$$

Here we have suppressed flavour and isospin indices. \mathcal{L}_{SM} is the Lagrangian of the SM. F is a matrix of Yukawa couplings and M_M a Majorana mass term for the right handed neutrinos ν_R . $l_L = (\nu_L, e_L)^T$ are the left handed lepton doublets in the SM and Φ is the Higgs doublet. $\tilde{\Phi} = (\epsilon\Phi)^\dagger$, where ϵ is the $SU(2)$ antisymmetric tensor, and $\nu_R^c = C\overline{\nu_R}^T$, where the charge conjugation matrix is $C = i\gamma_2\gamma_0$ in the Weyl representation. We chose a basis where the charged lepton Yukawa couplings and M_M are diagonal. Throughout this article we assume that there are only three “active” neutrinos ν_L that are charged under the weak interaction. If there are more families, then these must be heavier than $m_Z/2$, otherwise they would give visible contributions to the width of the Z-boson [8], see [9] for some recent discussion and references.

In the Lagrangian (1) the fields ν_R only interact via the Yukawa couplings F . In the early universe, when the temperature was high enough that Higgs particles were present in the primordial plasma ($T > T_{EW} \sim 140$ GeV for a Higgs mass $m_H \sim 125$ GeV [11, 12]), this interaction allowed ν_R -particles to participate in various different scattering processes. At energies much below the mass of the W-boson one can in good approximation replace the Higgs field Φ by its vacuum expectation value $v = 174$ GeV. Then (1) can be written as

$$\mathcal{L} = \mathcal{L}_{SM} + i\overline{\nu_{R,I}}\not{\partial}\nu_{R,I} - (m_D)_{\alpha I}\overline{\nu_{L,\alpha}}\nu_{R,I} - (m_D^*)_{\alpha I}\overline{\nu_{R,I}}\nu_{L,\alpha} - \frac{1}{2}[(M_M)_{IJ}\overline{\nu_{R,I}^c}\nu_{R,J} + (M_M)^*_{IJ}\overline{\nu_{R,I}}\nu_{R,J}^c] \quad (2)$$

⁸In this article “RH” and “LH” always refer to the chirality of the fields and *not* to helicity eigenstates.

⁹Here we refer to the $SU(3) \otimes SU(2) \otimes U(1)$ gauge group of the SM. They can of course be charged under some extended gauge group, which either acts only in a “hidden sector” or is broken at energies above the electroweak scale.

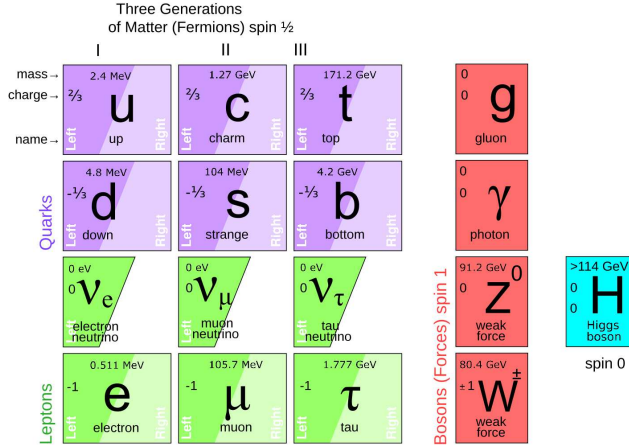


Figure 1: The particle content of the SM. Are we missing the right handed partner of the neutrinos? Picture taken from [10].

where we defined the *Dirac mass matrix* $m_D = Fv$. Thus, at $T \ll T_{EW}$ the only effect of the Yukawa interaction is the generation of the Dirac mass term m_D , and the only way how the fields ν_R interact with the SM is via their mixing with ν_L due to m_D .

1.2 The range of RH neutrino masses

While in the SM the Higgs mass m_H is the only dimensionful parameter (apart from the Planck mass), the Lagrangian (1) introduces n new dimensional parameters in M_M . The scale(s) associated with these provide a convenient way to classify different RH neutrino scenarios. Various embeddings of (1) into a bigger framework make different predictions for M_M (see e.g. [13–15] for a general overview and [16–18] for recent developments in model building), but empirically there are only few constraints. The following scenarios are particularly motivated, a summary in table form is given in appendix A. Of course, M_M can have eigenvalues in several different mass ranges, so that several of these scenarios may be combined in nature.

$M_M \gtrsim 10^9$ GeV - This range is motivated by embeddings of (1) into GUT scenarios [19], such as $SO(10)$ unification [20, 21]. $SO(10)$ models necessarily require the existence of ν_R .¹⁰ For Yukawa couplings F of order one, RH neutrinos with masses near the GUT scale reproduce the scale of observed neutrino oscillations (I) via (9). In addition, typical parameter values allow to generate the observed baryon density in the universe (II) in CP-violating decays of RH neutrinos, see section 5.1. The regime $M_M < 10^{15}$ GeV is favoured [22].

$M_M \sim \text{TeV}$ - Theoretically this mass range is interesting because it follows from a *no new scale* principle of minimality: If M_M is near the electroweak scale, the origin of both scales may be related. The origin of matter (II) may be explained by CP-violating ν_R -oscillations (see section 5.2) or, if two ν_R masses are degenerate, decays (see section 5.1). Neutrino masses (I) are explained by the seesaw mechanism. From an experimental viewpoint this mass range is favourable because it is accessible by high energy experiments, such as LHC.

¹⁰Any model that contains a $U(1)_{B-L}$ gauge symmetry requires this for anomaly freedom. This can be used as an argument for the existence of ν_R : The conservation of $B - L$ in the SM is not related to a gauge symmetry. If there is such symmetry, then ν_R must exist.

$M_M \sim \text{GeV}$ - If M_M has at least two eigenvalues $\gtrsim 2 \text{ GeV}$ and another eigenvalue in the keV range, then the observations (I)-(III) can be described by (1) alone, and no other physics between the electroweak and Planck scales is required, see section 7. Experimentally ν_R with GeV masses may be found using high intensity experiments, see section 3.4.

$M_M \sim \text{keV}$ - RH neutrinos with keV masses are promising DM candidates (III), see section 6.

$M_M \sim \text{eV}$ - RH neutrinos with eV masses can provide an explanation for the anomalies (i) and/or (ii), which are observed in some neutrino experiments (see section 4.2) and cosmological data (see section 4).

$M_M = 0$ - For $n = 3$ the leptonic sector exactly resembles the quark sector without strong interactions. In this case neutrinos are Dirac particles.¹¹ Then neutrino masses are generated by the Higgs mechanism in precisely the same way as other fermion masses, and their smallness can only be assigned to very tiny Yukawa couplings. Though in principle possible, this may appear “unnatural” unless there is a deeper reason for it¹². Furthermore, there is no known principle that forbids M_M for the gauge singlet fields ν_R ¹³. This is in contrast to quarks and charged leptons, for which an explicit mass term is forbidden by gauge symmetry.

2 Neutrino oscillations

The probably strongest motivation for the existence of ν_R are neutrino oscillations, the only processes amongst (I)-(IV) that have been observed in the laboratory. The neutrinos ν_L are massless in the SM¹⁴. In the past two decades an increasing number of neutrino experiments has observed neutrino flavour changes, which indicate that neutrinos are massive and oscillate, see e.g. [16, 26] for reviews with many references. The experimental results can be divided into two categories: the *standard 3-scenario* (SS) of three massive neutrinos, which we discuss here, and deviations from it, which we discuss in section 3.

The interactions of neutrinos in the SM are described by the Lagrangian term

$$- \frac{G_F}{2\sqrt{2}} \bar{\nu}_L \gamma^\mu e_L W_\mu - \frac{G_F}{4 \cos \theta_W} \bar{\nu}_L \gamma^\mu \nu_L Z_\mu + h.c., \quad (3)$$

where G_F is the Fermi constant. This defines the basis of weak interaction eigenstates (electron, muon and tau neutrino).¹⁵ If neutrinos have a mass, then the mass term need not be diagonal in this basis in flavour space. In the SS, the weak interaction eigenstates $\nu_{L,e}$, $\nu_{L,\mu}$ and $\nu_{L,\tau}$ are superpositions of three mass eigenstates $\nu_{L,i}$ with masses m_i . For a given momentum, these have different energies if their masses are different, and their wave functions oscillate with different frequencies. Thus, the flavour decomposition of a neutrino state changes in time. This can explain the observed neutrino oscillations.

¹¹For $n \neq 3$ it is in general not possible to combine all ν_L and ν_R into Dirac spinors, see appendix B.

¹²Some speculations on such reasons can e.g. be found in [23–25].

¹³A small value of M_M is, however, “natural” in the technical sense because the symmetry of \mathcal{L} increases in the limit $M_M \rightarrow 0$ (there is a global $U(1)_{B-L}$).

¹⁴We do not consider neutrino masses as a part of the SM because we do not know what the nature (Dirac or Majorana) or absolute scale of the mass term is.

¹⁵More precisely, if one considers the general form of the interaction $\frac{G_F}{2\sqrt{2}} \bar{\nu}_{L,\alpha} \gamma^\mu U_{\alpha\beta} e_{L,\beta} W_\mu$ in the basis where charged Yukawa couplings are diagonal, then the basis of weak interaction eigenstates for ν_L is the one where $U_{\alpha\beta} = \delta_{\alpha\beta}$.

2.1 The standard scenario of massive neutrinos

There are two different ways to effectively realize the SS of three massive neutrinos with no extra particles.

Majorana neutrinos - A Majorana mass term of the form

$$\frac{1}{2}\overline{\nu_L}m_\nu\nu_L^c + h.c. \quad (4)$$

can be constructed without adding any new degrees of freedom to the SM. This term, however, breaks gauge invariance unless it is generated by spontaneous symmetry breaking from a gauge invariant term like [27]

$$\frac{1}{2}\overline{l_L}\tilde{\Phi}f\tilde{\Phi}^Tl_L^c + h.c., \quad (5)$$

where f is some flavour matrix of dimension 1/mass. The dimension-5 operator (5) is not renormalizable; in an effective field theory approach it can be understood as the low energy limit of renormalizable operators that is obtained after "integrating out" heavier degrees of freedom. These can, for example (but not necessarily!), be right handed neutrinos, cf. (10). Therefore a Majorana mass term (4) clearly hints towards the existence of new physics although it can be constructed from SM fields only. At low energies one effectively observes the SS with only three massive neutrinos if the energy scale related to the new physics (in case of RH neutrinos the mass M_M) is sufficiently high that all new particles are too heavy to be seen in neutrino experiments. The Majorana mass term (4) can be diagonalized by a transformation $m_\nu = U_\nu \text{diag}(m_1, m_2, m_3) U_\nu^T$. In the mass base, the neutrino mixing matrix U_ν appears in the coupling to W_μ in (3).

Dirac neutrinos - If neutrinos are Dirac particles, the existence of ν_R is directly required to construct the mass term

$$\overline{\nu_L}m_D\nu_R + h.c.. \quad (6)$$

Though this means adding new degrees of freedom to the SM at low energies, it is still a realization of the SS, i.e. only three massive neutrinos are observed. The ν_R can be combined with the ν_L into Dirac spinors and there are only three different masses. One could say that there are no new particles in the strict sense, but just additional spin states for neutrinos. We refer to both of these scenarios as the SS.

A bi-unitary transformation $m_D = U_\nu \text{diag}(m_1, m_2, m_3) V_\nu^\dagger$ can diagonalize the mass term (6), with real and positive m_i . The matrix V_ν is not physical and can be absorbed into a redefinition of the flavour vector ν_R . One can define a Dirac spinor $\nu_R + U_\nu \nu_L$ with a diagonal mass term $\text{diag}(m_1, m_2, m_3)$. The neutrino mixing matrix U_ν then appears in the coupling of that Dirac spinor to W_μ in (3). A phenomenological prediction of Dirac neutrinos is that there is no neutrinoless double β -decay. In order to be consistent with observations, the Yukawa couplings F have to be very small ($F \sim 10^{-12}$) compared to those of the charged leptons and quarks.

The neutrino mixing matrix - In the basis where charged Yukawa couplings are diagonal, the mixing matrix U_ν is identical to the Pontecorvo-Maki-Nakagawa-Sakata matrix [28, 29] and can be parametrized as

$$U_\nu = V^{(23)}U_\delta V^{(13)}U_{-\delta}V^{(12)}\text{diag}(e^{i\alpha_1/2}, e^{i\alpha_2/2}, 1) \quad (7)$$

with $U_{\pm\delta} = \text{diag}(e^{\mp i\delta/2}, 1, e^{\pm i\delta/2})$. The non-zero entries of the matrices V are given by

$$V_{ii}^{(ij)} = V_{jj}^{(ij)} = c_{ij}, \quad V_{ij}^{(ij)} = s_{ij}, \quad V_{ji}^{(ij)} = -s_{ij}, \quad V_{kk}^{(ij)} = 1, \quad k \neq i, j, \quad (8)$$

where c_{ij} and s_{ij} denote $\cos(\theta_{ij})$ and $\sin(\theta_{ij})$, respectively. θ_{ij} are the neutrino mixing angles, α_1 , α_2 and δ are CP -violating phases. Many parameters of the mixing matrix U_ν have been measured in recent years. In particular, two mass square differences have been determined as $\Delta m_{\text{sol}}^2 \equiv m_2^2 - m_1^2 \simeq 7.5 \times 10^{-5} \text{eV}^2$ and $\Delta m_{\text{atm}}^2 \equiv |m_3^2 - m_1^2| \simeq 2.4 \times 10^{-3} \text{eV}^2$, the mixing angles are $\theta_{12} \simeq 34^\circ$, $\theta_{23} \simeq 39^\circ$ and $\theta_{13} \simeq 9^\circ$; the precise best fit values differ for normal and inverted hierarchy (but the difference is smaller than the within the 1σ ranges) and are given in [1, 30–32], see also [33] for a recent summary. What remains unknown are

- *the hierarchy of neutrino masses* - One can distinguish between two non-equivalent setups. The *normal hierarchy* corresponds to $m_1 < m_2 < m_3$, with $\Delta m_{\text{sol}}^2 = m_2^2 - m_1^2$ and $\Delta m_{\text{atm}}^2 = m_3^2 - m_1^2 \simeq m_3^2 - m_2^2 \gg \Delta m_{\text{sol}}^2$. The *inverted hierarchy* corresponds to $m_2 > m_1 > m_3$, with $\Delta m_{\text{sol}}^2 = m_2^2 - m_1^2$ and $\Delta m_{\text{atm}}^2 = m_1^2 - m_3^2 \simeq m_2^2 - m_3^2 \gg \Delta m_{\text{sol}}^2$.
- *the CP -violating phases* - The Dirac phase δ is the analogue to the CKM phase and remains present even for $M_M = 0$. Global fits to neutrino data tend to prefer $\delta \sim \pi$ [30], but are not conclusive. The Majorana phases α_1 and α_2 become unphysical in the limit $M_M \rightarrow 0$ because they can be absorbed into redefinitions of the fields.
- *the absolute mass scale* - The mass of the lightest neutrino is unknown, but the sum of masses is bound from above as $\sum_i m_i < 0.23 \text{ eV}$ [34] by cosmology¹⁶. It is also bound from below by the measured mass squares, $\sum_i m_i > 0.06 \text{ eV}$ for normal and $\sum_i m_i > 0.1 \text{ eV}$ for inverted hierarchy.

2.2 Neutrino masses from RH neutrinos

In this section we discuss how sterile neutrinos described by the Lagrangian (1) can give Dirac or Majorana mass terms to the active neutrinos. It is obvious that the Lagrangian (2) with $M_M = 0$ represents Dirac neutrinos with a mass term (6). For $M_M \neq 0$ they generate a Majorana mass term (4). If the mass M_M is sufficiently large, RH neutrinos are heavy and neutrino oscillation experiments can be described by an effective Lagrangian that is obtained by integrating them out of (2),

$$\mathcal{L} = \mathcal{L}_{SM} - \frac{1}{2} \overline{\nu_L} m_\nu \nu_L^c \text{ with } m_\nu = -m_D M_M^{-1} m_D^T. \quad (9)$$

If the Majorana mass is above the electroweak scale ($M_M \gg v$) one can already integrate out the ν_R in (1) to obtain (5) with $f = F M_M^{-1} F^T$,

$$\mathcal{L} = \mathcal{L}_{SM} + \frac{1}{2} \overline{l_L} \tilde{\Phi} F M_M^{-1} F^T \tilde{\Phi}^T l_L^c. \quad (10)$$

Hence, the SS with three massive neutrinos is effectively realized if M_M is either zero or so much bigger than the observed neutrino masses that (9) can be used to describe neutrino oscillations. If one or more eigenvalues of M_M are not that large, then the light sterile neutrinos

¹⁶The bound and preferred value for $\sum_i m_i$ slightly change, depending on the dataset and analysis.

appear as new particles in neutrino experiments. To explore the full range of masses, we write the mass term as

$$\frac{1}{2}(\overline{\nu_L} \ \overline{\nu_R^c})\mathfrak{M} \begin{pmatrix} \nu_L^c \\ \nu_R \end{pmatrix} + h.c. \equiv \frac{1}{2}(\overline{\nu_L} \ \overline{\nu_R^c}) \begin{pmatrix} 0 & m_D \\ m_D^T & M_M \end{pmatrix} \begin{pmatrix} \nu_L^c \\ \nu_R \end{pmatrix} + h.c. \quad (11)$$

If ν_R exist, they always generate a mass term for ν_L (except for $F = 0$ ¹⁷); this is seen as a strong motivation to postulate their existence¹⁸. The relative size of M_M and m_D (i.e. their eigenvalues) allows to distinguish different scenarios. Note that this does not say anything about the absolute scale of m_D , which may lie anywhere between 0 and the electroweak scale (assuming perturbative couplings F).

$M_M \ll m_D$ - This is a pseudo-Dirac scenario; for $n = 3$ the neutrinos in this case effectively behave like Dirac particles¹⁹. This case is excluded unless $M_M \lesssim 10^{-9}$ eV, as otherwise solar neutrino oscillations into ν_R should have been observed [49].

$M_M \sim m_D$ - In this case M_M and m_D should both be of the order of the observed neutrino mass differences. The full mass term can be diagonalized by a $(3 + n) \times (3 + n)$ matrix \mathcal{U} as $\mathfrak{M} = \mathcal{U} \text{diag}(m_1, m_2, m_3, M_1, \dots, M_n) \mathcal{U}^T$. This can lead to rather large mixing between ν_L and ν_R .

$M_M \gg m_D$ - This is the seesaw limit, in which the neutrino mass term is described by (9). This scenario is discussed in detail in the following section 2.3. The seesaw limit roughly applies if $M_M > 1$ eV.

2.3 The seesaw mechanism

In the limit $m_D \ll M_M$ (in terms of eigenvalues), the full $(3 + n) \times (3 + n)$ mass matrix \mathfrak{M} for ν_L and ν_R has two distinct sets of eigenvalues. n of them (M_I) are of the order of the eigenvalues of M_M , the remaining three (m_i) are suppressed by two powers of the *active - sterile mixing matrix*

$$\theta = m_D M_M^{-1}. \quad (12)$$

The seesaw hierarchy $\theta \ll 1$ separates two distinct sets of mass eigenstates. One can block-diagonalize (11) by expanding in $\theta \ll 1$; on one hand one obtains the 3×3 mass matrix

$$m_\nu = -\theta M_M \theta^T, \quad (13)$$

with eigenvalues m_i ; it corresponds to the operator (9). The known bounds on neutrino masses impose constraints between the values of F and M_M , see figure 2. On the other hand there is the $n \times n$ matrix

$$M_N = M_M + \frac{1}{2}(\theta^\dagger \theta M_M + M_M^T \theta^T \theta^*) \quad (14)$$

¹⁷In this case it is not clear from the viewpoint of (1) why the fields ν_R should be called “neutrinos”, as they have nothing in common with the known neutrinos except being neutral. Of course, such *pariah neutrinos* [which only interact gravitationally in (1)] can be charged in a way that justifies this classification under a gauge group that it broken at high energies.

¹⁸Of course there are alternative ways to generate a neutrino mass term, see e.g. [35–48] or [13–15] for a general overview with many references.

¹⁹This is not only way how Dirac fermions can arise. For instance, if the splitting between two eigenvalues of M_M is sufficiently small, then one can form Dirac spinor by combining different flavours, see appendix B.

with eigenvalues M_I . These matrices m_ν and M_N are not diagonal and lead to flavour oscillations. Diagonalizing them yields the mass term

$$\frac{1}{2} \left(\overline{\nu_L} m_\nu^{\text{diag}} \nu_L^c + \overline{\nu_R} M_N^{\text{diag}} \nu_R^c \right) + h.c. \quad (15)$$

with

$$m_\nu^{\text{diag}} = \text{diag}(m_1, m_2, m_3), \quad M_N^{\text{diag}} = (M_1, \dots, M_n) \quad (16)$$

In summary, the full matrix \mathcal{U} that diagonalizes \mathfrak{M} reads

$$\mathcal{U} = \left[\begin{pmatrix} \mathbb{1} - \frac{1}{2} \theta \theta^\dagger & \theta \\ -\theta^\dagger & \mathbb{1} - \frac{1}{2} \theta^\dagger \theta \end{pmatrix} + \mathcal{O}[\theta^3] \right] \begin{pmatrix} U_\nu & \\ & U_N \end{pmatrix}. \quad (17)$$

Three mass states have light masses $m_i \sim \mathcal{O}[\theta^2 M_M]$ and are mainly mixings of the SU(2) charged fields ν_L ,

$$\nu_L = U_\nu^\dagger \left(\left(\mathbb{1} - \frac{1}{2} \theta \theta^\dagger \right) \nu_L - \theta \nu_R^c \right) \quad (18)$$

The remaining n mass states have masses $M_I \sim \mathcal{O}[M_M]$ and are mainly mixings of the singlet fields ν_R ,

$$\nu_R = U_N^\dagger \left(\left(\mathbb{1} - \frac{1}{2} \theta^T \theta^* \right) \nu_R + \theta^T \nu_L^c \right). \quad (19)$$

We refer to ν_L as *active neutrinos* because they take part in the weak interactions (3). The ν_R participate in the weak interaction (3), but only with an amplitude suppressed by θ ; hence they are *sterile neutrinos*. The matrix U_N diagonalises the sterile neutrino mass matrix M_N ,²⁰ it can be seen as analogue to U_ν . The diagonal elements of M_N are much bigger than the off-diagonals and very close to the entries of M_M . Therefore one can in most cases neglect all terms of second order in θ and approximate $M_N = M_M$, $U_N = \mathbb{1}$. However, if two eigenvalues of M_M are degenerate, then the U_N can contain large sterile-sterile mixing angles. The active-sterile mixing angles are determined by the entries of the matrix θ and always small. More precisely, the experimentally relevant coupling between active and sterile species is given by the matrix Θ with²¹

$$\Theta_{\alpha I} \equiv (\theta U_N^*)_{\alpha I} \quad (20)$$

Practically, experiments to date constrain the quantities

$$U_\alpha^2 \equiv \sum_I \Theta_{\alpha I} \Theta_{\alpha I}^* = \sum_I \theta_{\alpha I} \theta_{\alpha I}^* \quad (21)$$

and combinations thereof.

This is known as the seesaw mechanism [50–53] because increasing the eigenvalues of M_M pushes the masses of the sterile neutrinos up and those of active neutrinos down, just as if they sat on a seesaw²². If the couplings F are of order one and M_M in the range suggested by GUT models, then m_ν roughly reproduces the observed neutrino mass splittings. Hence, the mechanism provides a natural explanation for the smallness of neutrino masses. However, the scale M_M of the seesaw is phenomenologically almost unconstrained and may be as low as 1 eV [55].

²⁰We choose the phase convention in U_N such that $M_N = U_N \text{diag}(M_1, \dots, M_n) U_N^T$ with M_I real and positive.

²¹In (19) the matrix $U_N^\dagger \theta^T = \Theta^T$ appears (rather than Θ) because the N_I couple to $\nu_{L,\alpha}$, but overlap with $\nu_{L,\alpha}^c$.

²²The term “seesaw” is also used for several modifications of this idea, such as the “type-II seesaw” [36, 38–41], “type-III” seesaw [44], “split seesaw” [54] or “inverse seesaw” [42, 43].

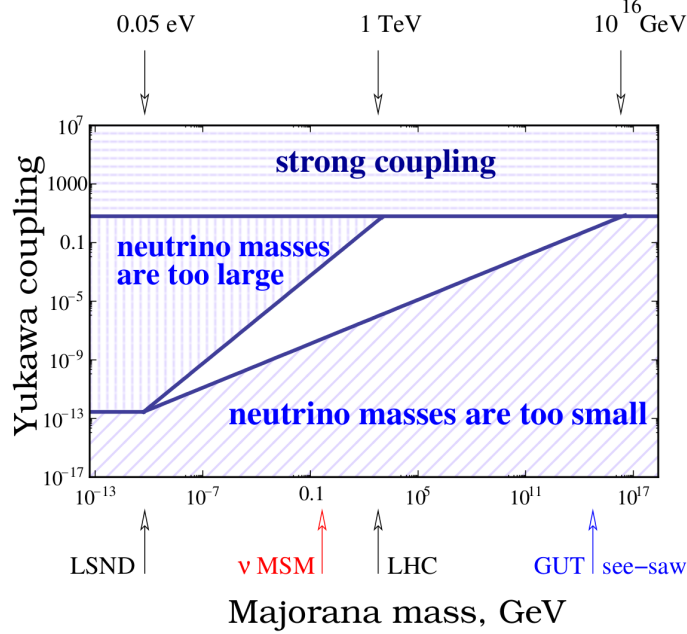


Figure 2: A schematic illustration of the relation between F and M_M in the seesaw limit $m_D \ll M_M$. Individual elements of the matrices F and M_M can deviate considerably from this if there are cancellations in (13). Plot taken from [16].

To make the Majorana nature of the fields explicit (and get rid of the charge conjugation matrix in the mass term) one can describe them in terms of Majorana spinors; we define the flavour vectors²³

$$N = v_R + v_R^c, \quad \nu = v_L + v_L^c. \quad (22)$$

Obviously, the elements ν_i are active neutrinos and the N_I sterile neutrinos. The mass and kinetic terms then can be combined as

$$\frac{1}{2} \bar{N} (i \not{\partial} - M_N^{\text{diag}}) N + \frac{1}{2} \bar{\nu} (i \not{\partial} - m_\nu^{\text{diag}}) \nu \quad (23)$$

This looks like the Lagrangian for a Dirac field, but one has to keep in mind the Majorana conditions $N_I = N_I^c$, $\nu_i = \nu_i^c$.

3 Other laboratory experiments

At energies $\gtrsim M_I$, the N_I particles can be produced and studied in the laboratory. This is in principle possible if M_I is below the electroweak scale. At energies $\ll M_I$, the N_I only leave indirect traces in the laboratory. They manifest as higher dimensional operators [56], such as the mass term (9). These can lead to deviations from SM predictions in different observables, such as lepton number violation or β -decays. These signatures provide valuable information, but are usually not specific to RH neutrinos. Here we list a number of experimental setups that can constrain the properties of N_I . So far almost all but those in section 3.1 have reported negative results, i.e. only allow to exclude certain parameter regions.

²³Obviously $v_R = P_R N$ and $v_L = P_L \nu$, where $P_{R,L}$ are chiral projectors.

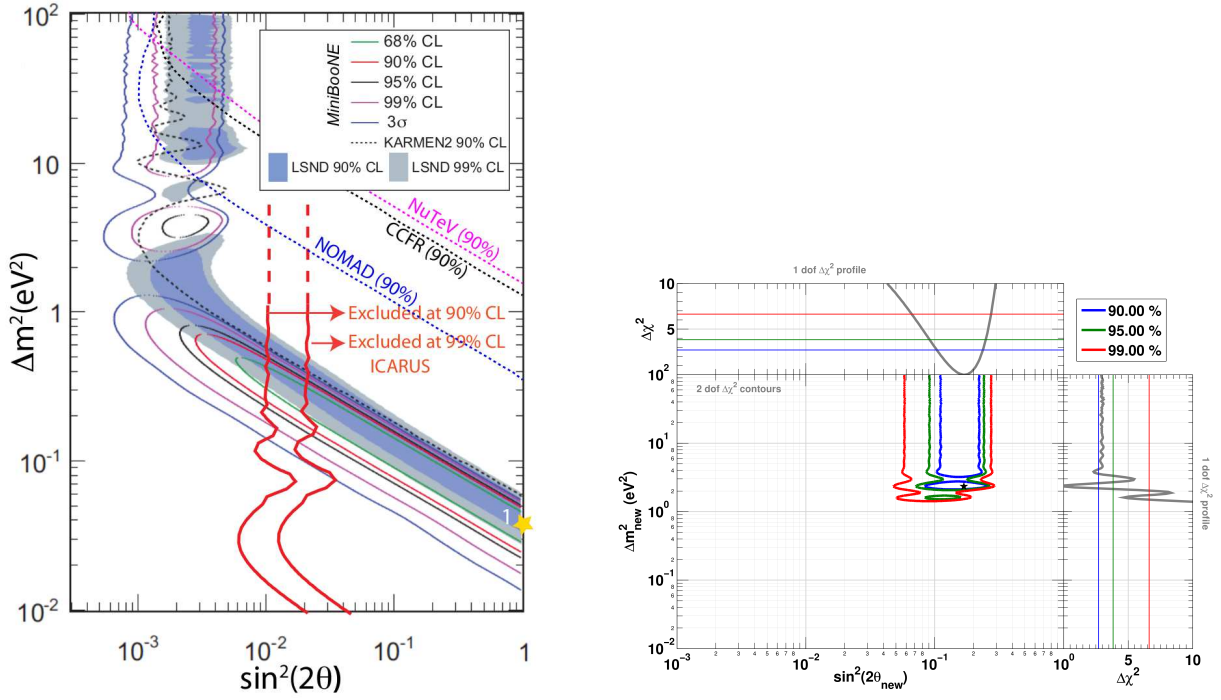


Figure 3: *Left plot:* The region in the mass-mixing plane preferred by the LSND anomaly (coloured bands) is compared to the region allowed by MiniBooNe (coloured lines) and exclusion plots by other experiments as indicated in the plot; plot taken from [63]. *Right plot:* region allowed by the combined reactor and gallium anomalies, taken from [16]. Data from both is e.g. combined in figure 4 in [64].

3.1 Neutrino oscillation anomalies

Accelerator experiments - Some short baseline and reactor neutrino experiments have reported deviations (ii) from the SS. A more detailed review of these results can be found in [57], which we follow closely here. The most prominent findings come from the LSND experiment [58, 59], which studied transitions $\bar{\nu}_\mu \rightarrow \bar{\nu}_e$ and saw an excess of $\bar{\nu}_e$ -events. The similar KARMEN experiment did not see such excess [60], but could not exclude the entire parameter space of the LSND anomaly [61], mostly due to its shorter baselength. The most recent results from the MiniBooNE experiment [62] from $\nu_\mu \rightarrow \nu_e$ and $\bar{\nu}_\mu \rightarrow \bar{\nu}_e$ studies seem compatible with the LSND anomaly, which is in contrast to previous results. However, it has been pointed out that much of the signal comes from energies below 475 MeV, where the background evaluation is problematic [57]. The ICARUS experiment [63] is also sensitive to sterile neutrinos; active-sterile oscillations get averaged over, but lead to an energy independent enhancement of event rates. Together these experiments roughly restrict the parameter space for one sterile neutrino to a mass splitting $\Delta m^2 \sim 0.5 \text{ eV}^2$ and mixing $\sin^2 2\theta \sim 5 \times 10^{-3}$ [57], see figure 3.

Reactor and gallium anomalies - There are two more anomalies that can be interpreted as a sign for sterile neutrinos with eV masses. One is the reactor anomaly [65]. The neutrino fluxes from nuclear reactors appeared to be in agreement with theory until recently. It was not new experimental data, but more refined theoretical calculations that lead to tension with the SS [66, 67]. However, it should be pointed out that even in these results, about 10% of the β -decay

branches are not known and can only be estimated. This involves using the ILL-experiment's measurement for the electron spectrum [68, 69] as a reference point, hence the anomaly could be due to a systematic in that measurement. The other anomaly arises in the calibration of the GALLEX and SAGE experiments [70, 71].

These anomalies have resulted in a great interest in searches for eV-mass sterile neutrinos. Global fits to all data have e.g. been performed in [64, 72, 73]. As discussed in detail in [64], the situation at this stage is not clear. The accelerator anomalies come from appearance measurements (muon to electron). If they are caused by sterile neutrino oscillations, there should also be a ν_μ disappearance, which is not observed. This tension is present in $3 + 1$ (three active and one eV sterile neutrino) model and remains in $3 + 2$ scenarios (three active plus eV sterile). It reduces a bit in a $1 + 3 + 1$ model (where one sterile mass square difference is negative). The reactor and gallium anomalies, which are due to disappearance, do not show such tension to other experiments. They come, however, from ν_e disappearance, which is controlled by other parameters than ν_μ disappearance. Hence, the situation remains puzzling. A detailed list of various proposals for future experiments [74, 75] can be found in [16].

3.2 Lepton flavour violation

The lepton number violation in the neutrino sector in (1) also mediates lepton number violation in the charged lepton sector [39, 76–78], leading e.g. to muon decays $\mu \rightarrow e\gamma$ and unitarity violation of the PMNS matrix [79]. For a generic choice of parameters the seesaw relation (13) implies that it is hard to observe these processes; either the suppressing scale M_I is too heavy or the Yukawa couplings F are too small. A class of models that offers relatively good chances to observe such processes are those where the structure of F and M_M is such that an approximately conserved lepton number can be defined [80]. In this case the scales where lepton flavour violation and total lepton number violation occur can be rather different. In such models RH neutrinos responsible for the baryon asymmetry of the universe may give a measurable contribution to $\mu \rightarrow e\gamma$ [81].

3.3 Neutrinoless double β -decay

If neutrinos are Majorana particles, neutrinoless double- β decays ($0\nu\beta\beta$) are possible [41] (see [82] for a general review). Whether $0\nu\beta\beta$ -decay occurs at observable rates depends on the Majorana mass matrix M_M . The lepton number violation is sufficient if at least one eigenvalue of M_M is larger than ~ 100 MeV [83, 84], see also [76, 85]. The $0\nu\beta\beta$ -decay can be pictured as exchange of an electron neutrino that acts as its own antiparticle between the nuclei, see figure 4. The relevant quantity from neutrino physics is the "effective Majorana mass" $m_{ee} = |\sum_i \mathcal{U}_{ei}^2 m_i|$.²⁴ If all N_I are heavy compared to the momentum exchange ($M_I \gg \text{keV}$), then the exchanged flavour state effectively is a superposition of the active neutrino mass states only. In this case there exists a lower bound $m_{ee} > 20$ meV if active neutrinos have an inverted mass hierarchy [86]. If some sterile neutrinos are lighter, they can also contribute and m_{ee} receives corrections [87–91] and there is no lower bound. This may in particular be the case for N_I with keV masses, which are

²⁴The effective Majorana mass is different from the kinetic mass $m_\beta^2 = \sum_i |\mathcal{U}_{ei}|^2 m_i^2$.

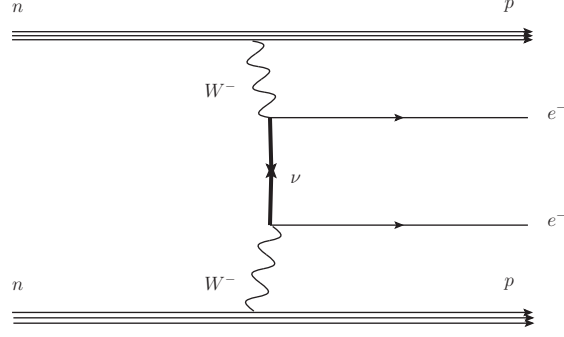


Figure 4: Diagram for neutrinoless double beta decay. Here we have made the lepton number flow explicit by assigning arrows to fermion lines. The “clashing arrows” in the center of the diagram are allowed because neutrinos and antineutrinos are indistinguishable if they are Majorana particles. If some N_I are light enough, they may also be exchanged instead of ν_i . The amplitude for this process vanishes in the limit $M_M \rightarrow 0$.

DM candidates. The effective Majorana mass m_{ee} is given by

$$m_{ee} = \left| \sum_i (U_{\nu})_{ei}^2 m_i + \sum_{\text{all light } I} \Theta_{eI}^2 M_I \right|. \quad (24)$$

For very light N_I one has to go beyond the seesaw approximation (20) to calculate the active-sterile mixing matrix Θ .

So far there is no clear observation of neutrinoless double- β decays. The only claim of a detection [92, 93] suggests $m_{ee} = 0.32 \pm 0.03$ eV [94], but is disputed, as it appears to be in conflict with other observations [95]. For instance, the EXO-200 experiment finds $m_{ee} < 0.14 - 0.38$ eV [86]. Other experiments so far only put upper bounds on the rate for this process, see e.g. [86, 96] for an overview.

3.4 Collider searches

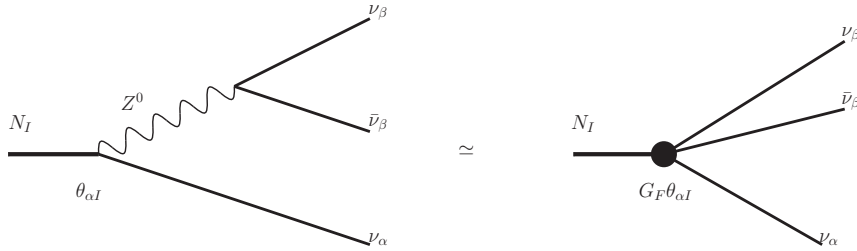


Figure 5: Example for a N_I -decay at low energies. The N_I itself can be produced in meson decays. Instead of the $\bar{\nu}_\beta$ - ν_β pair there can also be charged lepton-antilepton pairs or quark-antiquark pairs (which hadronize) in the final state if this is kinematically allowed.

Intensity frontier - If kinematically possible, the sterile neutrinos N_I participate in all processes that involve active neutrinos, but with a probability that is suppressed by the small mixings

U_α^2 . This makes it possible to produce them in meson decays for $M_I \lesssim$ a few GeV [97–102]. One can distinguish two ways to look for N_I . First, they could be seen as missing energy in the meson decays that produce them; in two body decays this allows to determine their mass and (via the branching ratio) their mixing. Second, the subsequent decay of the N_I shown in figure 5 may also be observed (e.g. as “nothing \rightarrow leptons” process) if one places a detector along the beamline. For some parameter choices, it can even be possible to observe both events in the same detector [103]. Several experiments of this type have been set up in the past [104, 105], in particular CERN PS191 [106, 107], NuTeV [108], CHARM [109], NOMAD [110] and BEBC [111] (see [112] for a review). The bounds derived from these for $n = 2$ are shown in figure 10. They are valid under the assumption that N_I have no interactions other than those in (1) below the electroweak scale. If the mass M_I is larger than a few GeV, the N_I are too heavy to be produced efficiently (D or B meson decays are not possible) and it is unlikely that direct searches in the near future can find them. If they are, on the other hand, lighter than \sim MeV, then their Yukawa coupling F must be very small due to (13) and the branching ration is too small²⁵.

High energy frontier - Sterile neutrinos with masses up to a few TeV in principle are within reach of the LHC. However, if they only interact via the Yukawa couplings F , the branching ratio is usually too small; a detection is only possible if F has a particular structure that leads to cancellations in the contributions of different elements to m_ν [114, 115], hence allows for larger individual entries of F . If the ν_R have additional interactions at high energy, the perspectives are better. For instance, in *left - right symmetric models* [116–118] they are charged under a right chiral $SU(2)$ gauge symmetry, which can be broken near the TeV scale. One promising possibility to test such models is to search for the associated gauge bosons [119], but also the N_I themselves can be searched for [120–122]. Current bounds are given in [123, 124]. Also in other scenarios LHC searches can be promising [125, 126], including those where N_I are responsible for leptogenesis [127].

3.5 Direct DM searches

Sterile neutrinos are a promising DM candidate, which we discuss in detail in section 6. If they compose all DM, then bounds from X-ray and structure formation imply that their Yukawa couplings are so small that they cannot contribute to the observed neutrino oscillations [128]²⁶. This means that, if one at the same time requires RH neutrinos to explain the two observed neutrino mass differences, there must be at least three of them. The small coupling also makes it practically impossible to directly observe these particles in collider experiments due to the tiny branching ratio for their production. They could at least in principle be found in direct detection experiments that look for interactions of DM sterile neutrinos from the interstellar medium with atomic nuclei in the laboratory, and some experiments have been suggested [130, 131]. However, such detection would be extremely challenging due to the small mixing angle and the background from solar and stellar active neutrinos [132].

²⁵If M_M is generated by spontaneous symmetry breaking below the electroweak scale, it may be possible to detect even lighter (keV) sterile neutrinos [113].

²⁶It has been shown that the bounds on DM sterile neutrinos can constrain the active neutrino mass spectrum if additional assumptions are made [129].

3.6 Other constraints

Several other ways to constrain N_I properties have been suggested. If they have eV masses as suggested by the oscillation anomalies (ii), they should affect β -decays [55, 133–135], which has not been observed. They may also leave traces in neutrino telescopes like IceCube [136–138] or detectors for direct DM searches [139]. Also keV sterile neutrinos may have an effect on nuclear decays [140]. In [141] it was found that sterile neutrinos with TeV masses can improve the fits to electroweak precision data.

4 Thermal history of the universe

If RH neutrinos ν_R with $F \neq 0$ exist, they are necessarily produced thermally in the early universe²⁷. At temperatures above the electroweak scale $T_{EW} \sim 140$ GeV (assuming a Higgs mass of ~ 125 GeV [11, 12]), Higgs particles are present in the plasma. This allows for N_I production as long as the temperature is high enough [$T \gtrsim M_N(T)$, where $M_N(T)$ is an effective mass in the plasma]. The relevant processes are decays and inverse decays $N_I \leftrightarrow \Phi l_\alpha$ (or $\Phi \leftrightarrow N_I l_\alpha$, depending on the effective masses of the (quasi)particles in the plasma [143–145]) and scatterings (such as $\bar{t}t \leftrightarrow N_I l_\alpha$). If the masses M_N are below the electroweak scale, N_I are produced at $T < T_{EW}$ via active-sterile mixing [The same process can be viewed as a ν_L - ν_R oscillation in the flavour basis used in (1)]. In addition to that, there may be other production mechanisms if ν_R have additional interactions with a hidden sector or extended Higgs sector, couple directly to the inflaton or are charged under a gauge symmetry that is broken above the electroweak scale. The presence of N_I in the plasma can have different effects in the early universe, which we will summarize in the following.

All astronomical observations to date are in rather good agreement with the Λ CDM model of cosmology²⁸, sometimes dubbed the “Concordance Model” or “Standard Model of Cosmology” in analogy to the SM. The most important cosmological parameters in the context of RH neutrinos are the fractions of the total energy budget of the observable universe from baryons ($\Omega_B \sim 0.049$) and dark matter ($\Omega_{DM} \sim 0.265$ without active neutrinos) [34], as well as the *effective number of neutrino species* N_{eff} in the radiation dominated epoch²⁹. The latter can be understood as a measure for the expansion history of the universe. The (Hubble) rate of the universe’s expansion is given by

$$H^2 = \frac{8\pi}{3}G\rho, \quad (25)$$

where $G = M_P^{-2}$ is Newton’s constant and ρ the energy density of the universe. The contribution of “known neutrinos plus unknown physics” to ρ is usually parametrized as $N_{\text{eff}} \times \rho_\nu$, where ρ_ν is the contribution from one ultrarelativistic species and N_{eff} is the *effective number of neutrino species*. It can be identified with the actual number of neutrino species if all neutrinos are effectively massless and there is no other “new physics”. It is common to parametrize

$$\rho_\gamma + \rho_{\text{neutrinos}} + [\text{new physics effects}] \equiv \rho_\gamma + N_{\text{eff}}\rho_\nu = \frac{\pi^2}{15}T_\gamma^4 \left[1 + N_{\text{eff}}\frac{7}{8} \left(\frac{4}{11} \right)^{4/3} \right], \quad (26)$$

²⁷See [142] for an early discussion.

²⁸A brief review of the Λ CDM model is given in [1], see e.g. [146, 147] for detailed introductions.

²⁹“Radiation dominated epoch” refers to the period in the universe’s history when more energy was stored in relativistic than in nonrelativistic degrees of freedom.

where T_γ and ρ_γ are temperature and energy density of photons and $\rho_{\text{neutrinos}}$ is the energy density of the SM-neutrinos. The second equality holds only for $T < 0.2$ MeV, i.e. after electrons and positrons annihilated. This is the temperature regime where N_{eff} is practically tested by observations. In the standard scenario $N_{\text{eff}} = 3$.³⁰ This assumes that each neutrino flavour has two internal degrees of freedom. In the SM (without neutrino masses), these are particles and antiparticles. In contrast to charged leptons and quarks, ν_L do not have a spin degree of freedom in the SM: For massless particles, the helicity must be equal to the chirality, hence ν_L must have left helicity. If additional particles were present in the early universe, this would lead to a larger value of N_{eff} [149, 150]. Each $\nu_{R,I}$ adds two neutrino degrees of freedom. If $n = 3$ and all of these were thermalized, N_{eff} would be 6. However, if neutrinos are Dirac fields, then the Yukawa couplings F must be tiny to explain the smallness of the neutrino masses. Then the ν_R degrees of freedom do not get populated significantly by thermal production. In other words, the helicity changing processes are so suppressed at $T \gg m_i$ that practically all neutrinos are produced by the weak interaction and have left helicity. This argument of course assumes that ν_R have no other couplings than F that could contribute to thermal production. Hence, the fact that we observe $N_{\text{eff}} \simeq 3 - 4$ strongly constrains models of Dirac neutrinos in which ν_R are charged under some gauge group at high energies or otherwise produced in the early universe. If neutrinos are Majorana fields and $M_M \gtrsim 100$ MeV, then the heavy particles N_I have decoupled and decayed long before big bang nucleosynthesis (BBN) and do not affect light element abundances or the CMB. Lighter sterile neutrinos can be long lived enough to contribute to N_{eff} during BBN and afterwards. If they are in thermal equilibrium and ultrarelativistic, then each N_I increases N_{eff} by one. If their abundance is below equilibrium or their mass not negligible, they contribute less.

Since (26) assumes that all neutrinos are massless and in thermal and chemical equilibrium, any deviation of the momentum distribution from $(e^{\mathbf{p}/T} + 1)^{-1}$ [such as a chemical potential, non-negligible mass³¹ or a nonequilibrium distribution] leads to non-integer contribution to N_{eff} ; this applies to both, active and sterile neutrinos.

4.1 A brief history of the universe

Observations of the CMB show that the universe was homogeneous and isotropic to one part in ~ 100000 at redshift $z \sim 1100$, when photons decoupled from the primordial plasma [153]. This is puzzling, as the radiation we receive from different directions originates from regions that were causally disconnected at that time if the universe only contained radiation and matter (“horizon problem”). Furthermore, the inferred overall spatial curvature is zero or very small [153], which means that it was extremely close to zero at earlier times (“flatness problem”). Both problems can be understood as the result of cosmic inflation [154, 155], a phase of accelerated expansion in the universe’s very early history. Inflation can also explain the small density perturbations that served as seeds for structure formation in the universe as quantum fluctuations that were “stretched out” to macroscopic scales by the rapid expansion, and predict the correct properties of their spectrum. However, while inflation is an excellent model for cosmology, we do not know much about the fundamental physics mechanism that drove it.

If inflation was driven by the potential energy of an inflaton field, then the quantum fluc-

³⁰At the time of CMB decoupling $N_{\text{eff}} = 3.046$ in the SM, where the deviation from 3 parametrises a deviation from the equilibrium distribution of neutrinos caused by e^\pm annihilation [148].

³¹For eV masses the deviation here is small, see [151, 152] for a detailed discussion of the effects of neutrino masses.

tuations of this field lead to small perturbations in the (otherwise homogeneous) gravitational potential. After the inflaton dissipates its energy into relativistic particles during *cosmic reheating* [156, 157], these lead to density fluctuations in the primordial plasma, which manifest in temperature fluctuations in the CMB and form the seeds for the formation of structures in the universe [158]. The power spectrum of CMB fluctuations is in very good agreement with the above hypothesis [153]. After reheating, N_I can affect the thermal history of the expanding universe in several ways.

Baryogenesis via leptogenesis ($T > T_{EW}$) - There is good evidence [159] that the observed Ω_B is the thermal relic of a small matter-antimatter asymmetry in order $\sim 10^{-10}$ of the early universe (BAU), which survived after all other particles and antiparticles annihilated into CMB photons and neutrinos and is reflected in today's baryon to photon ratio³² $\eta_B \sim 10^{-10}$. If this asymmetry was produced by *leptogenesis*, then the observed Ω_B allows to constrain F and M_M , cf. section 5.

Dark Matter production ($T \sim 100$ MeV if produced by mixing) - If DM consists of thermally produced N_I , then there are various different bounds on their properties, which we discuss in section 6.

Late time leptogenesis ($T_{EW} > T > \text{few MeV}$) - Sphaleron processes [160, 161] are the only source of baryon number violation in (1). They freeze out³³ at $T \sim T_{EW}$, below which baryon number is conserved. The production of a lepton asymmetry can, however, continue afterwards if some N_I are out of equilibrium (e.g. during their freezeout and decay) because F and M_M violate flavoured and total lepton number, respectively. The generated asymmetries can be much bigger than η_B and differ in each flavour [162, 163]. A weak constraint on the asymmetry may be derived from its effect on hadronisation at $T \sim 200$ MeV [164]. Stronger constraints can be derived from BBN, see below. Late time asymmetries can be very important if there are long lived sterile neutrinos because they can amplify or suppress their production rate. For keV-mass sterile neutrinos an amplification of their production rate [165, 166] can be so efficient that they are abundant enough to constitute all DM [162]. A suppression of the thermal production rate, on the other hand, can help to ease the tension between cosmological and laboratory hints for eV-mass sterile neutrinos, see section 4.2. In return, light sterile neutrinos can also amplify an active neutrino asymmetry [167].

Neutrino freezeout ($T \sim 1.1$ MeV for active neutrinos) - The freezeout of active neutrinos leads to a cosmic background of relativistic neutrinos, analogue to the CMB. They affect the expansion by their energy density $\rho_{\text{neutrinos}}$. The neutrino background may carry a lepton asymmetry that is orders of magnitude larger than the baryon asymmetry $\sim \eta_B \sim 10^{-10}$. The main constraints on such asymmetry come from BBN [168]. In the SS, active neutrino oscillations tend

³²The relation between these parameters is given by $\eta_B \simeq 2.739 \cdot 10^{-8} h^2 \Omega_B$.

³³A reaction “freezes out” when the temperature dependent rate at which it occurs falls below the Hubble rate H of cosmic expansion. This essentially means that the density of the primordial plasma has become so low that the rate at which the participating particles meet is negligible. A particle freezes out when the last process (other than decay) that changes its comoving number density freezes out.

to make the asymmetries in individual flavours equal³⁴ [169–171]. How complete this equilibration is depends on the mixing angle θ_{13} . The measured value for θ_{13} suggests a high degree of equilibration [172]. Lepton asymmetries in the neutrino background can be constrained due to their effect on the momentum distribution, which changes the relation between temperature and energy density (26) and mimics an $N_{\text{eff}} \neq 3$. The bounds on N_{eff} from BBN (see below) allow to constrain the asymmetry to roughly $|\eta_L| \lesssim 0.1$ [172], where η_L is defined analogously to (27); see also [173–176].

If sterile neutrinos are relativistic, then they can form a similar background and contribute to N_{eff} . For an active-sterile mass splitting $\Delta m^2 < 1.3 \times 10^{-7} \text{eV}^2$ active-sterile oscillations are effective only after the active neutrino freezeout, then they simply distort the momentum distributions [152]. For much larger splittings they can be produced efficiently via their mixing at $T > 1 \text{ MeV}$. The preference for $N_{\text{eff}} > 3$ in different cosmological data sets (see below) can be interpreted as a hint for eV mass sterile neutrinos as DR, see section 4.2. However, the constraints on N_{eff} from BBN, see below, imply that such background must either have frozen out considerably earlier if it ever was in equilibrium or never thermalized (e.g. because the production was suppressed by some mechanism).

Big bang nucleosynthesis ($T \lesssim 100 \text{ keV}$) - There was a brief period in the early universe during which the temperature was low enough for nuclei heavier than hydrogen (H) to exist and still high enough for thermonuclear reactions to occur. During this period most of the deuterium (D), helium (^3He , ^4He) and lithium (mainly ^7Li) in the universe were formed [177], see e.g. chapter 22 in [1] for a review. These light elements, in particular ^4He , make up the vast majority of all nuclei other than H in the universe. Sterile neutrinos can affect this big bang nucleosynthesis (BBN) in different ways, depending on their mass. N_I with masses far above the electroweak scale have no effect on BBN, as they have decayed long before. If the masses are in the GeV to TeV range, these particles can be long lived enough that the entropy released during their decay affects BBN or the thermal history afterwards. The good agreement between BBN calculations and the observed H and He abundances implies that, if sterile neutrinos with $\text{GeV} \lesssim M_I \lesssim \text{TeV}$ exist, they must have decayed sufficiently long before BBN. The resulting bounds [162, 163, 178] in the mass-mixing plane are plotted in figure 10. If DM is composed of keV-mass sterile neutrinos, these would have no visible effect on BBN because their number density is too low to affect the expansion history in that era. Light sterile neutrinos (with eV masses) would, on the other hand, significantly contribute to N_{eff} [151, 179, 180] as additional radiation and increase the rate of expansion of the universe via (25) and (26). This, for instance, determines the precise moment of neutron freeze-out ($T \sim 0.8$), which roughly occurs when the expansion rate (25) equals the rate for the reaction $n + e^+ \leftrightarrow p + \bar{\nu}_e$. It also affects the amount of time that passes until the formation of elements ($T \sim 10 - 100 \text{ keV}$) and during which neutrons decay. Both determine the number of neutrons available for fusions [181, 182]. However, a change in the expansion rate is not specific to light neutrinos, hence the resulting change in the value for N_{eff} extracted from fits to light element abundances does not actually “measure” the number of light neutrinos or other particles (see e.g. [183] for a summary of examples). It simply parametrizes any deviation from the SM prediction. Sterile neutrinos can also affect BBN if they cause deviations of the neutrino momentum distributions from a Fermi-Dirac spectrum, e.g. by active-sterile oscillations or by

³⁴This is often referred to as “flavour equilibration”, though the process occurs close to the neutrino freezeout and neutrinos may not reach thermal equilibrium. This means that the lepton asymmetry cannot be translated into a chemical potential in the strict sense.

inducing chemical potentials [184]. On one hand, this slightly modifies the relation (26) between T and ρ_ν , which again affects the rate of expansion. More importantly, the He abundance is directly affected by a distortion of the ν_e spectrum [151]. D is less affected, hence provides a more direct probe of the expansion rate [185].

BBN depends on Ω_B , N_{eff} and the lepton asymmetries Y_α . In the SM, where $N_{\text{eff}} = 3$ is fixed and $Y_\alpha = 0$, the only free parameter during BBN is Ω_B (or η_B), and there is a rather impressive agreement between theoretical predictions and the value obtained from the light elements, see e.g. [186]. If one treats N_{eff} as a free parameter using (26), a deviation from 3 mainly reflects in the ^4He abundance. The values for N_{eff} obtained from BBN alone (see e.g. [186–188], cf. also [189, 190]) show a slight preference for $N_{\text{eff}} > 3$, but are consistent with $N_{\text{eff}} = 3$. Different interpretation of the data are discussed in [182]: In absence of significant lepton asymmetry, BBN alone yields $N_{\text{eff}} = 3.71^{+0.47}_{-0.45}$. If one fixes the He abundance to the value inferred from the CMB, this tightens to $N_{\text{eff}} = 3.53^{+0.66}_{-0.63}$ ($N_{\text{eff}} = 3.22 \pm 0.55$ when using the D abundance measured in [188] alone). The likelihood functions given in [187] show a preference for $N_{\text{eff}} > 0$, but clearly constrain $N_{\text{eff}} < 4$. Hence, sterile neutrinos with eV masses, as motivated by the oscillation anomalies (ii), can only be made consistent with BBN if they are not thermalized. This strongly constrains models of light sterile neutrinos unless some mechanism suppresses their production. If DM is composed of sterile neutrinos with keV masses (see section 6), these do not affect N_{eff} because their number density is well below the equilibrium value (their number density can simply be obtained by putting today’s Ω_B in relation to their mass). Hence, they are unaffected by these bounds.

Matter - radiation equality ($T \sim 0.8$ eV) - As the universe expands, the matter density is diluted as $\propto a^3$, where a is the scale factor, due to the increasing physical volume. The radiation energy density is diluted faster ($\propto a^4$) due to the stretching of the wavelengths, hence an initially radiation dominated universe becomes matter dominated at the point of *matter-radiation equality*. In cosmology, one refers to all relativistic degrees of freedom (particle energy dominated by momentum) as “radiation”, while nonrelativistic degrees of freedom (particle energy dominated by mass) are “matter”. A first principles derivation of the kinetic equation in the expanding universe that covers both regimes is given in [191]. Due to Hubble expansion, constituents of the primordial plasma change their identity from “radiation” to “matter” when T (more precisely: their average momentum) falls below their mass, which has to be taken into account when determining the point of equality. If sterile neutrinos are relativistic near $T \sim 1$ eV, they change the temperature of matter radiation equality. This is crucial for the growth of density perturbations in the primordial plasma, see following paragraph. If they become nonrelativistic just around this time, their equation of state is neither that of “radiation” nor “matter” in the intermediate regime. The effect of the time dependence of the equation of state has e.g. been studied in [192].

Photon decoupling ($T \sim 0.25$ eV) - The universe becomes transparent when the temperature is so low that photons cannot dissociate H atoms any more³⁵. While photons previously scattered frequently with free electrons, the cross section with neutral atoms is so small that the average

³⁵The temperature at which this happens is much lower than the H binding energy because of the small baryon to photon ratio η_B , which implies that there are enough photons in the high energy tail of the Bose-Einstein distribution to dissociate the atoms.

photon has not interacted with matter ever since. The cosmic microwave background (CMB) formed by these primordial photons allows us to observe the universe at a very early stage (redshift $z \sim 1100$). The CMB contains an enormous amount of information and is, altogether, one of the most impressive confirmations of the Λ CDM model. The vast amount of data also makes it an excellent tool to look for hints of physics beyond Λ CDM and the SM. The small temperature fluctuations (of relative order $\delta T/T \sim 10^{-5}$) in the CMB yield the earliest probe of structure in the universe. They were generated by acoustic oscillations of the coupled baryon-photon plasma in the primordial gravitational potential wells (DM also falls into these wells, but does not feel the radiation pressure and does not oscillate).

The fluctuations can be decomposed into modes with wave numbers k , their spatial extension is characterized by the inverse of k . When $1/k$ is larger than the causal horizon, the mode remains “frozen”. After the end of inflation, density fluctuations successively “(re)enter the horizon”; that is, the causal horizon becomes bigger than their spatial extension. Then their amplitude starts to grow due to gravitational infall. The evolution in the radiation dominated era is governed by the competition between gravity and the radiation pressure (which depends on N_{eff}); this competition leads to *baryon acoustic oscillations* (BAO) of the plasma. The modes oscillate under the action of both forces until they decouple when the baryons stop feeling the pressure and start to collapse under the action of gravity, eventually forming the structures that we observe in the universe. The observed peaks in the CMB power spectrum can be identified with multipoles l in the multipole expansion of the CMB fluctuations that correspond to the modes k which reached the maximal elongation at that moment. The first peak corresponds to the smallest k that reached maximal compression by the time of decoupling and so on. The evolution of perturbations can be studied quantitatively by a coupled set of Boltzmann and Einstein equations. Before photon decoupling, the density perturbations are small and $\delta_k \rho / \rho \ll 1$ ³⁶ can be used as an expansion parameter in calculations.

The power spectrum of temperature fluctuations can be affected by RH neutrinos in different ways [16, 152, 193]. If they are nonrelativistic, they act as DM. Then they only affect the growth of perturbations via their free streaming length (the DM sterile neutrinos discussed in section 6 are relativistic at freezeout, but become nonrelativistic between BBN and the decoupling of photons). If they are relativistic (as e.g. the eV-mass- N_I motivated by oscillation anomalies), they act as radiation and modify the power spectrum in several ways [193–199]. Their contribution to $N_{\text{eff}} > 3$ increases the rate of expansion (25), hence reduces the comoving sound horizon, which moves the peaks in the power spectrum to higher multipoles. It also enhances the height of the first two peaks via the integrated Sachs-Wolfe effect [195]. Light sterile neutrinos are essentially collisionless and can, in contrast to baryons and photons, not be treated as a perfect fluid. Their anisotropic stress affects the gravitational potential via Einstein’s equations. Since this effect is more relevant in the radiation dominated era, it affects modes that enter the horizon before and after matter-radiation equality in a different way, which reflects in a change in the relative height of high and low l peaks [197]; it suppresses the modes $l \gtrsim 200$ and also shifts the positions of the peaks [193]. Finally, sterile neutrinos contribute to the damping of small scales via their free streaming and affect the high- l modes [193, 194, 200]. All these effects can be parametrized in terms of N_{eff} .³⁷

³⁶Here $\delta \rho_k / \rho$ collectively refers to the contrasts in the densities of photons, baryons, neutrinos and metric degrees of freedom, which of course have to be studied independently.

³⁷Note that individually they are degenerate with other effects, cf. e.g. the discussion in [16] and references therein, and only a global fit allows to reliably determine N_{eff} .

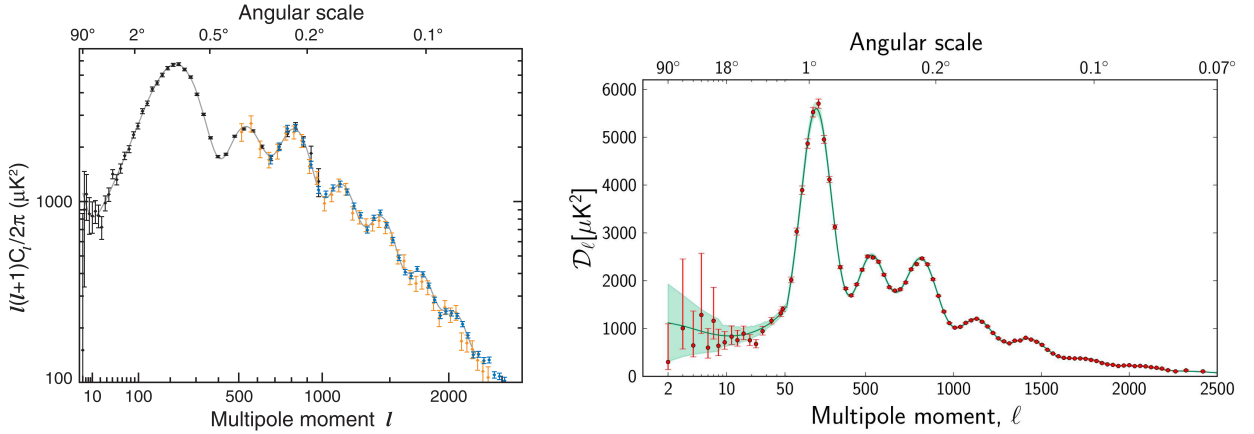


Figure 6: *Left plot: CMB power spectrum as measured by WMAP [153], SPT [201] and ACT [202]; plot taken from [153]. Right plot: CMB power spectrum as measured by Planck [203].*

The CMB power spectrum has been studied with different instruments, including the Wilkinson Microwave Anisotropy Probe (WMAP) satellite, South Pole Telescope (SPT), Atacama Cosmology Telescope (ACT) and Planck satellite, see figure 6. A few years ago these datasets consistently preferred $N_{\text{eff}} > 3$. In order to constrain N_{eff} , it is crucial to have information from high and low multipoles l . While WMAP with its full sky coverage can measure the low l at good precision, its angular resolution is not high enough to go beyond the third peak. ACT and SPT have a better resolution, but can only observe parts of the sky and cannot go below $l \sim 500$. Thus, these data sets need to be combined to reduce the degeneracies between N_{eff} and other parameters. Planck has, for the first time, measured low and high l with a single instrument. Combining WMAP 7 year data with ACT in 2011 preferred $N_{\text{eff}} = 5.3 \pm 1.3$ (which reduced to 4.6 ± 0.8 if data from BAO and measurements of the Hubble rate H_0 are added) [202], combining SPT with WMAP7 gave $N_{\text{eff}} = 3.85 \pm 0.62$ (3.86 ± 0.42 with BAO and H_0) [201]. More recent SPT results [204] continue to favour DR with $N_{\text{eff}} = 3.62 \pm 0.48$ (3.71 ± 0.43 when combined with BAO and H_0 data). In contrast to that, new ACT data [205, 206] favours $N_{\text{eff}} = 2.79 \pm 0.56$, in accord with the SS. This tension between SPT and ACT has e.g. been discussed in [73, 207]. The WMAP collaboration quotes $N_{\text{eff}} = 3.84 \pm 0.40$ using their 9 year data [153]. A combined analysis performed in [208] yields $N_{\text{eff}} = 3.28 \pm 0.40$. Very recently, Planck found $N_{\text{eff}} = 3.30 \pm 0.27$ [34], which is perfectly consistent with the SS. We discuss the implications of these measurements for sterile neutrinos as DR in section 4.2.

Large Scale Structure The formation of structures in the universe (see [210] for a review) after photon decoupling can roughly be divided into two parts. As long as $\delta\rho_k/\rho \ll 1$ can be used as an expansion parameter (“linear regime”), semianalytic methods [211] and fully automated codes (such as CAMB³⁸ [212, 213] or CLASS³⁹ [214]) are applicable. These can test a large number of cosmological parameter sets in a short time. For $\delta\rho_k/\rho > 1$ (“nonlinear regime”) the applicability of semianalytic methods (see e.g. [215–217]) is very limited; in general only

³⁸<http://camb.info>

³⁹<http://lesgourg.web.cern.ch/lesgourg/class.php>

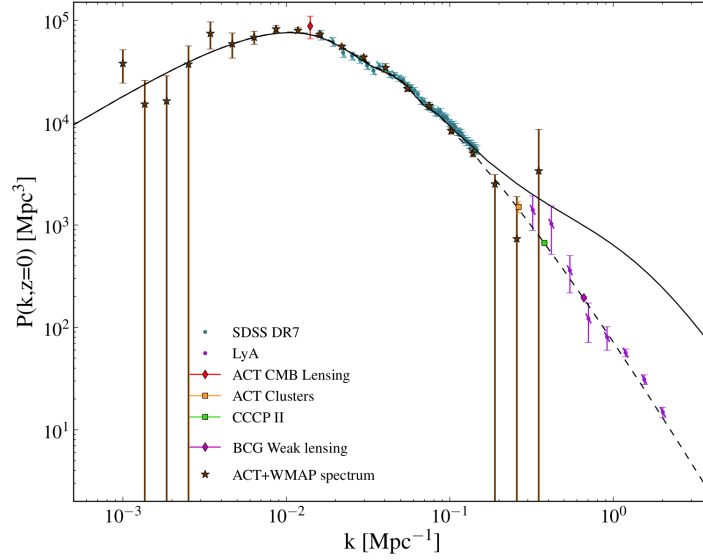


Figure 7: Matter power spectrum from different observations as indicated in the plot and combined in [209] (plot taken from there).

expensive numerical n-body simulations [218–224] allow to make predictions. In the intermediate range, some sophisticated methods have been suggested (see e.g. [225–231]). For perturbations on different scales, the evolution becomes nonlinear at different times; the behaviour on cosmic scales is still linear nowadays, while the matter distribution locally is extremely inhomogeneous. Sterile neutrinos can affect the structure formation if they act as DM or DR.

The implications of DM sterile neutrinos with keV masses are discussed in section 6, the only big difference to CDM scenarios lies in their free streaming length λ_{DM} . This leads to a suppression of structures on (comoving) scales smaller than λ_{DM} . Lighter sterile neutrinos with \sim eV masses as suggested by the oscillation anomalies (ii) would act as DR. The effect that they have on the expansion rate (25) would not only reflect in the abundances of light elements and the CMB, but also in the distribution of matter in the universe.

An important quantity that characterizes the distribution of large scale structures (LSS) in the universe is the *matter power spectrum*, cf. figure 7, which is obtained from large galaxy surveys [232–242] and measures fluctuations on smaller scales than the CMB. Apart from small wiggles (related to baryonic acoustic oscillations), the matter power spectrum shows a “turnover point”, the position of which is sensitive to N_{eff} . This feature occurs because perturbations oscillated in the radiation dominated era after they enter the horizon and grew only slowly, while in the matter dominated era they grew more quickly. The initial power spectrum is almost scale invariant, but those modes that entered the horizon during radiation domination grew only slowly until the moment of matter-radiation equality and are suppressed with respect to those that enter after that point. A larger N_{eff} leads to a later equality, which affects the position of the turnover point. The damping of modes right of the turnover point is controlled by the ratio $\Omega_B/(\Omega_B + \Omega_{DM})$. It is also affected by the velocity dispersion of massive neutrinos [16]. However, since the position of the turnover point is only known with limited accuracy [243] and LSS data cannot constrain all cosmological parameters, it is usually analysed in combination with CMB data (see below).

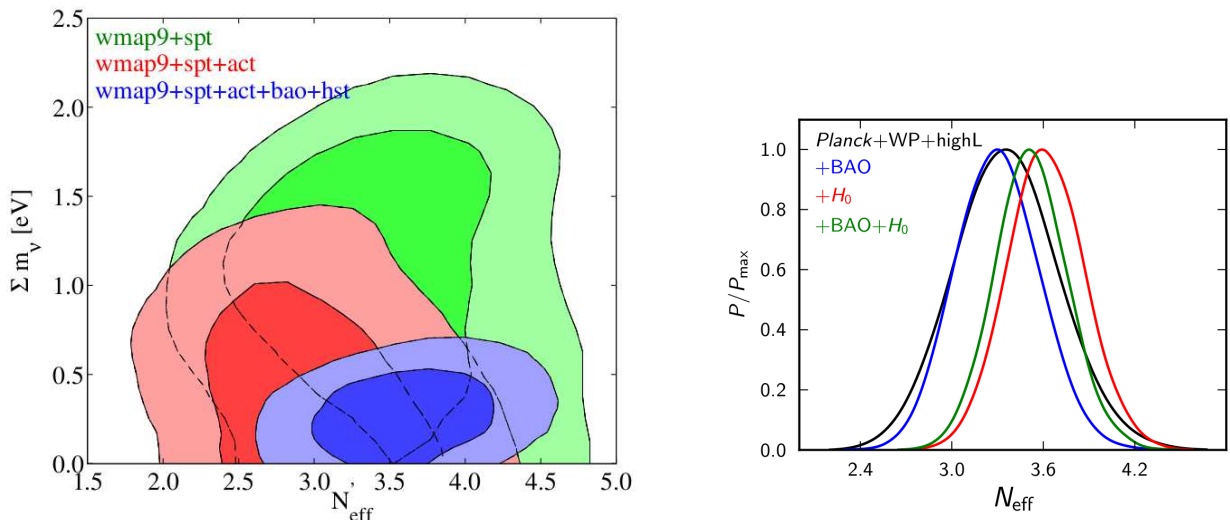


Figure 8: *Left plot:* Combinations of N_{eff} and the sum of neutrino masses favoured by the analysis in [73]. Note that the parameter N_{eff} on the horizontal axis is not exactly identical to the parameter in (26) because the authors allowed for a common neutrino mass. *Right plot:* Marginalized posterior distribution of N_{eff} from Planck (black) and Planck data supplemented by BAO data [235, 237, 238, 240, 242] (blue), a local H_0 measurement [247] (red), and both BAO and H_0 (green); plot from [34].

4.2 Sterile neutrinos as dark radiation

For the past decade, cosmological data generally favoured $N_{\text{eff}} > 3.046$, though the significance was not strong enough to rule out the SS. It is tempting to think that sterile neutrinos may be the common origin of the oscillation anomalies (ii) and these observations (i). For the masses and mixings indicated by LSND, the thermal production of the sterile neutrinos in the early universe would be efficient enough to thermalize them [244–246], leading to a contribution to N_{eff} of order one per species.

Unfortunately, the current situation is rather confusing. On one hand there is some tension amongst different oscillation experiments [64]; most of the region favoured by LSND is excluded by ICARUS, KARMEN and MiniBooNE. On the other hand, there is also tension between the latest results from the CMB. SPT+WMAP results [204] favour DR with $N_{\text{eff}} = 3.62 \pm 0.48$; this is consistent with the $N_{\text{eff}} \simeq 4$ predicted by a thermalized sterile neutrino with masses and mixing suggested by the oscillation anomalies, but also does not rule out the SS. In contrast, ACT+WMAP [205, 206] favours $N_{\text{eff}} = 2.79 \pm 0.56$, which would clearly rule out thermal DR. This is in contrast to earlier ACT results [202], which favoured DR. Planck found 3.30 ± 0.27 [34] (also using BAO data); though this shows a slight preference for $N_{\text{eff}} > 3$, it is perfectly consistent with the SS and clearly disfavors $N_{\text{eff}} = 4$.

The WMAP, ACT and SPT results have been combined with various other data sets, including measurements of the CMB, the LSS and BAO from galaxy surveys and measurements of the contemporary Hubble constant H_0 . For instance, in [73] it was recently argued that cosmology can be consistent with the neutrino oscillation anomalies. This conclusion was mainly possible because the authors excluded ACT and BBN data from the combined analysis. This can be seen in figure 8. For small masses < 0.5 eV, WMAP+SPT+ACT data prefer extra neutrinos; but

for masses around 1 eV the data favours $N_{\text{eff}} \sim 3$, as predicted by the SS. Including BAO and H_0 data indicates $N_{\text{eff}} > 3$, but also disfavours the ~ 1 eV region for the masses preferred by oscillation anomalies. Without ACT, $N = 4$ and a mass of 1 eV are perfectly consistent. Similar analyses, using pre-Planck data, have e.g. been performed in [190, 200, 207, 248–254]⁴⁰. The conclusions differ, depending on the selected data sets and statistical method. There is a general preference for $N_{\text{eff}} > 3$, but no exclusion of the SS.

However, while the authors of [73] presented arguments to exclude ACT from their analysis, the conclusions change dramatically when the Planck result 3.30 ± 0.27 [34] is included. Though a slight preference for N_{eff} so far seems to remain, the thermalized DR ($N_{\text{eff}} \geq 4$) that the oscillation anomalies hint at is clearly disfavoured [256]. The above result assumes massless neutrinos, but does not change significantly if the sum of neutrino masses is allowed to vary ($N_{\text{eff}} = 3.32^{+0.54}_{-0.52}$ and $\sum_I m_i < 0.28$ eV when combined with BAO [34]). There is some freedom to increase N_{eff} if local measurements are used to determine H_0 instead of the value obtained from the Planck data itself, see figure 8. Local measurements of cosmological quantities such as the Hubble rate or the age of the universe (by studying old objects) depend less on the assumed model of cosmology and can be used complementary to high redshift data, see [257] for a recent discussion. The Planck collaboration concludes that the tension between direct H_0 measurements and the CMB and BAO data in the Λ CDM model can be relieved by $N_{\text{eff}} > 3.046$, but there is no strong preference for this extension from the CMB damping tail [34]. It remains to be seen whether this tendency continues when the full Planck data is analysed, which will provide the most stringent constraint on N_{eff} from a single instrument [258].

The apparent tension between oscillation anomalies and the Planck and ACT results could be eased if the thermal production of light sterile neutrinos in the early universe is somehow suppressed, e.g. by a chemical potential [190, 259–261]. Quantitative studies of the flavour evolution [167, 169–171, 262–264] are required to answer the question to which degree a lepton chemical potential can prevent the thermalization [190, 246, 260, 261, 265–273].

If one, on the other hand, interprets the Planck and ACT results as indicators that there is no DR, then it remains to be understood why so many previous analyses seemed to point towards its existence. The possibility that the preference $N_{\text{eff}} > 3.046$ is an artefact of the prior choice in Bayesian analyses has been discussed and rejected in [274]. On the other hand, the authors of [254] found that Bayesian model selection prefers SS, despite the fact that parameter estimates for N_{eff} are larger than 3.046. In [275] it has been pointed out that there is no evidence for $N_{\text{eff}} > 3$ if one relaxes the assumptions on the late history of the universe suggested by Λ CDM when analysing the CMB. Generally, there is a lot more freedom if one allows for more physics beyond the Λ CDM scenario. In [276] it has been discussed in detail that different modifications of the SM can predict values $N_{\text{eff}} > 3$ or $N_{\text{eff}} < 3$, irrespective of the number of neutrino degrees of freedom. However, it seems that at least the simplest scenario in which light sterile neutrinos with generic couplings are the common explanation for the oscillation anomalies and the preference for $N_{\text{eff}} > 3$ is disfavoured by Planck unless more new physics is added. At the same time, it seems unlikely that the SS can be ruled out by CMB observations in foreseeable time.

4.3 Sterile neutrinos in astrophysics

In addition to possible signatures in high redshift observations, sterile neutrinos may also have an effect on astrophysical phenomena at present time. Their most studied role in astrophysics is that

⁴⁰A nice summary of various other ways to combine different data sets can be found in [255].

of a DM candidate, see section 4.2, but they may have effects on other phenomena. They can, for instance, affect the transport in supernova explosions if they have keV [277, 278] or GeV [279] masses. Sterile neutrinos with keV masses can also help to explain the high rotation velocities of pulsars [280, 281].

5 Baryogenesis via leptogenesis

The observable universe does not contain any significant amounts of antibaryons [159], i.e. it is highly matter-antimatter asymmetric. Given our knowledge about the thermal history of the universe, today’s baryon density Ω_B is easily explained as the remnant of a small matter-antimatter asymmetry at early times, when the temperature was high enough for pair creation processes to occur faster than the Hubble rate. The baryon asymmetry in the early universe (BAU) can be estimated by the baryon-to-photon ratio at later times,

$$\left. \frac{n_B - n_{\bar{B}}}{n_B + n_{\bar{B}}} \right|_{T \gg 1 \text{ GeV}} \sim \frac{n_B - n_{\bar{B}}}{s} \sim \left. \frac{n_B}{n_\gamma} \right|_{T \ll 1 \text{ GeV}} \equiv \eta_B. \quad (27)$$

Here n_B and $n_{\bar{B}}$ are comoving number densities for baryons and anti-baryons. η_B can be determined rather consistently from BBN [186] or the CMB and LSS [153],

$$\eta_B^{\text{BBN}} = 5.80 \pm 0.27, \quad \eta_B^{\text{CMB}} = 6.21 \pm 0.12, \quad (28)$$

both in units of 10^{-10} . A period of cosmic inflation, as suggested by the CMB, would have diluted any pre-inflationary asymmetry. Thus, the BAU must have been created dynamically afterwards. There are three conditions for the dynamical generation of a BAU (“baryogenesis”), known as Sakharov conditions [282]: Baryon number (B) violation, breaking of charge (C) as well as charge-parity (CP) symmetry and a deviation from thermal equilibrium. In principle, all of them are fulfilled in the SM: at the quantum level, baryon number is violated [160, 283] at $T > T_{EW}$ by nonperturbative sphaleron processes [161], C and CP are violated by the phase in the CKM matrix [284] and the weak interaction [285, 286], and a deviation from thermal equilibrium is caused by Hubble expansion. However, the CP violation and deviation from equilibrium are both too small in the SM to explain the observed η_B ; see [159] for a detailed account of the Sakharov conditions and baryogenesis in the SM.

RH neutrinos described by (1) can fix both of these shortcomings. As gauge singlets, they can be out of equilibrium at temperatures when all other particles are tightly coupled by gauge interactions, and their Yukawa couplings contain several unconstrained CP -violating phases. This makes baryogenesis via leptogenesis possible [287]⁴¹. Practically leptogenesis works as follows. As usual, we define the left handed lepton numbers $L_{L,\alpha}$ as the zero components of the currents $J_{L,\alpha}^\mu = \bar{\nu}_{L,\alpha} \gamma^\mu \nu_{L,\alpha} + \bar{e}_{L,\alpha} \gamma^\mu e_{L,\alpha}$. Analogously, we define lepton numbers $L_{R,I}$ and $L_{R,\alpha}$ from currents $J_I^\mu = \bar{\nu}_{R,I} \gamma^\mu \nu_{R,I}$ and $J_{R,\alpha}^\mu = \bar{e}_{R,\alpha} \gamma^\mu e_{R,\alpha}$ for the RH fields. This allows to define the active lepton numbers $L_\alpha = L_{L,\alpha} + L_{R,\alpha}$ as well as the LH and RH lepton numbers $L_L = \sum_\alpha L_{L,\alpha}$ and $L_R = \sum_I L_{R,I} + \sum_\alpha L_{R,\alpha}$. The total lepton number is $L = L_L + L_R$. The interactions in

⁴¹The term leptogenesis is often used in a wider sense, referring to all scenarios where the source of CP -violation lies in the leptonic sector. Here we only refer to those scenarios where the BAU is generated from the interactions in (1).

(1) violate individual lepton flavours L_α (via F) as well as total lepton number L (via M_M)⁴². When one or more of the N_I are out of equilibrium, they can generate lepton asymmetries via various processes, including decays and inverse decays, scatterings and flavour oscillations (the probability to decay/scatter/oscillate into leptons and antileptons is different at second order in F due to quantum interferences between CP-violating processes). Sphalerons violate B and L individually, but conserve $B - L$. At $T > T_{EW}$ they transform part of the lepton asymmetry into a baryon asymmetry; if all interactions are in equilibrium it is given by $B \sim \frac{28}{79}(B - L)$ [289, 290]. B is protected from washout after sphaleron freezeout around $T \sim T_{EW}$. Since sphalerons only couple to left chiral fields, they in fact only see the leptonic charge L_L stored in these fields, which may differ from the total lepton asymmetry L . Thus, the BAU we observe is determined by L_L at $T \sim T_{EW} \sim 140$ GeV. The nonequilibrium condition can be fulfilled three times for each N_I : during their production, their freezeout, and their decay.

5.1 Leptogenesis from N_I freezeout and decay

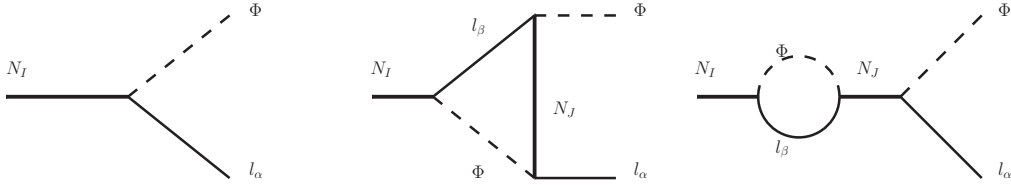


Figure 9: A dominant contribution to the CP-violation in the simplest version of “vanilla leptogenesis” comes from the quantum interference between the tree level diagram and radiative corrections to the decay $N_I \rightarrow \Phi l_\alpha$. Due to the CP-violation contained in the complex phases in F , the amplitudes for these processes with l_α in the final state differ from those with \bar{l}_α . At tree level this difference amounts to an overall phase, which does not affect the physical absolute square of the amplitude, but in the interference terms between tree level and loop diagrams it makes a physical difference. The rightmost diagram gets resonantly enhanced for $M_I \sim M_J$ because then the N_J propagator is nearly onshell. In more general scenarios, also scattering processes (such as $\Phi l_\alpha \rightarrow \Phi l_\beta$ with intermediate N_I) have to be considered.

It is common to split the lepton number violating processes into “source” and “washout”. The source consists of all contributions that violate active lepton numbers in the absence of an existing asymmetry (e.g. N_I -decays); these can generate asymmetries in the presence of a deviation from thermal equilibrium. The “washout” consists of all other processes, which tend to eliminate existing asymmetries (e.g. inverse N_I -decays). In addition, there are “spectator processes” [291, 292] that do not violate L themselves, but redistribute charges amongst different fields and thereby affect the time evolution of L . If the N_I have masses as suggested by GUT models, they are produced thermally, freeze out and decay at temperatures $T \gg T_{EW}$. Since L -violating processes are strongly suppressed at $T < M_I$, $B - L \neq 0$ is preserved from washout. This is the most studied version of leptogenesis, and there exist several detailed reviews, see e.g. [293] or, more recently, [294, 295]. This setup is very appealing because it can easily be integrated into a GUT-framework, provides a “natural” explanation for the smallness of the neutrino masses m_i via the seesaw mechanism and allows to probe at least some parameters of very high energy

⁴²If F and M_M have some particular structure, a combination of them may be exactly or approximately conserved, in which case a different generalization of the term “lepton number” to the RH neutrinos may be convenient, see e.g. [81, 288].

physics in low energy neutrino experiments via (9). The downside is that such heavy particles N_I cannot be studied in the laboratory. Out of the $7n - 3$ parameters in F and M_M , one can under ideal conditions probe the 3 neutrino masses and 6 angles and phases in U_ν experimentally (being very optimistic in case of the Majorana phases). The generated asymmetry η_B (the only observable number in leptogenesis) can in general depend on all $7n - 3$ parameters. Thus, the perspectives to constrain N_I -properties from leptogenesis are very limited. We therefore only recapitulate the basic ideas and refer the interested reader to the reviews named above.

Minimal “Vanilla” leptogenesis - In the simplest scenario one assumes that the N_I are very heavy, have hierarchical masses ($T_{EW} \ll M_1 \ll M_{I>1}$) and the washout is strong. The latter statement is usually parametrized in terms of the parameter $K_I = \Gamma_I|_{T=0}/H|_{T=M_I} \simeq (F^\dagger F)_{II} v^2 / (M_I \times 10^{-3} \text{eV})$, where Γ_I is the thermal width of N_I particles, $H \simeq 1.66 \sqrt{g_*} T^2 / M_P$ the Hubble rate and g_* the effective number of relativistic degrees of freedom in the plasma ($g_* = 106.75$ in the SM at $T \gg T_{EW}$). If $(F^\dagger F)_{11} \sim \text{eV} \times M_1 / v^2$, as suggested by the seesaw relation (13), then $K_1 \gg 1$ and one is in the *strong washout* regime. In this case the BAU responsible for the observed η_B may have been created by the freezeout and decay of the lightest sterile neutrino N_1 alone. This is possible if any pre-existing asymmetries, the asymmetries generated during the production of the N_I and the asymmetries from the $N_{I>1}$ -decays are all washed out efficiently by N_1 ⁴³. This scenario has the advantage that η_B is essentially independent of the initial conditions. A major contribution to the final asymmetry comes from the decay diagrams shown in figure 9. In addition, there are lepton number violating scatterings. However, vanilla leptogenesis can be qualitatively understood by considering the decays and inverse decays only [296]. This mechanism can reproduce η_B for $M_1 \gtrsim 4 \times 10^8 \text{ GeV}$ [297], which requires a rather large reheating temperature if N_I are mainly produced thermally (“thermal leptogenesis”). There is also a constraint on the mass of the lightest active neutrino as $m_1 \lesssim 0.1 \text{ eV}$ [298, 299]; see [300] for an review on the connection with neutrino masses. In the weak washout regime $K_1 \lesssim 1$ ⁴⁴ the predictive power is much smaller because asymmetries from processes at earlier time (nonthermal production during reheating, thermal N_I production, $N_{I>1}$ freezeout and decay...) are not washed out efficiently and contribute to η_B .

Flavour effects - In the simplest scenario it is assumed that only one sterile neutrino N_1 dynamically participates in leptogenesis and all three active flavours can be treated equivalently (“unflavoured regime”). In the unflavoured regime, only the linear combination $\sim F_{\alpha 1} |l_{L\alpha}\rangle$ of active leptons that couples to N_1 is relevant for leptogenesis. In the corresponding flavour basis one can ignore the directions in flavour space perpendicular to that, and the problem is equivalent to the one flavour case. Both of these assumptions do not hold in general.

Active flavours have to be treated separately when the Hubble rate drops below the rate at which interactions that distinguish active flavours, mediated by the charged Yukawa couplings, occur (“flavoured regime”). These interactions destroy the coherence of the flavour state that couples to N_1 because they have different strength for the different $l_{L,\alpha}$. For the τ -Yukawa, this happens below $T \sim 10^{12} \text{ GeV}$. The importance of flavour has been realized in [301] and [302–305] and meanwhile been studied by various authors, see [294, 295] for details and references. Once two

⁴³Though there are no $N_{I>1}$ particles in the plasma at $T \ll M_{I>1}$, the existence of more than one RH neutrino is crucial to provide CP-violation in the lepton sector.

⁴⁴This is possible in spite of (13) because M_M and F are matrices.

flavour states are distinguishable, one has to treat the asymmetries stored in each individually. They can differ considerable and even have opposite signs [306]. This can affect η_B if e.g. the washout is very different for different flavours; it makes leptogenesis possible even if the source term does not violate $\sum_\alpha L_\alpha$. Flavour effects can reduce the lower bound on M_1 in generic seesaw scenarios by 1 – 2 orders of magnitude [288, 307], which is still far out of experimental reach.

Also the assumption that the generation of today’s BAU only involved N_1 -dynamics does not hold in general. In the unflavoured regime, N_1 can only wash out the asymmetry that is stored in the combination $F_{\alpha 1} Y_\alpha$ in flavour space to which it couples. This singles out a particular direction in flavour space. If pre-existing asymmetries or those produced by $N_{I>1}$ have a component orthogonal to this, N_1 cannot wash them out efficiently [308, 309]. In fact, it is a rather special case that there is no such component. The effect of active flavours in scenarios where the heavier N_I contribute has been discussed in [310–314].

Flavour effects offer ways to circumvent the lower bound on M_I . One possibility is that the BAU originates from a purely flavoured asymmetry; i.e. the total asymmetry is vanishing or small ($L \simeq 0$), but the left handed asymmetry is non-vanishing ($|L_L| \gg |L|$). Since sphalerons only couple to LH fields, they convert part of L_L into a LH baryon asymmetry. This is possible for $M_I < v$ because in this case the seesaw relation (13) enforces Yukawa couplings that are so small that L_L and L_R may not equilibrate before sphaleron freezeout. This makes leptogenesis possible even for $M_M = 0$ [315] (Dirac leptogenesis), and it is also the basis of scenarios discussed in the following section 5.2. The mass bound may also be circumvented if the generated asymmetry is resonantly enhanced by a degeneracy between sterile neutrino masses [316] (resonant leptogenesis). This enhancement is discussed from first principles in [317, 318]; in [317] it is shown that the maximal enhancement (compared to the non-resonant case) of the total asymmetry L can be expressed in terms of the parameter⁴⁵

$$\frac{M_1 M_2}{2(M_1 \Gamma_1 + M_2 \Gamma_2)}. \quad (29)$$

The enhancement allows values of M_M in the TeV range, which raises hope to probe N_I in high energy experiments. In this case it is of course not only the lightest sterile neutrino N_1 that generates the asymmetry, but the interplay between the two mass-degenerate states, and flavour effects in the sterile sector have to be taken into account. This is generally the case when the spectrum of M_I is not hierarchical ($|M_1 - M_2| \lesssim M_1$), not only in the extreme case $M_1 \simeq M_2$.

5.2 Leptogenesis during N_I production

If some masses M_I are near the electroweak scale or below, the seesaw relation (13) requires the entries $F_{\alpha I}$ to be very small to be consistent with bounds on the active neutrino masses. That means that the rate $\Gamma_I \sim (F^\dagger F)_{II} T$ of thermal N_I production is so small that these particles may not come into thermal equilibrium until $T \sim T_{EW}$. During the thermal production before equilibration, the nonequilibrium condition is fulfilled and asymmetries L_α are generated. The total asymmetry L is suppressed by M_I/T unless there is a resonant enhancement à la (29), but the flavoured asymmetries L_α are unsuppressed [324]. In contrast to the $M_I \gg T_{EW}$ scenarios discussed in section 5.1, L is not conserved near T_{EW} ; once the N_I reach thermal equilibrium, the L_α are washed out. If N_I have not thermalized or this washout is not efficient enough to eliminate

⁴⁵See [316, 317, 319–323] for earlier discussions of this point.

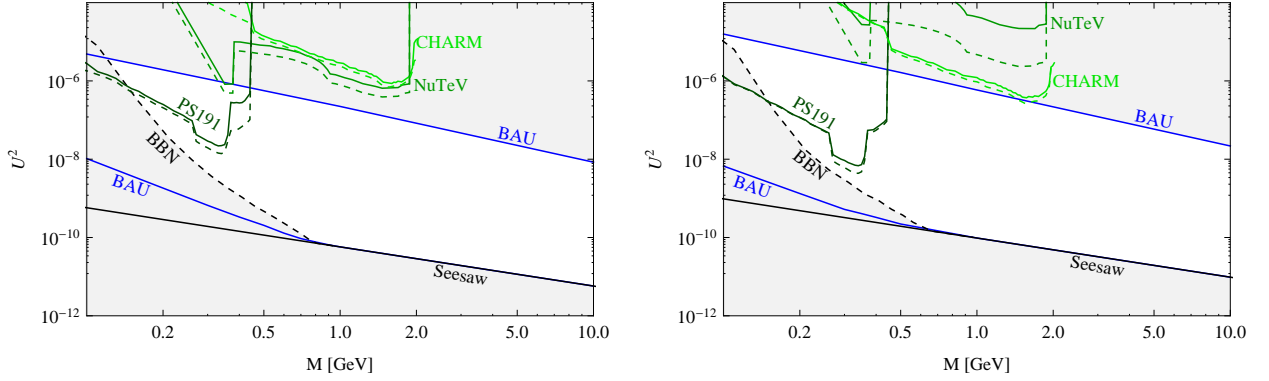


Figure 10: Constraints on the sterile neutrino masses and mixing $U^2 = \text{tr}(\theta^\dagger \theta)$ for $n = 2$ from baryogenesis; left panel - normal hierarchy, right panel - inverted hierarchy. For the displayed case of $n = 2$ RH neutrinos, baryogenesis can only be successful if their masses are degenerate, the parameter M refers to their mean value. For $n = 3$ RH neutrinos no mass degeneracy is required [324]. The observed BAU can be generated in the region between the solid blue “BAU” lines. The regions below the solid black “seesaw” line and dashed black “BBN” line are excluded by neutrino oscillation experiments and BBN, respectively. The areas above the green lines of different shade are excluded by direct search experiments, as indicated in the plot. The solid lines are exclusion plots for all choices of parameters, for the dashed lines the phases were chosen to maximize the asymmetry, consistent with the blue lines. Plots taken from [163].

L_L before sphaleron freezeout, then a baryon asymmetry can be generated despite $L \simeq 0$ due to the fact that sphalerons only see $L_L \simeq -L_R \neq 0$. This scenario is often referred to as *baryogenesis via neutrino oscillations* [325], though oscillations are not always crucial. One advantage of this mechanism is that the N_I are light enough to be within reach of laboratory experiments. This makes it one of the few known models of baryogenesis that are empirically testable (the other two much studied testable mechanisms are resonant leptogenesis and electroweak baryogenesis [326]). If the N_I interact with the SM only via the Yukawa couplings F , then a clear detection is realistically only possible for masses $M_I \lesssim$ a few GeV unless F has some special structure leading to cancellations in (13) that allow for larger individual elements $F_{\alpha I}$ [114, 115]. If they have additional interactions, masses up to a few TeV are in reach of high energy experiments (see section 3.4 and references therein). The perspectives to study the N_I responsible for baryogenesis in the laboratory have been studied in detail in [162, 163, 324, 327]. In the minimal scenario with $n = 2$ sterile neutrinos a mass degeneracy $|M_1 - M_2|/(M_1 + M_2) \sim 10^{-3}$ is required to produce the observed BAU (or η_B). Bounds on mass and mixing from the baryogenesis requirement in this case are shown in figure 10 together with other experimental and astrophysical constraints. For $n > 2$ and M_I in the GeV range no mass degeneracy is necessary [324].

The number of possible leptogenesis scenarios increases greatly when (1) is extended by additional degrees of freedom or embedded into a bigger framework (e.g. supersymmetry); we do not discuss these here in detail and refer the interested reader to the reviews [293–295].

Finally, the CP- and B-violation that make leptogenesis possible can also “work backwards” and rule out or constrain other baryogenesis scenarios because they wash out matter-antimatter asymmetries created by those mechanisms at higher temperatures. The mass spectrum of the N_I can be constrained by the requirement that they do not wash out the baryon asymmetry in the

early universe [328], though these conclusions rely on assumptions about additional interactions of N_I . A similar argument was suggested in [329] to constrain the properties of a fourth neutrino generation.

5.3 Towards a quantitative treatment

Transport equations - Most quantitative studies of leptogenesis solve a set of momentum integrated Boltzmann equations (“rate equations”) to predict η_B as a function of the parameters in (1). In the case of “vanilla leptogenesis”, these can be written as [296]

$$HX \frac{dY_1}{dX} = -\Gamma_1(Y_1 - Y_1^{eq}) \quad (30)$$

$$HX \frac{dY_{B-L}}{dX} = \epsilon_1 \Gamma_1(Y_1 - Y_1^{eq}) - c_W \Gamma_1 Y_{B-L}. \quad (31)$$

Here Y_1 is the abundance of N_1 particles, i.e. the momentum integral over the phase space distribution function divided by the entropy density s . Y_1^{eq} is its value in thermal equilibrium and Y_{B-L} the difference between baryon and lepton abundances (particles minus antiparticles for each of them). We use the variable $X = M_1/T$ instead of time, which leads to a factor $dX/dt \simeq HX$ on the left hand side⁴⁶. The factor $HX \simeq \frac{dX}{dt}$ on the left hand side ϵ_1 is a parameter that characterizes the amount of CP-violation,

$$\epsilon_1 \simeq -\frac{3}{16\pi} \frac{1}{(F^\dagger F)_{11}} \sum_I \text{Im} \left[\left(F^\dagger F \right)_{I1}^2 \right] \frac{M_1}{M_I} \simeq \frac{3}{16\pi} \frac{M_1}{(F^\dagger F)_{11} v^2} \text{Im} [(F^T m_\nu F)_{11}] \quad (32)$$

The constant c_W in the simplest case (washout by inverse decays) is given by 1/2 times the ratio between the number densities of N_1 and active leptons. Calculation of the final Y_{B-L} requires solving the rate equations (30) and (31), it can be estimated as $Y_{B-L} \sim \kappa \epsilon_1 / g_*$ [287],⁴⁷ where the number $\kappa < 1$ is called efficiency factor and is related to the washout.

Equations (30) and (31) can be used when only one sterile neutrino dynamically contributes to the BAU and the SM leptons can be described in an effective one flavour treatment (unflavoured regime). In the fully flavoured regime flavour dependent interactions act sufficiently fast (compared to the time scale $\sim 1/\Gamma_1$ related to the N_1 dynamics) to fully decohere the different contributions in the state $F_{\alpha 1} |l_{L\alpha}\rangle$ that couples to N_1 . Then (31) has to be replaced by three different equations for the asymmetries Y_α in the individual flavours. In the intermediate regime between these two cases, there is no full decoherence. In this case flavour oscillations have to be taken into account. This is usually done by *density matrix equations* [330], see [301, 304] for early applications to leptogenesis. These are matrix valued generalizations of the rate equations (30) and (31) in which the lepton charges $Y_{\alpha\beta}$ carry two indices. The diagonal elements $Y_{\alpha\alpha}$ of these simply describe the lepton abundance in flavour α , the off-diagonal components describe correlations between different flavours. A first principles approach that allows to study the flavoured, unflavoured and intermediate regimes consistently was presented in [331].

If more than one RH neutrino is relevant for leptogenesis, also the different sterile flavours have to be treated independently. For a hierarchical mass spectrum, this usually amounts to simply

⁴⁶The expression for dX/dt can be complicated when g_* changes during leptogenesis. This can e.g. affect the generation of lepton asymmetries at $T \ll T_{EW}$.

⁴⁷Our notation is more close to that in [293].

replacing (30) by n different equations for the abundances Y_I of all relevant sterile flavours N_I . In scenarios of resonant leptogenesis or leptogenesis during N_I production, oscillations between the different flavours may be relevant. In these scenarios, leptogenesis typically happens at temperatures $T \gg M_I$. In this situation transitions between the different helicity states are strongly suppressed and the different helicity states of N_I evolve independently. Effectively, they act as “particle” and “antiparticle” for the N_I , though this notion can of course not be taken literally for a Majorana field⁴⁸. Correlations between different helicities are usually negligible, and it is justified to describe the N_I by two matrices Y_N and $Y_{\bar{N}}$ for the two helicity states. In the mass basis, the abundances Y_I can be identified with the elements $(Y_N)_{II}$. In the fully flavoured regime, where leptogenesis during N_I production and resonant leptogenesis usually take place, the kinetic equations then read

$$iHX \frac{dY_N}{dX} = [H_N, Y_N] - \frac{i}{2} \{\Gamma_N, Y_N - Y_N^{eq}\} + \frac{i}{2} Y_\alpha \tilde{\Gamma}_N^\alpha, \quad (33)$$

$$iHX \frac{dY_{\bar{N}}}{dX} = [H_N^*, Y_{\bar{N}}] - \frac{i}{2} \{\Gamma_N^*, Y_{\bar{N}} - Y_{\bar{N}}^{eq}\} - \frac{i}{2} Y_\alpha \tilde{\Gamma}_N^{\alpha*}, \quad (34)$$

$$iHX \frac{dY_\alpha}{dX} = -i\Gamma_L^\alpha Y_\alpha + i\text{tr} \left[\tilde{\Gamma}_L^\alpha (Y_N - Y_N^{eq}) \right] - i\text{tr} \left[\tilde{\Gamma}_L^{\alpha*} (Y_{\bar{N}} - Y_{\bar{N}}^{eq}) \right]. \quad (35)$$

The flavour-matrix H_N is the dispersive part of the effective N_I -Hamiltonian, which leads to sterile neutrino oscillations; the rate-matrices Γ_N , $\tilde{\Gamma}_N$ and Γ_L^α form the dissipative part, which acts as collision term. These transport coefficients have to be computed from the real- and imaginary parts of the N_I and $l_{L,\alpha}$ self energies in thermal field theory. More precise definitions are given in [163], along with a derivation of (33)-(35).

The equations (30)-(35) are *rate equations* for momentum integrated abundances. They provide a good approximation if the momentum distributions are proportional for equilibrium distributions (this is often called *kinetic equilibrium*). If this is not the case, each momentum mode has to be tracked independently by a Boltzmann equation, see e.g. [332, 333]. In numerical simulations, one of course has to sample a finite number of representative momenta. In addition, one needs to calculate the collision term as a function of momentum and temperature. This makes the treatment technically much more challenging.

Conceptual issues - A question that has received much attention in recent years is whether Boltzmann equations for particle abundances are in principle suitable to describe leptogenesis. For instance, calculations based on Boltzmann equations are plagued with a double-counting problem [334]. The reason is that Boltzmann equations somewhat artificially distinguish the external and internal lines of a Feynman diagram; only the external lines are associated with physical particles that appear in the phase space distribution functions. If one simply introduces collision terms for N_I -mediated scatterings in addition to those for N_I decays and inverse decays shown in figure 9, one counts the same processes twice: If the intermediate N_I in a scattering is on-shell, then the scattering $l_\alpha \Phi \rightarrow \Phi l_\beta$ is identical to an inverse decay $l_\alpha \Phi \rightarrow N_I$ followed by a decay $N_I \rightarrow \Phi l_\beta$ and should not be counted independently. This particular problem can be fixed by hand within the Boltzmann approach by performing a real intermediate state subtraction (RIS) and using finite temperature field theory to calculate the amplitudes, see [335] and references therein for a detailed account of this issue.

⁴⁸At $T \gg M_I$ the average momentum of particles is so large that the Majorana mass is kinematically negligible, hence ν_R effectively behaves like a massless Weyl field up to corrections $\mathcal{O}[M_M/T]$.

In leptogenesis, the leading order processes that contribute to the generation of a matter-antimatter asymmetry comes from an interference with loop diagrams as e.g. shown in figure 9, hence leptogenesis is a pure quantum effect. This is in contrast to many other processes that are well-described by Boltzmann equations, such as CMB decoupling or BBN. Boltzmann equations are semi-classical. The dynamical quantities are phase space distribution functions for particles and antiparticles, i.e. classical quantities. The collision terms, on the other hand, are calculated from S-matrix elements. This treatment is based on a number of assumptions that may be questionable in the dense primordial plasma. The definition of particle numbers and the S-matrix are both based on the notion of asymptotic states, the meaning of which is not clear in a dense plasma, where particles are never “far away” from their neighbours. Even if the plasma can be described as an ensemble of (quasi)particles, the dispersion relations of these differ considerably from those in vacuum. Finally, the collision terms are affected by thermodynamic effects (such as Bose enhancement, Pauli blocking, Landau-Pomeranchuk-Migdal effect, possible enhancements from multiple scatterings...) and cannot be calculated from the (vacuum) S-matrix. The range of validity of the Boltzmann equations and size of possible corrections cannot be estimated within this framework and requires a first principles treatment. This has lead to a great interest in nonequilibrium quantum field theory [191, 336–340] and applications to leptogenesis [144, 191, 317, 318, 331, 335, 341–354] in recent years.

At a fundamental level, the state of a quantum system can be described by an infinite tower of n-point correlation functions. In practice, it is usually sufficient to consider two-point functions. The leptonic charge can conveniently be described in terms of the correlation function⁴⁹ $S_L^+(x_1, x_2)_{\alpha\beta} = \frac{1}{2} \langle \bar{l}_{L,\alpha}(x_1) l_{L,\beta}(x_2) - l_{L,\beta}(x_2) \bar{l}_{L,\alpha}(x_1) \rangle$, where the average $\langle \dots \rangle = \text{Tr}(\varrho \dots)$ includes quantum mechanical and thermodynamic fluctuations (ϱ is the density operator). The definition of this function does not depend on any notion of asymptotic states or (quasi)particles. From the Fourier transform of this function in the relative coordinate $x_1 - x_2$ one can define the momentum integrated lepton abundance matrices

$$Y_l(t) \equiv - \int \frac{d^4 p}{(2\pi)^4} \frac{\text{tr}[\gamma^0 S_L^+(p; t)]}{s} = - \int d\mathbf{p} \frac{\mathbf{p}^2}{2\pi^2} \int \frac{dp_0}{2\pi} \frac{\text{tr}[\gamma^0 S_L^+(p; t)]}{s}. \quad (36)$$

Here $x_i = (t_i, \mathbf{x}_i)$, $t = (t_1 + t_2)/2$ ⁵⁰ and the trace runs over Dirac indices. The diagonal elements $Y_l(t)_{\alpha\alpha}$ correspond the lepton numbers in flavour α , the off-diagonals describe correlations between different flavours, related to flavour oscillations. For the sterile neutrinos we define the propagator $G_{IJ}^+(x_1, x_2) = \frac{1}{2} \langle \bar{N}_I(x_1) N_J(x_2) - N_J(x_2) \bar{N}_I(x_1) \rangle$. The matrices Y_N and $Y_{\bar{N}}$ can be extracted from it as

$$Y_N(t) \equiv - \int \frac{d^4 p}{(2\pi)^4} \frac{\text{tr}[P_+ \gamma^0 G^+(p; t)]}{s}, \quad Y_{\bar{N}}(t) \equiv - \int \frac{d^4 p}{(2\pi)^4} \frac{\text{tr}[P_- \gamma^0 G^+(p; t)]}{s} \quad (37)$$

where P_{\pm} are helicity projectors. The time evolution of G^+ and S_L^+ is governed by the Kadanoff-Baym equations, which can be obtained from a Dyson-Schwinger equation on a complex time path [355–358]. The Kadanoff-Baym equations are exact integro-differential equations; There are different ways to derive effective kinetic equations for Y_N , $Y_{\bar{N}}$ and Y_l from them [191, 318, 331, 335, 349, 353]. In the fully flavoured or unflavoured regime, one can neglect active flavour oscillations and find a flavour basis in which Y_l is diagonal. In this case we can, assuming

⁴⁹We use the notation of [349].

⁵⁰In the homogeneous and isotropic early universe there is no dependence on $\mathbf{x}_1 + \mathbf{x}_2$.

that sphalerons act rapidly on the time scale related to the N_I -evolution with a rate that is in good approximation given by the equilibrium one⁵¹, relate Y_l to the quantities in (33)-(35) as $Y_\alpha = (Y_l)_{\alpha\alpha} - (n_B - n_{\bar{B}})/3$.

Though the above approach provides a controlled approximation scheme to formally obtain effective kinetic equations from first principles, it is not yet a complete theory of leptogenesis because the computation of the transport coefficients in practice can be complicated [145, 165, 361–366]. It requires knowledge of the quasiparticle spectrum in the plasma [143, 318, 353, 367–369] and inclusion of all processes in the plasma [143, 144, 364, 366]. In the regime $M_I \ll T$ it is still not clear which effect corrections from soft and collinear gauge boson exchange have [145, 364–366].

The conclusion on this point is that it is possible to describe leptogenesis in the unflavoured [346, 349], flavoured [331, 348] and resonant [317, 318] regimes by effective kinetic equations. By that, we mean differential equations that are local and of first order in time [191], which is in contrast to the non-local second order fundamental Kadanoff-Baym equations. The situation is relatively simple if the lepton asymmetry is generated at $T \ll M_I$ and the M_I spectrum is hierarchical. Then first principles calculations suggest that in the unflavoured [346, 349] and fully flavoured [331] cases standard Boltzmann equations give results which are correct up to factors $\mathcal{O}[1]$, provided that the RIS is performed consistently. When flavour oscillations are relevant, one has to use their matrix-valued generalisation, the density matrix equations, as e.g. derived in [163, 331, 353]. For $T > M$ or when two masses are degenerate, one can still formulate effective kinetic equations, such as (33)-(35). However, these cannot be obtained by inserting S-matrix elements into the classical Boltzmann equation. Instead, they should be derived using controlled approximations to the full nonequilibrium field theory, which take into account the modified (quasi)particle spectrum and dispersion relations in the plasma, the effect of (possibly multiple) scatterings with quanta from the thermal bath and other thermodynamic effects. Though great progress has been made in this regime [145, 163, 317, 318, 324, 347, 364–366], the accurate quantitative description is not complete at this stage.

6 RH Neutrinos as dark matter

Over the past 80 years⁵², overwhelming evidence has accumulated that most of the mass in the observable universe is not composed of *baryonic matter*⁵³ as we know it. The presence of large amounts of non-luminous matter can on one hand be inferred by comparing the observed gravitational potential⁵⁴ to the density of visible matter. Independently of that, it is also required in order to explain the clustering of matter and formation of structures in the universe, e.g. the power spectrum shown in figure 7. This process can be studied by the analysis of density

⁵¹See [359, 360] for some discussion of this point.

⁵²The term “dark matter” was already used in [370, 371], but in that context simply referred to non-luminous matter. Zwicky concluded that the velocities in the Coma-system are an “unsolved problem”, which, however, did not receive much attention for decades.

⁵³In this context all matter that is composed of SM fermions (including leptons) is usually referred to as “baryonic”.

⁵⁴The gravitational potential can be studied by tracking the dynamics of astrophysical objects on various scales such as stars in galaxies (in particular rotation curves) as well as galaxies and ionized gas clouds within galaxy clusters and by gravitational lensing (weak and strong).

perturbations in the CMB⁵⁵ and by observations of the structure in the universe, such as galaxy surveys, gravitational lensing or the absorption in the spectra of distant quasars (“Ly α forest”).

Numerous attempts to simultaneously explain these phenomena by modifications of gravity or the presence of compact macroscopic objects (such as lonely planets, black holes or other non-luminous star remnants) have failed. In contrast to that, they can easily be understood if one assumes the existence of (one or several) new particles that are massive, electrically neutral, long lived (compared to the age of the universe), collisionless and have a free streaming length in the matter dominated era that is sufficiently small to be consistent with the observed structure in the universe.

One can qualitatively distinguish three types of DM candidates. *cold dark matter* (CDM) is composed of particles that were nonrelativistic at the time of decoupling. *hot dark matter* (HDM) particles were relativistic at the time of decoupling and remain so into the matter dominated epoch, when structures can grow nonlinearly due to gravitational collapse. *warm dark matter* is relativistic at the time of freezeout, but becomes nonrelativistic during the radiation dominated epoch.

CDM scenarios predict that smaller scale objects form first and then merge into bigger structures (“bottom up”) [372, 373]. This is in good agreement with observations as well as numerical simulations of LSS. On smaller scales, it was noticed more than a decade ago [374, 375] and remains an unsolved puzzle that CDM simulations tend to predict more objects (satellite galaxies and subhalos) than observed. Furthermore, they do not reproduce shape of galactic halos (“cusp/core issue”). However, at this stage this is far from being a reason to disregard CDM because the discrepancy may be related to the resolution or other technical limitations of the simulations (to date, most of them are pure DM simulations that do not include baryons consistently). Furthermore, small objects are hard to observe if they fail to confine gas and form stars, see e.g. [376–379], though this may not explain the discrepancy for objects that are *too big to fail* to attract gas, see e.g. [380]. A recent summary on issues and possible solutions in the Λ CDM model can be found in [381].

In contrast to that, HDM predicts that large structures form first because primordial fluctuations in the gravitational potential have been erased due to the large free streaming length of DM particles (“top down”). This is in contradiction to the observed LSS, which rules out the only potential DM candidate within the SM, the neutrinos ν_L .⁵⁶ In WDM scenarios, structure formation on scales larger than the particles’ average free streaming length λ_{DM} is similar to CDM, but differences on smaller scales are expected to be visible in various observables, such as the matter power spectrum, halo density profile, halo mass function, subhalo density profile and subhalo mass function. Qualitatively, structures on scales smaller than λ_{DM} are suppressed due to the free streaming.

Sterile neutrinos are collisionless and can be very long lived, hence they are an obvious DM candidate. This scenario has been studied by a large number of authors, see e.g. [54, 128, 129, 224, 265, 277, 382–391, 393, 394, 394–424]. Formally, sterile neutrinos are WDM candidates, though this classification is slightly ambiguous because momentum distribution may be very different from Fermi-Dirac. Their properties are constrained by the requirements outlined below. In what follows, we require that all DM is composed of sterile neutrinos. If they make up only a

⁵⁵The fact that most of the matter started to cluster before the decoupling of photons implies that it had decoupled considerable earlier, hence is not composed of (electrically charged) SM particles.

⁵⁶The active neutrino background can be viewed as a small HDM contribution to the matter density in the universe.

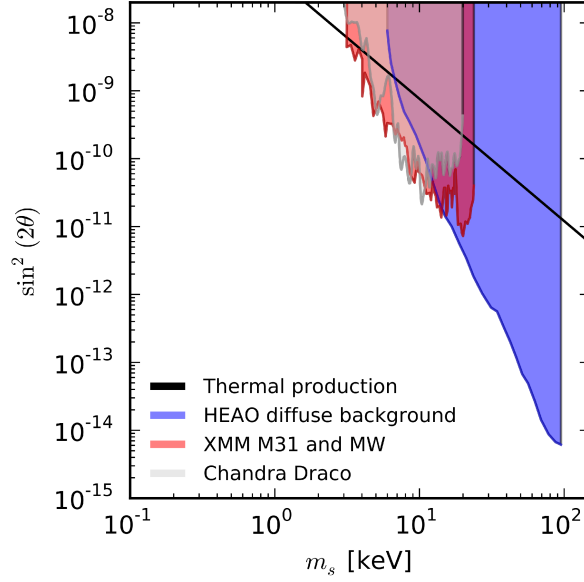


Figure 11: *Different constraints on sterile neutrino DM mass and mixing from X-ray observations. The constraints are taken from [382] (red), rescaled by a factor of two due to mass estimate uncertainties as recommended in [128], [383] (grey) and [384] (purple). Some analyses have claimed stronger constraints, but were later found to be too optimistic. In [385, 386] it was found that [387] underestimated the flux by two orders of magnitude. According to [382] the mass was overestimated in [388] leading to too restrictive constraints. The constraints in [389] might be too restrictive due to the choice of source profile [390]. The spectral resolution seems to be overestimated in [391], cf. Chandra Proposers Guide; this seems to be the main reason for the stronger bounds used in [91]. Thanks to Signe Riemer-Sørensen for the plot and comments.*

fraction of Ω_{DM} , then the bounds weaken considerably. For instance, sterile neutrinos with eV masses could give a subdominant HDM contribution to Ω_{DM} if there are other CDM particles that ensure consistency with structure formation.

Stability - N_I particles are unstable and decay via the θ -suppressed weak interaction. If they are DM, their lifetime must be longer than the age of the universe.

X-ray bounds - The radiative decay $N_I \rightarrow \gamma \nu_\alpha$ via processes as shown in figure 13 predicts the emission of photons with energy $M_I/2$ from DM dense regions [385, 422]⁵⁷. The non-observation of such signal in the data of different X-ray observatories (such as XMM, Chandra and Suzaku) [128, 382–391, 398, 399, 407, 416–419] imposes upper bounds in the mass-mixing plane; these are displayed in figure 11. In figure 12 X-ray bounds are combined with other constraints. For decaying DM, the signal strength scales only linear with the DM column density along the line of sight, hence one can expect a signal from wider range of astrophysical objects than for annihilating DM. This makes future searches promising despite the fact that there are various astrophysical sources in the keV range. The perspectives for future searches have e.g. been

⁵⁷Here we assume that ν_R have (at least) the Yukawa interactions in (1). If such interactions are suppressed, the RH neutrinos that constitute DM can be much heavier and may even be related to the observed excess [425] of γ -ray emission near the galactic center [426].

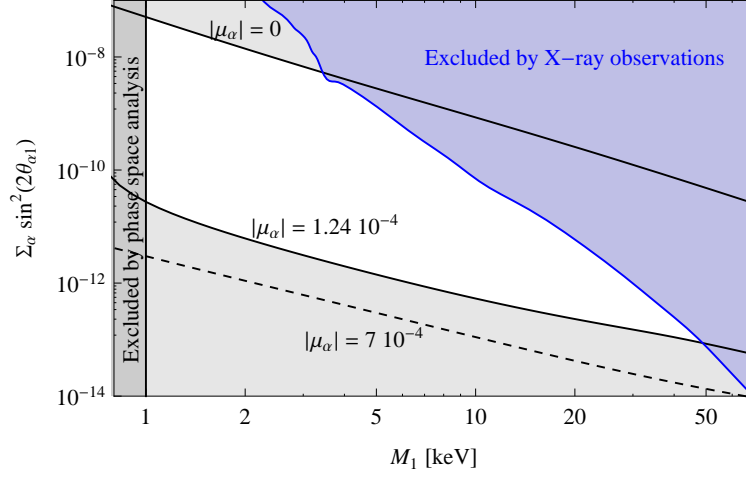


Figure 12: Different constraints on sterile neutrino DM mass and mixing, assuming ν_R interactions (1). The blue region is excluded by X-ray observations, the dark gray region $M < 1$ keV by the Tremaine-Gunn bound [392–394]. The solid black lines are “production curves” for thermal production. For all points on the upper black line the observed Ω_{DM} is produced in the absence of lepton asymmetries (for $Y_\alpha = 0$, non-resonant production) [165]. Points on the lower solid black line yield the correct Ω_{DM} for $|Y_\alpha| = 1.24 \cdot 10^{-4}$ at $T = 100$ MeV, the dashed line for $|Y_\alpha| = 7 \cdot 10^{-4}$. For these values the resonant production mechanism contributes. The region between these lines is accessible for intermediate values of Y_α . We do not display bounds derived from structure formation because they depend on Y_α in a complicated way and there are considerable uncertainties. Plot taken from [162].

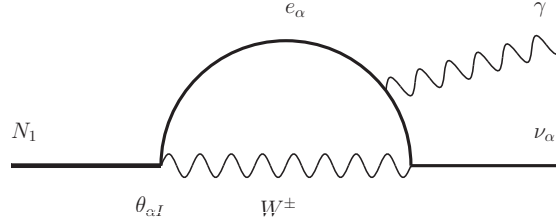


Figure 13: Radiative decay of a DM sterile neutrino $N_1 \rightarrow \gamma \nu_\alpha$. The coupling of N_1 to the W -boson is suppressed by the mixing $\theta_{\alpha 1}$ as indicated.

outlined in [16, 409, 422–424]. Finally, it is worth to emphasize that this scenario is falsifiable: if DM is made of RH neutrinos that are produced thermally in the early universe through their mixing with active neutrinos, their mass and mixing are constrained in all directions in figure 12 and this scenario can be found or falsified on human time scales.

Phase space analysis - As a fermionic DM candidate, the mass of RH neutrinos is constrained by the Tremaine-Gunn bound [392] on the phase space density in the Milky way’s dwarf spheroidal galaxies [393, 394]. This yields a lower bound of $M_N > 1$ keV. In [420] it has been shown that phase space arguments on the galactic scale indeed favour a keV DM particle. The same authors have argued in [421] that, due to the high phase space density, a quantum mechanical treatment is necessary on these scales, which may solve the “cusp issue”.

Production in the early universe It is not known when and how DM was produced in the early universe. If it is composed of sterile neutrinos, then there are several possible production mechanisms.

- **Thermal production via mixing** (non-resonant) - If ν_R have nonzero Yukawa couplings F (i.e. $m_D \neq 0$), then they are produced thermally from the primordial plasma via their mixing with the SM neutrinos ν_L [427]. If this production was efficient enough to bring them into thermal equilibrium, their density would be bigger than Ω_{DM} and “overclose” the universe unless they are diluted by entropy production at some later stage [428–430]. This puts an upper bound on the mixing angle, given by the upper production curve in figure 12. The production can yield the correct Ω_{DM} if θ is small enough that the DM sterile neutrino never reach thermal equilibrium. In that case they still have a momentum distribution that is proportional to a Fermi-Dirac spectrum [396, 427, 431, 432], which makes them a WDM candidate that is at least disfavoured by structure formation arguments (see below).
- **Resonant thermal production** - The properties of (quasi)particles in the primordial plasma are modified by the interactions with the medium [433–435]. In the presence of a lepton asymmetry, the Mikheev-Smirnov-Wolfenstein effect [436, 437] can lead to a level crossing between active and sterile neutrino dispersion relations [165, 438]. This results in a resonant enhancement of the sterile neutrino production rate. The resulting spectrum is nonthermal, with higher occupation numbers for low momentum modes [165]. Production curves for two different values of the asymmetry are also given in figure 12. Note that these have to be taken with some care because in the calculation of the production efficiency [165] it was assumed that $Y_e = Y_\nu = Y_\tau$. In reality the asymmetries in different flavours may be different and can even have opposite sign (see e.g. [163] for a particular model).
- **Thermal production beyond the SM** - The fields ν_R are singlet under SM the gauge group and only interact with SM particles via their Yukawa couplings F . However, if there exists an extended “hidden sector” [439] or extended Higgs sector, they may have additional interactions with these. They may also be charged under some extended gauge group that is broken at high energies, as e.g. in the left-right-symmetric model [415]. Such additional interactions would contribute to the thermal production [429] in the early universe. Since they usually increase the production rate, the universe may overclose unless the DM abundance is diluted by additional entropy production at later times [440].
- **Nonthermal production** - RH neutrinos can also be produced nonthermally, e.g. due to a coupling to an inflaton [441–443], the SM Higgs [444], other scalars [113, 445] or modified gravity [446].

All these scenarios are constrained by the requirements to produce the correct Ω_{DM} and a momentum distribution that is consistent with the observed LSS.

Structure formation - The masses dictated by the above bounds suggest that, if RH neutrinos mix with LH neutrinos, then they formally are WDM, but their momentum distribution can be non-thermal. Structure formation in WDM scenarios on scales above the free streaming length is similar to CDM. On smaller scales the formation of structures is affected in different ways, the study of which is in general complicated due to the nonlinear nature of the clustering process. Most importantly, one expects a cut in the matter power spectrum at scales below the free

streaming length [447]. In addition, the suppression of small scale structures should be visible in the halo mass function (which counts the number of haloes per unit volume per unit mass at given redshift) [448] and affect the gravitational collapse leading to the formation of the first stars [449, 450]. Unfortunately, these arguments do not directly constrain M_N , but the free streaming length. Furthermore, structure formation is a highly nonlinear problem in the regime $\delta\rho_k/\rho > 1$ that can only be studied quantitatively with expensive many body simulations. With few exceptions [224], these simulations assume that the DM distribution is proportional to a Fermi-Dirac distribution [396]. If this is the case, then the comoving free streaming length λ_{DM} is simply related to the mass by [424]

$$\lambda_{DM} \sim 1\text{Mpc} \left(\frac{\text{keV}}{M_N} \right) \frac{\langle p_N \rangle}{\langle p_\nu \rangle}, \quad (38)$$

where p_N and p_ν are the spatial momenta of sterile and active neutrinos. Such spectra are produced by the non-resonant thermal production from the primordial plasma. In that case Ly α forest observations strongly constrain the viability of WDM [224, 401–403, 405, 412, 413, 451–456]; for sterile neutrinos they impose a lower bound of $M_N > 8$ keV [405]. Then it may be very difficult to distinguish RH neutrino WDM from CDM observationally [405, 457]. If, on the other hand, RH neutrino DM is produced by some other mechanism and has a nonthermal spectrum, the relation (38) between mass and free streaming length does not apply, and simulations of structure formation based on thermal WDM do not allow to draw any general conclusions. In case of the resonant thermal production mechanism, the resulting spectrum has been calculated for $Y_e = Y_\mu = Y_\tau$ [128, 165]. It can be viewed as a superposition of a WDM component and a nonthermal cold component [405, 406], where the Ly α forest bounds allow the warm component to be much “warmer” than in conventional WDM scenarios. First simulations [224] indicate that this scenario may perform better than CDM in predicting the abundance of small scale structures (such as satellite/dwarf galaxies), but the question is not settled at this stage. On one hand, only little is known about how much structure actually exists at small (sub-galactic) scales. While lensing flux and stellar streams suggest the existence of subhalos [381], there is no direct observation of such structures and their existence is disfavoured by some stability considerations [458]. On the other hand there are no systematic studies of structure formation in the nonlinear regime that include the nonthermal component. Arguments against sterile neutrino DM are essentially based on extrapolations of results from simulations that assume purely thermal spectra.

7 A theory of almost everything

Right handed neutrinos ν_R , described by the Lagrangian (1), provide plausible explanations for the phenomena (I), (II), (III), (i) and (ii) named in the introduction. In this section we address the question how many of these phenomena can be explained *simultaneously* by RH neutrinos *alone*.

Minimal case $n = 3$ - The Lagrangian (1) with $n = 3$ RH neutrinos and M_M at or below the electroweak scale [459, 460] is an extension of the SM motivated by the principle of minimality (or Ockham’s razor); it makes only minimal modifications to the known principles and particles in nature. There is no modification to the SM gauge group, the number of fermion families is unchanged, there is no modification to the bosonic field content of the SM or the mechanism of

electroweak symmetry breaking, and no new scale above the electroweak scale is introduced⁵⁸. In [162] it has been shown that this model can indeed simultaneously explain (I)-(III); that is, all known *evidence* for particle physics beyond the SM. This minimal scenario is known as Neutrino Minimal Standard Model (ν MSM). Various aspects of this model have been studied in the past by different authors [88, 90, 97, 98, 101, 114, 128, 162, 165, 178, 324, 327, 361, 384, 385, 417, 428, 432, 441, 442, 444, 459, 460, 462–476], see [128, 163] for a detailed introduction and review.

In the ν MSM, two sterile neutrinos ($N_{2,3}$) have degenerate masses between roughly a GeV and the electroweak scale; the third one (N_1) has a mass in the keV range and acts as DM candidate. $N_{2,3}$ generate active neutrino masses via the seesaw mechanism; at the same time, the CP-violating oscillations during their thermal production at temperatures $T > T_{EW}$ produce the baryon asymmetry of the universe via the mechanism outlined in section 5.2. The lepton asymmetries generated during $N_{2,3}$ production are washed out after sphaleron freezeout at $T \sim T_{EW}$. The freezeout ($T \sim M_{2,3}$) and decay ($T < M_{2,3}$) of the $N_{2,3}$ particles produce new, late time lepton asymmetries, which can be orders of magnitude bigger than the baryon asymmetry. The late time asymmetries are capable of enhancing the rate of N_1 production sufficiently to explain the observed Ω_{DM} for $|Y_\alpha| \gtrsim 10^{-5}$, while being in agreement with all known constraints on DM properties.

The minimal extension of the particle content in the ν MSM comes at the price of a “fine tuning” in the mass splitting of two RH neutrinos: M_2 and M_3 have to be equal to a level of precision $\sim 10^{-13}$ [163]. This degeneracy may be related to new symmetries [114, 470], but cannot be explained in the framework of the ν MSM itself. The tuning mainly arises from the requirement to produce a late time lepton asymmetry $|Y_\alpha| \gtrsim 10^{-5}$; this is necessary to sufficiently enhance the N_1 production to explain the observed Ω_{DM} . If some of the asymmetries generated before sphaleron freezeout can be preserved from washout [477] or N_1 is produced by some other mechanism (e.g. during reheating), then the required degree of degeneracy reduces to $\sim 10^{-3}$. This weaker degeneracy is necessary for baryogenesis, i.e. to explain the observed Ω_B from CP-violating oscillations of two sterile neutrinos $N_{2,3}$. The third sterile neutrino N_1 cannot contribute significantly to leptogenesis if it is DM because in this case its couplings $F_{\alpha 1}$ are constrained to be tiny by X-ray bounds on its decay width, cf. section 6. For the same reason it also cannot make a significant contribution to neutrino masses via the seesaw mechanism (13); this implies that the lightest active neutrino is effectively massless in the ν MSM.

The particles N_2 and N_3 can be searched for in collider experiments, cf. section 3.4. Known bounds on their mass and mixing are summarized in figure 14. The DM candidate N_1 is too weakly coupled to be studied at colliders, but can be found by indirect DM searches for the X-ray emission line from the decay $N_1 \rightarrow \gamma \nu$, cf. figure 13. Its properties are also constrained by phase space and structure formation considerations. Figure 12 summarizes different bounds on N_1 mass and mixing.

More than three sterile neutrinos - The required amount of “fine tuning” can be considerably reduced if there are more than three sterile neutrinos. For instance, if three sterile neutrinos participate in baryogenesis, then there is no need for degenerate masses even if they are as light as a few GeV [324]. If one at the same time requires one sterile neutrino with keV mass to compose DM, then that means there must be at least $n = 4$ of them altogether. If one, in addition to the evidence (I)-(III), also wants to address the hints (i) and (ii) in this framework,

⁵⁸This implies that the hierarchy problem of the SM can be avoided [461–463].

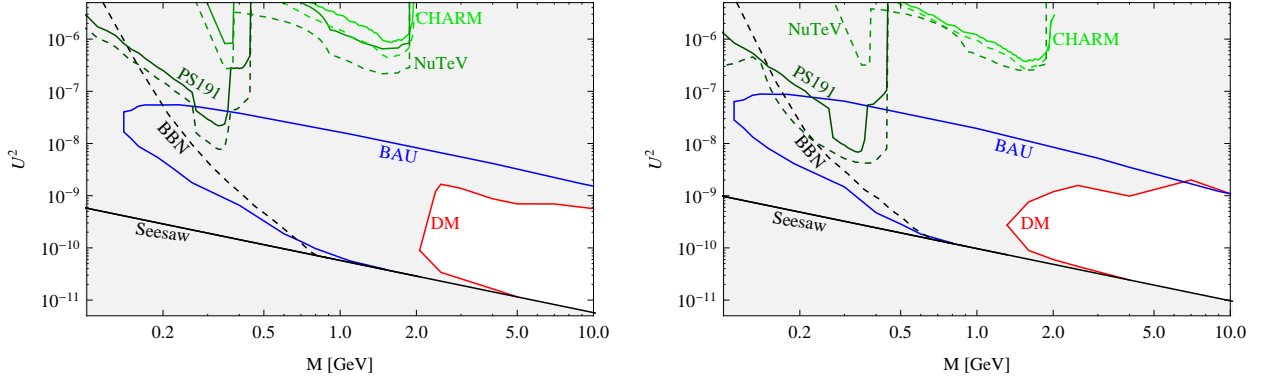


Figure 14: Constraints on the $N_{2,3}$ masses $M_{2,3} \simeq M$ and mixing $U^2 = \text{tr}(\theta^\dagger \theta)$ in the νMSM ; upper panel - normal hierarchy, lower panel - inverted hierarchy. In the region between the solid blue “BAU” lines, the observed BAU can be generated. The lepton asymmetry at $T = 100$ MeV can be large enough that the resonant enhancement of N_1 production is sufficient to explain the observed Ω_{DM} inside the solid red “DM” line. The CP-violating phases were chosen to maximize the asymmetry at $T = 100$ MeV. The regions below the solid black “seesaw” line and dashed black “BBN” line are excluded by neutrino oscillation experiments and BBN, respectively. The areas above the green lines of different shade are excluded by direct search experiments, as indicated in the plot. The solid lines are exclusion plots for all choices of νMSM parameters, for the dashed lines the phases were chosen to maximize the late time asymmetry, consistent with the red line. Plot taken from [162].

then there must be at least one more sterile neutrino with an eV mass. This light sterile neutrino, responsible for the oscillation anomalies, would leave the thermal history of the universe before BBN essentially unaffected due to the smallness of its couplings enforced by the seesaw relation (13). At the same time it can be responsible for the $N_{\text{eff}} > 3$ inferred from BBN and the CMB, see section 4. The late time lepton asymmetries generated by the freezeout and decay of its $M_I \gtrsim 1$ GeV siblings could help to suppress the efficiency of its thermal production and ease the tension between oscillation anomaly and dark radiation signals, see section 4.2. Thus, $n \geq 4$ RH neutrinos described by the Lagrangian (1) alone can be capable of explaining the points (I)-(III) as well as (i) and (ii) simultaneously without “new physics” above the electroweak scale; that is all confirmed fundamental physics phenomena that cannot be explained in the SM except those that are likely to involve accelerated cosmic expansion. Hence, this framework at the current stage provides a phenomenologically complete description of particle physics.

8 Conclusions

Right handed neutrinos provide plausible explanations for neutrino oscillations, the observed dark matter and the baryon asymmetry of the universe, which cannot be understood within the SM. They may also be responsible for the anomalies reported by some short baseline neutrino experiments and hints for dark radiation in cosmological data. Right handed neutrinos can be embedded naturally into bigger frameworks, such as left-right symmetric theories, grand unified theories, supersymmetric extensions of the SM and various models of neutrino mass generation. The different phenomena point towards different right handed neutrino mass ranges, which may of course coexist in nature. Several of these can be probed by direct and indirect laboratory searches, astrophysical observations and cosmological data in the near future. We summarize

well-motivated mass ranges and their phenomenological relevance in the overview table appendix A.

Acknowledgements

I would like to thank Signe Riemer-Sørensen and Yvonne Wong for valuable discussions on astrophysical and cosmological bounds. I am also grateful to Björn Garbrecht, Pasquale Di Bari, Signe Riemer-Sørensen and Yvonne Wong for their comments on different sections of the manuscript. Thanks also to Oleg Ruchayskiy and Viviana Niro for their comments on X-ray bounds and neutrinoless double β -decay, respectively. Finally, I would like to thank Mikhail Shaposhnikov for proof-reading of the manuscript. This work was supported by the Gottfried Wilhelm Leibniz program of the Deutsche Forschungsgemeinschaft.

A Overview Table: Majorana mass scales and observables

M_M	Motivation	ν -oscillations	laboratory searches	CMB	BBN	DM	Leptogenesis
eV	ν -oscillations anomalies, dark radiation	masses by seesaw, explain anomalies ^a	oscillation anomalies, β -decays	explain $N_{\text{eff}} > 3$	may explain $N_{\text{eff}} > 3$	no	no
keV	DM	no if DM ^b	direct searches? ^c , nuclear decays	act as DM, no effect on N_{eff}	effect on N_{eff} too small if DM	good candidate	no
MeV	testability, why not?	masses by seesaw	intensity frontier	unaffected	constrains $M_I \gtrsim 200$ MeV	no ^d	possible (fine tuning)
GeV	testability, minimality	masses by seesaw	intensity frontier, EW precision data, $0\nu\beta\beta$	unaffected	unaffected	no ^d	possible
TeV	minimality, testability	masses by seesaw	LHC	unaffected	unaffected	no ^d	possible
$\gtrsim 10^9\text{GeV}$	grand unification, “naturally” small ν -masses	masses by seesaw	too heavy to be found	unaffected	unaffected	no ^d	works naturally

Colour code: green = can affect, red = does not affect

^a This assumes that the observed Δm_{atm} and Δm_{sol} are generated by ν_R other than those responsible for the anomalies, i.e. $n > 2$.

^b ν_R with keV-masses can generate neutrino masses via the seesaw mechanism, but then they are too short lived to be DM. If they are DM, then their Yukawa coupling is too small to contribute to the seesaw - they can *either* be DM *or* contribute to the seesaw mechanism.

^c It is disputed whether the signal can be distinguished from the active neutrino background.

^d This applies to sterile neutrinos thermally produced via their mixing. Sterile neutrinos with $M_I \gg \text{keV}$ can be DM if $F \simeq 0$ ensures their stability and the production in the early universe is due to an unknown interaction.

B Dirac and Majorana masses

This appendix summarizes some basic aspects of Majorana fermions, see [13, 14] for details. In the SM, matter is composed of fermions. In relativistic quantum field theory these can be described by two component (Weyl) spinors ψ_L and ψ_R , which transform under the (irreducible) left or right handed representations of the Poncaré group, respectively. For historical and computational reasons fermions are, however, often represented by four component spinors. In this review we adopt this common “overnotation”; using the Weyl representation of γ^μ matrices, we define four component spinors $\Psi_L = (\psi_L, 0)^T$ and $\Psi_R = (0, \psi_R)^T$. Consider sets of left and right handed spinors $\Psi_{L,i}$ and $\Psi_{R,j}$, where the indices i and j run from 1 to n and m , respectively, and label individual fields (“flavours”). The most general free Lagrangian reads

$$\frac{i}{2} (\overline{\Psi}_L \not{\partial} \Psi_L + \overline{\Psi}_R \not{\partial} \Psi_R) - \overline{\Psi}_L m_D \Psi_R - \frac{1}{2} (\overline{\Psi}_L m_M \Psi_L^c + \overline{\Psi}_R M_M \Psi_R^c) + h.c., \quad (39)$$

where we have suppressed flavour indices (Ψ_R, Ψ_L are now flavour vectors with components $\Psi_{R,i}$ and $\Psi_{L,j}$). The matrices m_D, m_M and M_M can be combined into a $(n+m) \times (n+m)$ matrix \mathfrak{M} , the physical mass squares are the eigenvalues of $\mathfrak{M}^\dagger \mathfrak{M}$. The mass term reads

$$\frac{1}{2} (\overline{\Psi}_L \ \overline{\Psi}_R^c) \mathfrak{M} \begin{pmatrix} \Psi_L^c \\ \Psi_R \end{pmatrix} + h.c. \equiv \frac{1}{2} (\overline{\Psi}_L \ \overline{\Psi}_R^c) \begin{pmatrix} m_M & m_D \\ m_D^T & M_M^\dagger \end{pmatrix} \begin{pmatrix} \Psi_L^c \\ \Psi_R \end{pmatrix} + h.c. \quad (40)$$

All fermions in the SM are charged under some gauge group, thus any intrinsic mass terms are forbidden by gauge invariance. Terms as m_D are generated by the Higgs mechanism. For $M_M = 0, m_M = 0$ one can express (39) in terms of Dirac spinors $\Psi \equiv \Psi_R + \Psi_L$ as $\mathcal{L} = \overline{\Psi}(i\not{\partial} - m_D)\Psi$. This is the reason why one can describe charged leptons and quarks by Dirac spinors though the basic building blocks of matter are Weyl fermions: the conserved charge related to the unbroken $U(1)$ subgroup in the electroweak theory leads to mass matrix that allows to combine two Weyl fields into a Dirac spinor. If, on the other hand, $m_M, M_M \neq 0$, then one can form $n+m$ Majorana spinors. In the simplest case, when $m_D = 0$ and m_M and M_M are diagonal, one can define $\chi_i = \Psi_{L,i} + \Psi_{L,i}^c$ and $\psi_j = \Psi_{R,j} + \Psi_{R,j}^c$. Formally χ and ψ are four component objects, and the Lagrangian can be written in analogy to the Dirac equation, $\overline{\chi}(i\not{\partial} - m_M)\chi + \overline{\psi}(i\not{\partial} - M_M)\psi$, but they obey the additional Majorana conditions $\chi = \chi^c, \psi = \psi^c$ and have only two independent components. Due to this property the neutral fermions can annihilate with themselves (are their own antiparticles).

Because of these considerations m_D is usually referred to as *Dirac mass term*, while m_M and M_M are called *Majorana mass terms*. However, apart from the two special cases discussed above, they have not much to do with the appearance of Dirac or Majorana particles. Even for $m_D = 0$ the particle spectrum may contain Dirac spinors. Consider, for instance, a set of three fields $\Psi_L, \Psi_{R,1}$ and $\Psi_{R,2}$ with $m_D, m_M = 0$ and $M_M = M \mathbb{1}_{2 \times 2}$. Then one can combine $\Psi_{R,1}$ and $\Psi_{R,2}$ into a Dirac spinor $\Psi = (i\psi_1 + \psi_2)/\sqrt{2}$. On the other hand, one can split any Dirac spinor into two Majorana spinors in this way.

Thus, fermions can generically be described by two component Weyl spinors. If one, for computational convenience, prefers to use four component spinors, one can use the chiral spinors $\Psi_{R,L}$. Only in special cases one can combine these into Dirac spinors. This is possible whenever the full mass matrix \mathfrak{M} has degenerate eigenvalues (with opposite sign), and not necessarily related to the presence of “Dirac” or “Majorana mass terms”.

References

- [1] J. Beringer et al. (Particle Data Group), Phys.Rev. **D86**, 010001 (2012).
- [2] H. Murayama, H. Suzuki, T. Yanagida, and J. Yokoyama, Phys.Rev.Lett. **70**, 1912 (1993).
- [3] M. Shaposhnikov and C. Wetterich, Phys. Lett. **B683**, 196 (2010), 0912.0208.
- [4] F. Bezrukov, M. Y. Kalmykov, B. A. Kniehl, and M. Shaposhnikov, JHEP **1210**, 140 (2012), 1205.2893.
- [5] G. Degrandi, S. Di Vita, J. Elias-Miro, J. R. Espinosa, G. F. Giudice, et al., JHEP **1208**, 098 (2012), 1205.6497.
- [6] S. Alekhin, A. Djouadi, and S. Moch, Phys.Lett. **B716**, 214 (2012), 1207.0980.
- [7] J. Elias-Miro, J. R. Espinosa, G. F. Giudice, G. Isidori, A. Riotto, et al., Phys.Lett. **B709**, 222 (2012), 1112.3022.
- [8] S. Schael et al. (ALEPH Collaboration, DELPHI Collaboration, L3 Collaboration, OPAL Collaboration, SLD Collaboration, LEP Electroweak Working Group, SLD Electroweak Group, SLD Heavy Flavour Group), Phys.Rept. **427**, 257 (2006), hep-ex/0509008.
- [9] D. Delepine, C. Lujan-Peschard, and M. Napsuciale (2013), 1303.4687.
- [10] M. Shaposhnikov, J.Phys.Conf.Ser. **408**, 012015 (2013).
- [11] G. Aad et al. (ATLAS Collaboration), Phys.Lett.B (2012), 1207.7214.
- [12] S. Chatrchyan et al. (CMS Collaboration), Phys.Lett.B (2012), 1207.7235.
- [13] R. Mohapatra and P. Pal, World Sci.Lect.Notes Phys. **72**, 1 (2004).
- [14] M. Fukugita and T. Yanagida, Springer (Berlin) pp. 1–593 (2003).
- [15] R. Mohapatra, S. Antusch, K. Babu, G. Barenboim, M.-C. Chen, et al., Rept.Prog.Phys. **70**, 1757 (2007), hep-ph/0510213.
- [16] K. Abazajian, M. Acero, S. Agarwalla, A. Aguilar-Arevalo, C. Albright, et al. (2012), 1204.5379.
- [17] S. Antusch (2013), 1301.5511.
- [18] A. Merle (2013), 1302.2625.
- [19] H. Georgi and S. L. Glashow, Phys. Rev. Lett. **32**, 438 (1974).
- [20] H. Georgi, AIP Conf.Proc. **23**, 575 (1975).
- [21] H. Fritzsch and P. Minkowski, Annals Phys. **93**, 193 (1975).
- [22] F. Maltoni, J. Niczyporuk, and S. Willenbrock, Phys.Rev.Lett. **86**, 212 (2001), hep-ph/0006358.

- [23] K. R. Dienes, E. Dudas, and T. Gherghetta, Nucl.Phys. **B557**, 25 (1999), [hep-ph/9811428](#).
- [24] N. Arkani-Hamed, S. Dimopoulos, G. Dvali, and J. March-Russell, Phys.Rev. **D65**, 024032 (2002), [hep-ph/9811448](#).
- [25] Y. Grossman and M. Neubert, Phys.Lett. **B474**, 361 (2000), [hep-ph/9912408](#).
- [26] A. Strumia and F. Vissani, [hep-ph/0606054](#) (2006), [hep-ph/0606054](#).
- [27] S. Weinberg, Phys.Rev.Lett. **43**, 1566 (1979).
- [28] Z. Maki, M. Nakagawa, and S. Sakata, Prog.Theor.Phys. **28**, 870 (1962).
- [29] B. Pontecorvo, Sov.Phys.JETP **26**, 984 (1968).
- [30] G. Fogli, E. Lisi, A. Marrone, D. Montanino, A. Palazzo, et al., Phys.Rev. **D86**, 013012 (2012), [1205.5254](#).
- [31] M. Gonzalez-Garcia, M. Maltoni, J. Salvado, and T. Schwetz, JHEP **1212**, 123 (2012), [1209.3023](#).
- [32] D. Forero, M. Tortola, and J. Valle, Phys.Rev. **D86**, 073012 (2012), [1205.4018](#).
- [33] S. Petcov (2013), [1303.5819](#).
- [34] P. Ade et al. (Planck Collaboration) (2013), [1303.5076](#).
- [35] C. Froggatt and H. B. Nielsen, Nucl.Phys. **B147**, 277 (1979).
- [36] J. Schechter and J. Valle, Phys.Rev. **D22**, 2227 (1980).
- [37] G. Gelmini and M. Roncadelli, Phys.Lett. **B99**, 411 (1981).
- [38] M. Magg and C. Wetterich, Phys.Lett. **B94**, 61 (1980).
- [39] T. Cheng and L.-F. Li, Phys.Rev. **D22**, 2860 (1980).
- [40] G. Lazarides, Q. Shafi, and C. Wetterich, Nucl.Phys. **B181**, 287 (1981).
- [41] R. N. Mohapatra and G. Senjanovic, Phys.Rev. **D23**, 165 (1981).
- [42] R. Mohapatra and J. Valle, Phys.Rev. **D34**, 1642 (1986).
- [43] R. Mohapatra, Phys.Rev.Lett. **56**, 561 (1986).
- [44] R. Foot, H. Lew, X. He, and G. C. Joshi, Z.Phys. **C44**, 441 (1989).
- [45] M. Roncadelli and D. Wyler, Phys.Lett. **B133**, 325 (1983).
- [46] E. Ma, Phys.Rev.Lett. **81**, 1171 (1998), [hep-ph/9805219](#).
- [47] T. Gherghetta, Phys.Rev.Lett. **92**, 161601 (2004), [hep-ph/0312392](#).
- [48] P.-H. Gu and H.-J. He, JCAP **0612**, 010 (2006), [hep-ph/0610275](#).

- [49] A. de Gouvea, W.-C. Huang, and J. Jenkins, Phys.Rev. **D80**, 073007 (2009), 0906.1611.
- [50] P. Minkowski, Phys. Lett. **B67**, 421 (1977).
- [51] M. Gell-Mann, P. Ramond, and R. Slansky, in Supergravity, ed. by D. Freedman et al., North Holland (1979).
- [52] R. N. Mohapatra and G. Senjanovic, Phys. Rev. Lett. **44**, 912 (1980).
- [53] T. Yanagida, Prog.Theor.Phys. **64**, 1103 (1980).
- [54] A. Kusenko, F. Takahashi, and T. T. Yanagida, Phys.Lett. **B693**, 144 (2010), 1006.1731.
- [55] A. de Gouvea, Phys.Rev. **D72**, 033005 (2005), hep-ph/0501039.
- [56] A. Abada, C. Biggio, F. Bonnet, M. Gavela, and T. Hambye, JHEP **0712**, 061 (2007), 0707.4058.
- [57] A. Palazzo (2013), 1302.1102.
- [58] C. Athanassopoulos et al. (LSND Collaboration), Phys.Rev.Lett. **77**, 3082 (1996), nucl-ex/9605003.
- [59] A. Aguilar-Arevalo et al. (LSND Collaboration), Phys.Rev. **D64**, 112007 (2001), hep-ex/0104049.
- [60] B. Armbruster et al. (KARMEN Collaboration), Phys.Rev. **D65**, 112001 (2002), hep-ex/0203021.
- [61] E. Church, K. Eitel, G. B. Mills, and M. Steidl, Phys.Rev. **D66**, 013001 (2002), hep-ex/0203023.
- [62] A. Aguilar-Arevalo et al. (MiniBooNE Collaboration) (2012), 1207.4809.
- [63] M. Antonello, B. Baibussinov, P. Benetti, E. Calligarich, N. Canci, et al. (2012), 1209.0122.
- [64] J. Kopp, P. A. N. Machado, M. Maltoni, and T. Schwetz (2013), 1303.3011.
- [65] G. Mention, M. Fechner, T. Lasserre, T. Mueller, D. Lhuillier, et al., Phys.Rev. **D83**, 073006 (2011), 1101.2755.
- [66] T. Mueller, D. Lhuillier, M. Fallot, A. Letourneau, S. Cormon, et al., Phys.Rev. **C83**, 054615 (2011), 1101.2663.
- [67] P. Huber, Phys.Rev. **C84**, 024617 (2011), 1106.0687.
- [68] F. Von Feilitzsch, A. Hahn, and K. Schreckenbach, Phys.Lett. **B118**, 162 (1982).
- [69] A. Hahn, K. Schreckenbach, G. Colvin, B. Krusche, W. Gelletly, et al., Phys.Lett. **B218**, 365 (1989).
- [70] J. Abdurashitov, V. Gavrin, S. Girin, V. Gorbachev, P. Gurkina, et al., Phys.Rev. **C73**, 045805 (2006), nucl-ex/0512041.

- [71] C. Giunti, M. Laveder, Y. Li, Q. Liu, and H. Long, Phys.Rev. **D86**, 113014 (2012), 1210.5715.
- [72] J. Conrad, C. Ignarra, G. Karagiorgi, M. Shaevitz, and J. Spitz (2012), 1207.4765.
- [73] M. Archidiacono, N. Fornengo, C. Giunti, S. Hannestad, and A. Melchiorri (2013), 1302.6720.
- [74] S. K. Agarwalla and P. Huber, Phys.Lett. **B696**, 359 (2011), 1007.3228.
- [75] A. de Gouvea and W.-C. Huang, Phys.Rev. **D85**, 053006 (2012), 1110.6122.
- [76] A. Ibarra, E. Molinaro, and S. Petcov, Phys.Rev. **D84**, 013005 (2011), 1103.6217.
- [77] L. Lello and D. Boyanovsky (2012), 1212.4167.
- [78] A. Abada, D. Das, A. Teixeira, A. Vicente, and C. Weiland, JHEP **1302**, 048 (2013), 1211.3052.
- [79] S. Antusch, C. Biggio, E. Fernandez-Martinez, M. Gavela, and J. Lopez-Pavon, JHEP **0610**, 084 (2006), hep-ph/0607020.
- [80] M. Gavela, T. Hambye, D. Hernandez, and P. Hernandez, JHEP **0909**, 038 (2009), 0906.1461.
- [81] S. Blanchet, T. Hambye, and F.-X. Josse-Michaux, JHEP **1004**, 023 (2010), 0912.3153.
- [82] W. Rodejohann, Int.J.Mod.Phys. **E20**, 1833 (2011), 1106.1334.
- [83] M. Blennow, E. Fernandez-Martinez, J. Lopez-Pavon, and J. Menendez, JHEP **1007**, 096 (2010), 1005.3240.
- [84] J. Barry, W. Rodejohann, and H. Zhang, JCAP **1201**, 052 (2012), 1110.6382.
- [85] M. Mitra, G. Senjanovic, and F. Vissani (2012), 1205.3867.
- [86] A. de Gouvea and P. Vogel (2013), 1303.4097.
- [87] P. Benes, A. Faessler, F. Simkovic, and S. Kovalenko, Phys.Rev. **D71**, 077901 (2005), hep-ph/0501295.
- [88] F. Bezrukov, Phys.Rev. **D72**, 071303 (2005), hep-ph/0505247.
- [89] M. Mitra, G. Senjanovic, and F. Vissani, Nucl.Phys. **B856**, 26 (2012), 1108.0004.
- [90] T. Asaka, S. Eijima, and H. Ishida, JHEP **1104**, 011 (2011), 1101.1382.
- [91] A. Merle and V. Niro (2013), 1302.2032.
- [92] H. Klapdor-Kleingrothaus, A. Dietz, H. Harney, and I. Krivosheina, Mod.Phys.Lett. **A16**, 2409 (2001), hep-ph/0201231.
- [93] H. Klapdor-Kleingrothaus, I. Krivosheina, A. Dietz, and O. Chkvorets, Phys.Lett. **B586**, 198 (2004), hep-ph/0404088.

- [94] H. Klapdor-Kleingrothaus and I. Krivosheina, *Mod.Phys.Lett.* **A21**, 1547 (2006).
- [95] G. Fogli, E. Lisi, A. Marrone, A. Melchiorri, A. Palazzo, et al., *Phys.Rev.* **D78**, 033010 (2008), 0805.2517.
- [96] B. Schwingenheuer (2012), 1210.7432.
- [97] D. Gorbunov and M. Shaposhnikov, *JHEP* **10**, 015 (2007), 0705.1729.
- [98] O. Ruchayskiy and A. Ivashko, *JHEP* **1206**, 100 (2012), 1112.3319.
- [99] D. Gorbunov and M. Shaposhnikov, Contribution to Open Symposium - European Strategy Preparatory Group, Krakow, Poland, September 2012, <https://indico.cern.ch/contributionDisplay.py?contribId=17&confId=175067> (2012).
- [100] L. Lello and D. Boyanovsky (2012), 1208.5559.
- [101] T. Asaka, S. Ejima, and A. Watanabe (2012), 1212.1062.
- [102] S. Gninenko, D. Gorbunov, and M. Shaposhnikov, *Adv.High Energy Phys.* **2012**, 718259 (2012), 1301.5516.
- [103] P. Achard et al. (L3), *Phys. Lett.* **B517**, 75 (2001), hep-ex/0107015.
- [104] T. Yamazaki et al. (1984), in *LEIPZIG 1984, Proceedings, High Energy Physics, Vol. 1*, 262.
- [105] M. Daum et al., *Phys. Rev. Lett.* **85**, 1815 (2000), hep-ex/0008014.
- [106] G. Bernardi et al., *Phys. Lett.* **B166**, 479 (1986).
- [107] G. Bernardi et al., *Phys. Lett.* **B203**, 332 (1988).
- [108] A. Vaitaitis et al. (NuTeV), *Phys. Rev. Lett.* **83**, 4943 (1999), hep-ex/9908011.
- [109] F. Bergsma et al. (CHARM), *Phys. Lett.* **B166**, 473 (1986).
- [110] P. Astier et al. (NOMAD), *Phys. Lett.* **B506**, 27 (2001), hep-ex/0101041.
- [111] A. M. Cooper-Sarkar et al. (WA66), *Phys. Lett.* **B160**, 207 (1985).
- [112] A. Atre, T. Han, S. Pascoli, and B. Zhang, *JHEP* **0905**, 030 (2009), 0901.3589.
- [113] I. M. Shoemaker, K. Petraki, and A. Kusenko, *JHEP* **1009**, 060 (2010), 1006.5458.
- [114] M. Shaposhnikov, *Nucl. Phys.* **B763**, 49 (2007), hep-ph/0605047.
- [115] J. Kersten and A. Y. Smirnov, *Phys.Rev.* **D76**, 073005 (2007), 0705.3221.
- [116] J. C. Pati and A. Salam, *Phys.Rev.* **D10**, 275 (1974).
- [117] R. N. Mohapatra and J. C. Pati, *Phys.Rev.* **D11**, 566 (1975).
- [118] G. Senjanovic and R. N. Mohapatra, *Phys.Rev.* **D12**, 1502 (1975).

- [119] W.-Y. Keung and G. Senjanovic, Phys.Rev.Lett. **50**, 1427 (1983).
- [120] A. Maiezza, M. Nemevsek, F. Nesti, and G. Senjanovic, Phys.Rev. **D82**, 055022 (2010), 1005.5160.
- [121] J. Aguilar-Saavedra, F. Deppisch, O. Kittel, and J. Valle, Phys.Rev. **D85**, 091301 (2012), 1203.5998.
- [122] M. Nemevsek, G. Senjanovic, and V. Tello (2012), 1211.2837.
- [123] S. Chatrchyan et al. (CMS Collaboration), Phys.Rev.Lett. **109**, 261802 (2012), 1210.2402.
- [124] G. Aad et al. (ATLAS Collaboration), Eur.Phys.J. **C72**, 2056 (2012), 1203.5420.
- [125] L. A. Anchordoqui, H. Goldberg, and G. Steigman, Phys.Lett. **B718**, 1162 (2013), 1211.0186.
- [126] V. Hoang, P. Q. Hung, and A. Kamat (2013), 1303.0428.
- [127] S. Blanchet, Z. Chacko, S. S. Granor, and R. N. Mohapatra, Phys.Rev. **D82**, 076008 (2010), 0904.2174.
- [128] A. Boyarsky, O. Ruchayskiy, and M. Shaposhnikov, Ann. Rev. Nucl. Part. Sci. **59**, 191 (2009), 0901.0011.
- [129] A. Merle, Phys.Rev. **D86**, 121701 (2012), 1210.6036.
- [130] Y. Li and Z.-z. Xing, Phys.Lett. **B695**, 205 (2011), 1009.5870.
- [131] W. Liao, Phys.Rev. **D82**, 073001 (2010), 1005.3351.
- [132] S. Ando and A. Kusenko, Phys.Rev. **D81**, 113006 (2010), 1001.5273.
- [133] A. de Gouvea, J. Jenkins, and N. Vasudevan, Phys.Rev. **D75**, 013003 (2007), hep-ph/0608147.
- [134] J. Formaggio and J. Barrett, Phys.Lett. **B706**, 68 (2011), 1105.1326.
- [135] C. Kraus, A. Singer, K. Valerius, and C. Weinheimer (2012), 1210.4194.
- [136] H. Nunokawa, O. Peres, and R. Zukanovich Funchal, Phys.Lett. **B562**, 279 (2003), hep-ph/0302039.
- [137] S. Choubey, JHEP **0712**, 014 (2007), 0709.1937.
- [138] A. Esmaili, F. Halzen, and O. Peres, JCAP **1211**, 041 (2012), 1206.6903.
- [139] A. Gutlein, C. Ciemniak, F. von Feilitzsch, N. Haag, M. Hofmann, et al., Astropart.Phys. **34**, 90 (2010), 1003.5530.
- [140] H. de Vega, O. Moreno, E. M. de Guerra, M. R. Medrano, and N. Sanchez, Nucl.Phys. **B866**, 177 (2013), 1109.3452.
- [141] E. Akhmedov, A. Kartavtsev, M. Lindner, L. Michaels, and J. Smirnov (2013), 1302.1872.

- [142] Y. Zeldovich and M. Y. Khlopov, Sov.Phys.Usp. **24**, 755 (1981).
- [143] G. Giudice, A. Notari, M. Raidal, A. Riotto, and A. Strumia, Nucl.Phys. **B685**, 89 (2004), hep-ph/0310123.
- [144] B. Garbrecht, Nucl.Phys. **B847**, 350 (2011), 1011.3122.
- [145] A. Anisimov, D. Besak, and D. Bodeker, JCAP **1103**, 042 (2011), 1012.3784.
- [146] V. Mukhanov, Cambridge University Press (2005).
- [147] S. Weinberg, Oxford University Press (2008).
- [148] G. Mangano, G. Miele, S. Pastor, T. Pinto, O. Pisanti, et al., Nucl.Phys. **B729**, 221 (2005), hep-ph/0506164.
- [149] V. Shvartsman, Pisma Zh.Eksp.Teor.Fiz. **9**, 315 (1969).
- [150] G. Steigman, D. Schramm, and J. Gunn, Phys.Lett. **B66**, 202 (1977).
- [151] A. Dolgov, Phys.Rept. **370**, 333 (2002), hep-ph/0202122.
- [152] J. Lesgourgues and S. Pastor, Adv.High Energy Phys. **2012**, 608515 (2012), 1212.6154.
- [153] G. Hinshaw, D. Larson, E. Komatsu, D. Spergel, C. Bennett, et al. (2012), 1212.5226.
- [154] A. A. Starobinsky, Phys. Lett. **B91**, 99 (1980).
- [155] A. H. Guth, Phys. Rev. **D23**, 347 (1981).
- [156] L. Kofman, A. D. Linde, and A. A. Starobinsky, Phys.Rev.Lett. **73**, 3195 (1994), hep-th/9405187.
- [157] L. Kofman, A. D. Linde, and A. A. Starobinsky, Phys. Rev. **D56**, 3258 (1997), hep-ph/9704452.
- [158] V. F. Mukhanov and G. Chibisov, JETP Lett. **33**, 532 (1981).
- [159] L. Canetti, M. Drewes, and M. Shaposhnikov, New J. Phys. **14**, 095012 (2012), 1204.4186.
- [160] G. 't Hooft, Phys.Rev.Lett. **37**, 8 (1976).
- [161] V. A. Kuzmin, V. A. Rubakov, and M. E. Shaposhnikov, Phys. Lett. **B155**, 36 (1985).
- [162] L. Canetti, M. Drewes, and M. Shaposhnikov, Phys. Rev. Lett. **110**, 061801 (2013), 1204.3902.
- [163] L. Canetti, M. Drewes, T. Frossard, and M. Shaposhnikov, Phys. Rev. D (accepted) (2012), 1208.4607.
- [164] D. J. Schwarz and M. Stuke, JCAP **0911**, 025 (2009), 0906.3434.
- [165] M. Laine and M. Shaposhnikov, JCAP **0806**, 031 (2008), 0804.4543.

- [166] C. T. Kishimoto and G. M. Fuller, Phys.Rev. **D78**, 023524 (2008), 0802.3377.
- [167] R. Foot, M. J. Thomson, and R. Volkas, Phys.Rev. **D53**, 5349 (1996), hep-ph/9509327.
- [168] H.-S. Kang and G. Steigman, Nucl.Phys. **B372**, 494 (1992).
- [169] A. Dolgov, S. Hansen, S. Pastor, S. Petcov, G. Raffelt, et al., Nucl.Phys. **B632**, 363 (2002), hep-ph/0201287.
- [170] Y. Y. Wong, Phys.Rev. **D66**, 025015 (2002), hep-ph/0203180.
- [171] K. N. Abazajian, J. F. Beacom, and N. F. Bell, Phys.Rev. **D66**, 013008 (2002), astro-ph/0203442.
- [172] G. Mangano, G. Miele, S. Pastor, O. Pisanti, and S. Sarikas, Phys.Lett. **B708**, 1 (2012), 1110.4335.
- [173] P. D. Serpico and G. G. Raffelt, Phys.Rev. **D71**, 127301 (2005), astro-ph/0506162.
- [174] S. Pastor, T. Pinto, and G. G. Raffelt, Phys.Rev.Lett. **102**, 241302 (2009), 0808.3137.
- [175] G. Mangano, G. Miele, S. Pastor, O. Pisanti, and S. Sarikas, JCAP **1103**, 035 (2011), 1011.0916.
- [176] E. Castorina, U. Franca, M. Lattanzi, J. Lesgourgues, G. Mangano, et al., Phys.Rev. **D86**, 023517 (2012), 1204.2510.
- [177] G. Gamow, Phys.Rev. **70**, 572 (1946).
- [178] O. Ruchayskiy and A. Ivashko (2012), 1202.2841.
- [179] R. Barbieri and A. Dolgov, Phys.Lett. **B237**, 440 (1990).
- [180] K. Kainulainen, Phys.Lett. **B244**, 191 (1990).
- [181] J. Lesgourgues and S. Pastor, Phys.Rept. **429**, 307 (2006), astro-ph/0603494.
- [182] G. Steigman, Adv.High Energy Phys. **2012**, 268321 (2012), 1208.0032.
- [183] C. Brust, D. E. Kaplan, and M. T. Walters (2013), 1303.5379.
- [184] M. Y. Khlopov and S. Petcov, Phys.Lett. **B99**, 117 (1981).
- [185] P. Di Bari, Phys.Rev. **D65**, 043509 (2002), hep-ph/0108182.
- [186] G. Steigman (2010), 1008.4765.
- [187] G. Mangano and P. D. Serpico, Phys.Lett. **B701**, 296 (2011), 1103.1261.
- [188] M. Pettini and R. Cooke, Monthly Notices of the Royal Astronomical Society **425**, 24772486 (2012), 1205.3785.
- [189] K. M. Nollett and G. P. Holder (2011), 1112.2683.

- [190] J. Hamann, S. Hannestad, G. G. Raffelt, and Y. Y. Wong, JCAP **1109**, 034 (2011), 1108.4136.
- [191] M. Drewes, S. Mendizabal, and C. Weniger, Phys. Lett. B **718**, 1119 (2013), 1202.1301.
- [192] H. Wei, Z.-C. Chen, and J. Liu (2013), 1302.0643.
- [193] S. Bashinsky and U. Seljak, Phys.Rev. **D69**, 083002 (2004), astro-ph/0310198.
- [194] J. Silk, Astrophys.J. **151**, 459 (1968).
- [195] W. Hu and N. Sugiyama, Astrophys.J. **444**, 489 (1995), astro-ph/9407093.
- [196] W. Hu, D. Scott, N. Sugiyama, and . White, Martin J., Phys.Rev. **D52**, 5498 (1995), astro-ph/9505043.
- [197] W. Hu and N. Sugiyama, Astrophys.J. **471**, 542 (1996), astro-ph/9510117.
- [198] W. Hu, D. J. Eisenstein, M. Tegmark, and M. J. White, Phys.Rev. **D59**, 023512 (1999), astro-ph/9806362.
- [199] R. Bowen, S. H. Hansen, A. Melchiorri, J. Silk, and R. Trotta, Mon.Not.Roy.Astron.Soc. **334**, 760 (2002), astro-ph/0110636.
- [200] Z. Hou, R. Keisler, L. Knox, M. Millea, and C. Reichardt (2011), 1104.2333.
- [201] R. Keisler, C. Reichardt, K. Aird, B. Benson, L. Bleem, et al., Astrophys.J. **743**, 28 (2011), 1105.3182.
- [202] J. Dunkley, R. Hlozek, J. Sievers, V. Acquaviva, P. Ade, et al., Astrophys.J. **739**, 52 (2011), 1009.0866.
- [203] P. Ade et al. (Planck Collaboration) (2013), 1303.5062.
- [204] Z. Hou, C. Reichardt, K. Story, B. Follin, R. Keisler, et al. (2012), 1212.6267.
- [205] J. Dunkley, E. Calabrese, J. Sievers, G. Addison, N. Battaglia, et al. (2013), 1301.0776.
- [206] J. L. Sievers, R. A. Hlozek, M. R. Nolta, V. Acquaviva, G. E. Addison, et al. (2013), 1301.0824.
- [207] E. Di Valentino, S. Galli, M. Lattanzi, A. Melchiorri, P. Natoli, et al. (2013), 1301.7343.
- [208] E. Calabrese, R. A. Hlozek, N. Battaglia, E. S. Battistelli, J. R. Bond, et al. (2013), 1302.1841.
- [209] R. Hlozek, J. Dunkley, G. Addison, J. W. Appel, J. R. Bond, et al., Astrophys.J. **749**, 90 (2012), 1105.4887.
- [210] F. Bernardeau, S. Colombi, E. Gaztanaga, and R. Scoccimarro, Phys.Rept. **367**, 1 (2002), astro-ph/0112551.
- [211] Y. Zeldovich, Astron.Astrophys. **5**, 84 (1970).

- [212] A. Lewis, A. Challinor, and A. Lasenby, *Astrophys. J.* **538**, 473 (2000), [astro-ph/9911177](#).
- [213] A. Lewis and S. Bridle, *Phys. Rev.* **D66**, 103511 (2002), [astro-ph/0205436](#).
- [214] D. Blas, J. Lesgourgues, and T. Tram, *JCAP* **1107**, 034 (2011), [1104.2933](#).
- [215] W. H. Press and P. Schechter, *Astrophys.J.* **187**, 425 (1974).
- [216] J. Peacock and A. Heavens, *Mon.Not.Roy.Astron.Soc.* **243**, 133 (1990).
- [217] J. Bond, S. Cole, G. Efstathiou, and N. Kaiser, *Astrophys.J.* **379**, 440 (1991).
- [218] J. S. Bullock, T. S. Kolatt, Y. Sigad, R. S. Somerville, A. V. Kravtsov, et al., *Mon.Not.Roy.Astron.Soc.* **321**, 559 (2001), [astro-ph/9908159](#).
- [219] V. Springel, S. D. White, A. Jenkins, C. S. Frenk, N. Yoshida, et al., *Nature* **435**, 629 (2005), [astro-ph/0504097](#).
- [220] V. Springel, *Mon.Not.Roy.Astron.Soc.* **364**, 1105 (2005), [astro-ph/0505010](#).
- [221] M. Boylan-Kolchin, V. Springel, S. D. White, A. Jenkins, and G. Lemson, *Mon.Not.Roy.Astron.Soc.* **398**, 1150 (2009), [0903.3041](#).
- [222] F. Prada, A. A. Klypin, A. J. Cuesta, J. E. Betancort-Rijo, and J. Primack, *Mon.Not.Roy.Astron.Soc.* **423**, 3018 (2011).
- [223] A. A. Klypin, S. Trujillo-Gomez, and J. Primack, *The Astrophysical Journal* **740** (2011).
- [224] M. R. Lovell, V. Eke, C. S. Frenk, L. Gao, A. Jenkins, et al., *Mon.Not.Roy.Astron.Soc.* **420**, 2318 (2012), [1104.2929](#).
- [225] S. Matarrese and M. Pietroni, *JCAP* **0706**, 026 (2007), [astro-ph/0703563](#).
- [226] H. de Vega, P. Salucci, and N. Sanchez, *New Astron.* **17**, 653 (2012), [1004.1908](#).
- [227] S. Tassev and M. Zaldarriaga, *JCAP* **1204**, 013 (2012), [1109.4939](#).
- [228] S. Anselmi and M. Pietroni, *JCAP* **1212**, 013 (2012), [1205.2235](#).
- [229] C. Rampf and T. Buchert, *JCAP* **1206**, 021 (2012), [1203.4260](#).
- [230] C. Rampf and G. Rigopoulos (2012), [1210.5446](#).
- [231] S. Tassev and M. Zaldarriaga, *JCAP* **1212**, 011 (2012), [1203.5785](#).
- [232] M. Maggiore and A. Riotto, *Astrophys.J.* **711**, 907 (2010), [0903.1249](#).
- [233] M. Maggiore and A. Riotto, *Astrophys.J.* **717**, 515 (2010), [0903.1250](#).
- [234] M. Maggiore and A. Riotto, *Astrophys.J.* **717**, 526 (2010), [0903.1251](#).
- [235] W. J. Percival et al. (SDSS Collaboration), *Mon.Not.Roy.Astron.Soc.* **401**, 2148 (2010), [0907.1660](#).

- [236] E. Papastergis, A. M. Martin, R. Giovanelli, and M. P. Haynes, *Astrophys.J.* **739**, 38 (2011), 1106.0710.
- [237] F. Beutler, C. Blake, M. Colless, D. H. Jones, L. Staveley-Smith, et al., *Mon.Not.Roy.Astron.Soc.* **416**, 3017 (2011), 1106.3366.
- [238] C. Blake, E. Kazin, F. Beutler, T. Davis, D. Parkinson, et al., *Mon.Not.Roy.Astron.Soc.* **418**, 1707 (2011), 1108.2635.
- [239] H. Aihara et al. (SDSS Collaboration), *Astrophys.J.Suppl.* **193**, 29 (2011), 1101.1559.
- [240] L. Anderson, E. Aubourg, S. Bailey, D. Bizyaev, M. Blanton, et al., *Mon.Not.Roy.Astron.Soc.* **428**, 1036 (2013), 1203.6594.
- [241] C. Blake, S. Brough, M. Colless, C. Contreras, W. Couch, et al., *Mon.Not.Roy.Astron.Soc.* **425**, 405 (2012), 1204.3674.
- [242] N. Padmanabhan, X. Xu, D. J. Eisenstein, R. Scalzo, A. J. Cuesta, et al. (2012), 1202.0090.
- [243] G. B. Poole, C. Blake, D. Parkinson, S. Brough, M. Colless, et al. (2012), 1211.5605.
- [244] A. Dolgov and F. Villante, *Nucl.Phys.* **B679**, 261 (2004), hep-ph/0308083.
- [245] M. Cirelli, G. Marandella, A. Strumia, and F. Vissani, *Nucl.Phys.* **B708**, 215 (2005), hep-ph/0403158.
- [246] A. Mirizzi, N. Saviano, G. Miele, and P. D. Serpico, *Phys.Rev.* **D86**, 053009 (2012), 1206.1046.
- [247] A. G. Riess, L. Macri, S. Casertano, H. Lampeitl, H. C. Ferguson, et al., *Astrophys.J.* **730**, 119 (2011), 1103.2976.
- [248] M. Gonzalez-Garcia, M. Maltoni, and J. Salvado, *JHEP* **1008**, 117 (2010), 1006.3795.
- [249] L. M. Krauss, C. Lunardini, and C. Smith, *Phys.Rev.D* (2010), 1009.4666.
- [250] M. Archidiacono, N. Fornengo, C. Giunti, and A. Melchiorri, *Phys.Rev.* **D86**, 065028 (2012), 1207.6515.
- [251] E. Giusarma, R. de Putter, and O. Mena (2012), 1211.2154.
- [252] S. Riemer-Sorensen, D. Parkinson, T. M. Davis, and C. Blake, *Astrophys.J.* **763**, 89 (2013), 1210.2131.
- [253] S. Joudaki, K. N. Abazajian, and M. Kaplinghat (2012), 1208.4354.
- [254] S. M. Feeney, H. V. Peiris, and L. Verde (2013), 1302.0014.
- [255] S. Riemer-Sorensen, D. Parkinson, and T. M. Davis (2013), 1301.7102.
- [256] A. Mirizzi, G. Mangano, N. Saviano, E. Borriello, C. Giunti, et al. (2013), 1303.5368.
- [257] L. Verde, R. Jimenez, and S. Feeney (2013), 1303.5341.

- [258] 713764 (2006), [astro-ph/0604069](#).
- [259] R. Foot and R. Volkas, Phys.Rev.Lett. **75**, 4350 (1995), [hep-ph/9508275](#).
- [260] C. M. Ho and R. J. Scherrer (2012), [1212.1689](#).
- [261] D. J. Schwarz and M. Stuke (2012), [1211.6721](#).
- [262] X.-D. Shi, Phys.Rev. **D54**, 2753 (1996), [astro-ph/9602135](#).
- [263] N. F. Bell, R. R. Volkas, and Y. Y. Wong, Phys.Rev. **D59**, 113001 (1999), [hep-ph/9809363](#).
- [264] S. Hannestad and G. Raffelt, Phys.Rev. **D59**, 043001 (1999), [astro-ph/9805223](#).
- [265] K. Abazajian, G. M. Fuller, and M. Patel, Phys. Rev. **D64**, 023501 (2001), [astro-ph/0101524](#).
- [266] K. Abazajian, N. F. Bell, G. M. Fuller, and Y. Y. Wong, Phys.Rev. **D72**, 063004 (2005), [astro-ph/0410175](#).
- [267] Y.-Z. Chu and M. Cirelli, Phys.Rev. **D74**, 085015 (2006), [astro-ph/0608206](#).
- [268] A. Melchiorri, O. Mena, S. Palomares-Ruiz, S. Pascoli, A. Slosar, et al., JCAP **0901**, 036 (2009), [0810.5133](#).
- [269] D. Kirilova, JCAP **1206**, 007 (2012), [1101.4177](#).
- [270] S. Hannestad, I. Tamborra, and T. Tram, JCAP **1207**, 025 (2012), [1204.5861](#).
- [271] T. D. Jacques, L. M. Krauss, and C. Lunardini (2013), [1301.3119](#).
- [272] N. Saviano, A. Mirizzi, O. Pisanti, P. D. Serpico, G. Mangano, et al. (2013), [1302.1200](#).
- [273] S. Hannestad, R. S. Hansen, and T. Tram (2013), [1302.7279](#).
- [274] J. Hamann, JCAP **1203**, 021 (2012), [1110.4271](#).
- [275] B. Audren, J. Lesgourgues, K. Benabed, and S. Prunet (2012), [1210.7183](#).
- [276] G. Steigman (2013), [1303.0049](#).
- [277] J. Hidaka and G. M. Fuller, Phys.Rev. **D74**, 125015 (2006), [astro-ph/0609425](#).
- [278] J. Hidaka and G. M. Fuller, Phys.Rev. **D76**, 083516 (2007), [0706.3886](#).
- [279] G. M. Fuller, A. Kusenko, and K. Petraki, Phys.Lett. **B670**, 281 (2009), [0806.4273](#).
- [280] A. Kusenko and G. Segre, Phys.Rev. **D59**, 061302 (1999), [astro-ph/9811144](#).
- [281] G. M. Fuller, A. Kusenko, I. Mocioiu, and S. Pascoli, Phys.Rev. **D68**, 103002 (2003), [astro-ph/0307267](#).
- [282] A. D. Sakharov, Pisma Zh. Eksp. Teor. Fiz. **5**, 32 (1967).
- [283] S. L. Adler, Phys.Rev. **177**, 2426 (1969).

- [284] M. Kobayashi and T. Maskawa, Prog.Theor.Phys. **49**, 652 (1973).
- [285] C. Wu, E. Ambler, R. Hayward, D. Hoppes, and R. Hudson, Phys.Rev. **105**, 1413 (1957).
- [286] J. Christenson, J. Cronin, V. Fitch, and R. Turlay, Phys.Rev.Lett. **13**, 138 (1964).
- [287] M. Fukugita and T. Yanagida, Phys. Lett. **B174**, 45 (1986).
- [288] J. Racker, M. Pena, and N. Rius, JCAP **1207**, 030 (2012), 1205.1948.
- [289] S. Y. Khlebnikov and M. Shaposhnikov, Nucl.Phys. **B308**, 885 (1988).
- [290] M. Laine and M. E. Shaposhnikov, Phys.Rev. **D61**, 117302 (2000), hep-ph/9911473.
- [291] W. Buchmuller and M. Plumacher, Phys.Lett. **B511**, 74 (2001), hep-ph/0104189.
- [292] E. Nardi, Y. Nir, J. Racker, and E. Roulet, JHEP **0601**, 068 (2006), hep-ph/0512052.
- [293] W. Buchmuller, R. Peccei, and T. Yanagida, Ann.Rev.Nucl.Part.Sci. **55**, 311 (2005), hep-ph/0502169.
- [294] S. Blanchet and P. Di Bari, New J.Phys. **14**, 125012 (2012), 1211.0512.
- [295] C. S. Fong, E. Nardi, and A. Riotto, Adv.High Energy Phys. **2012**, 158303 (2012), 1301.3062.
- [296] W. Buchmuller, P. Di Bari, and M. Plumacher, Annals Phys. **315**, 305 (2005), hep-ph/0401240.
- [297] S. Davidson and A. Ibarra, Phys.Lett. **B535**, 25 (2002), hep-ph/0202239.
- [298] W. Buchmuller, P. Di Bari, and M. Plumacher, Phys.Lett. **B547**, 128 (2002), hep-ph/0209301.
- [299] W. Buchmuller, P. Di Bari, and M. Plumacher, Nucl.Phys. **B665**, 445 (2003), hep-ph/0302092.
- [300] E. Nardi, Nucl.Phys.Proc.Suppl. **217**, 27 (2011).
- [301] R. Barbieri, P. Creminelli, A. Strumia, and N. Tetradis, Nucl.Phys. **B575**, 61 (2000), hep-ph/9911315.
- [302] S. Blanchet and P. Di Bari, JCAP **0703**, 018 (2007), hep-ph/0607330.
- [303] A. Abada, S. Davidson, A. Ibarra, F.-X. Josse-Michaux, M. Losada, et al., JHEP **0609**, 010 (2006), hep-ph/0605281.
- [304] A. Abada, S. Davidson, F.-X. Josse-Michaux, M. Losada, and A. Riotto, JCAP **0604**, 004 (2006), hep-ph/0601083.
- [305] E. Nardi, Y. Nir, E. Roulet, and J. Racker, JHEP **0601**, 164 (2006), hep-ph/0601084.
- [306] T. Endoh, T. Morozumi, and Z.-h. Xiong, Prog.Theor.Phys. **111**, 123 (2004), hep-ph/0308276.

- [307] S. Antusch, S. Blanchet, M. Blennow, and E. Fernandez-Martinez, JHEP **1001**, 017 (2010), 0910.5957.
- [308] P. Di Bari, Nucl.Phys. **B727**, 318 (2005), hep-ph/0502082.
- [309] G. Engelhard, Y. Grossman, E. Nardi, and Y. Nir, Phys.Rev.Lett. **99**, 081802 (2007), hep-ph/0612187.
- [310] O. Vives, Phys.Rev. **D73**, 073006 (2006), hep-ph/0512160.
- [311] S. Blanchet and P. Di Bari, Nucl.Phys. **B807**, 155 (2009), 0807.0743.
- [312] E. Bertuzzo, P. Di Bari, and L. Marzola, Nucl.Phys. **B849**, 521 (2011), 1007.1641.
- [313] S. Antusch, P. Di Bari, D. A. Jones, and S. F. King, Nucl.Phys. **B856**, 180 (2012), 1003.5132.
- [314] S. Blanchet, P. Di Bari, D. A. Jones, and L. Marzola, JCAP **1301**, 041 (2013), 1112.4528.
- [315] K. Dick, M. Lindner, M. Ratz, and D. Wright, Phys.Rev.Lett. **84**, 4039 (2000), hep-ph/9907562.
- [316] A. Pilaftsis and T. E. Underwood, Nucl.Phys. **B692**, 303 (2004), hep-ph/0309342.
- [317] M. Garny, A. Kartavtsev, and A. Hohenegger (2011), 1112.6428.
- [318] B. Garbrecht and M. Herranen, Nucl.Phys. **B861**, 17 (2012), 1112.5954.
- [319] J. Liu and G. Segre, Phys.Rev. **D49**, 1342 (1994), hep-ph/9310248.
- [320] M. Flanz, E. A. Paschos, U. Sarkar, and J. Weiss, Phys.Lett. **B389**, 693 (1996), hep-ph/9607310.
- [321] L. Covi and E. Roulet, Phys.Lett. **B399**, 113 (1997), hep-ph/9611425.
- [322] A. Pilaftsis, Nucl.Phys. **B504**, 61 (1997), hep-ph/9702393.
- [323] W. Buchmuller and M. Plumacher, Phys.Lett. **B431**, 354 (1998), hep-ph/9710460.
- [324] M. Drewes and B. Garbrecht (2012), 1206.5537.
- [325] E. K. Akhmedov, V. A. Rubakov, and A. Y. Smirnov, Phys. Rev. Lett. **81**, 1359 (1998), hep-ph/9803255.
- [326] D. E. Morrissey and M. J. Ramsey-Musolf, New J.Phys. **14**, 125003 (2012), 1206.2942.
- [327] L. Canetti and M. Shaposhnikov, JCAP **1009**, 001 (2010), 1006.0133.
- [328] S. Blanchet, Z. Chacko, and R. N. Mohapatra, Phys.Rev. **D80**, 085002 (2009), 0812.3837.
- [329] S. Hollenberg, H. Pas, and D. Schalla (2011), 1110.0948.
- [330] G. Sigl and G. Raffelt, Nucl. Phys. **B406**, 423 (1993).

- [331] M. Beneke, B. Garbrecht, C. Fidler, M. Herranen, and P. Schwaller, Nucl.Phys. **B843**, 177 (2011), 1007.4783.
- [332] F. Hahn-Woernle, M. Plumacher, and Y. Wong, JCAP **0908**, 028 (2009), 0907.0205.
- [333] T. Asaka, S. Eijima, and H. Ishida, JCAP **1202**, 021 (2012), 1112.5565.
- [334] E. W. Kolb and S. Wolfram, Nucl.Phys. **B172**, 224 (1980).
- [335] T. Frossard, M. Garny, A. Hohenegger, A. Kartavtsev, and D. Mitrouskas (2012), 1211.2140.
- [336] T. Prokopec, M. G. Schmidt, and S. Weinstock, Annals Phys. **314**, 208 (2004), hep-ph/0312110.
- [337] T. Prokopec, M. G. Schmidt, and S. Weinstock, Annals Phys. **314**, 267 (2004), hep-ph/0406140.
- [338] A. Anisimov, W. Buchmuller, M. Drewes, and S. Mendizabal, Annals Phys. **324**, 1234 (2009), 0812.1934.
- [339] M. Drewes (2010), 1012.5380.
- [340] P. Millington and A. Pilaftsis (2012), 1211.3152.
- [341] W. Buchmuller and S. Fredenhagen, Phys.Lett. **B483**, 217 (2000), hep-ph/0004145.
- [342] A. De Simone and A. Riotto, JCAP **0708**, 002 (2007), hep-ph/0703175.
- [343] M. Garny, A. Hohenegger, A. Kartavtsev, and M. Lindner, Phys.Rev. **D80**, 125027 (2009), 0909.1559.
- [344] V. Cirigliano, C. Lee, M. J. Ramsey-Musolf, and S. Tulin, Phys.Rev. **D81**, 103503 (2010), 0912.3523.
- [345] M. Garny, A. Hohenegger, A. Kartavtsev, and M. Lindner, Phys.Rev. **D81**, 085027 (2010), 0911.4122.
- [346] A. Anisimov, W. Buchmuller, M. Drewes, and S. Mendizabal, Phys.Rev.Lett. **104**, 121102 (2010), 1001.3856.
- [347] J.-S. Gagnon and M. Shaposhnikov, Phys.Rev. **D83**, 065021 (2011), 1012.1126.
- [348] M. Beneke, B. Garbrecht, M. Herranen, and P. Schwaller, Nucl.Phys. **B838**, 1 (2010), 1002.1326.
- [349] A. Anisimov, W. Buchmuller, M. Drewes, and S. Mendizabal, Annals Phys. **326**, 1998 (2011), 1012.5821.
- [350] M. Garny, A. Hohenegger, and A. Kartavtsev (2010), 1005.5385.
- [351] M. Herranen, K. Kainulainen, and P. M. R  h  k  la, JHEP **1012**, 072 (2010), 1006.1929.

- [352] M. Herranen, K. Kainulainen, and P. M. Rahkila, JHEP **1202**, 080 (2012), 1108.2371.
- [353] C. Fidler, M. Herranen, K. Kainulainen, and P. M. Rahkila, JHEP **1202**, 065 (2012), 1108.2309.
- [354] B. Garbrecht (2012), 1210.0553.
- [355] J. S. Schwinger, J.Math.Phys. **2**, 407 (1961).
- [356] P. M. Bakshi and K. T. Mahanthappa, J.Math.Phys. **4**, 1 (1963).
- [357] P. M. Bakshi and K. T. Mahanthappa, J.Math.Phys. **4**, 12 (1963).
- [358] L. Keldysh, Zh.Eksp.Teor.Fiz. **47**, 1515 (1964).
- [359] Y. Burnier, M. Laine, and M. Shaposhnikov, JCAP **0602**, 007 (2006), hep-ph/0511246.
- [360] M. D’Onofrio, K. Rummukainen, and A. Tranberg, PoS **LATTICE2012**, 055 (2012), 1212.3206.
- [361] T. Asaka, M. Laine, and M. Shaposhnikov, JHEP **06**, 053 (2006), hep-ph/0605209.
- [362] M. Laine and Y. Schroder, JHEP **1202**, 068 (2012), 1112.1205.
- [363] A. Salvio, P. Lodone, and A. Strumia, JHEP **1108**, 116 (2011), 1106.2814.
- [364] D. Besak and D. Bodeker, JCAP **1203**, 029 (2012), 1202.1288.
- [365] B. Garbrecht, F. Glowna, and M. Herranen (2013), 1302.0743.
- [366] B. Garbrecht, F. Glowna, and P. Schwaller (2013), 1303.5498.
- [367] C. P. Kiessig, M. Plumacher, and M. H. Thoma, Phys.Rev. **D82**, 036007 (2010), 1003.3016.
- [368] C. Kiessig and M. Plumacher, JCAP **1207**, 014 (2012), 1111.1231.
- [369] C. Kiessig and M. Plumacher (2011), 1111.1235.
- [370] J. H. Oort, Bulletin of the Astronomical Institutes of the Netherlands **6**, 249 (1932).
- [371] F. Zwicky, Helv.Phys.Acta **6**, 110 (1933).
- [372] G. R. Blumenthal, S. Faber, J. R. Primack, and M. J. Rees, Nature **311**, 517 (1984).
- [373] M. Davis, G. Efstathiou, C. S. Frenk, and S. D. White, Astrophys.J. **292**, 371 (1985).
- [374] A. A. Klypin, A. V. Kravtsov, O. Valenzuela, and F. Prada, Astrophys. J. **522**, 82 (1999), astro-ph/9901240.
- [375] B. Moore, S. Ghigna, F. Governato, G. Lake, T. R. Quinn, et al., Astrophys.J. **524**, L19 (1999), astro-ph/9907411.
- [376] J. S. Bullock, A. V. Kravtsov, and D. H. Weinberg, Astrophys.J. **539**, 517 (2000), astro-ph/0002214.

- [377] A. Benson, C. Frenk, C. G. Lacey, C. Baugh, and S. Cole, Mon.Not.Roy.Astron.Soc. **333**, 177 (2002), [astro-ph/0108218](#).
- [378] R. S. Somerville, Astrophys.J. **572**, L23 (2002), [astro-ph/0107507](#).
- [379] A. V. Maccio', X. Kang, F. Fontanot, R. S. Somerville, S. E. Koposov, et al. (2009), [0903.4681](#).
- [380] M. Boylan-Kolchin, J. S. Bullock, and M. Kaplinghat, Mon.Not.Roy.Astron.Soc. **415**, L40 (2011), [1103.0007](#).
- [381] J. R. Primack, Annalen Phys. **524**, 535 (2012).
- [382] A. Boyarsky, D. Iakubovskiy, O. Ruchayskiy, and V. Savchenko, Mon.Not.Roy.Astron.Soc. **387**, 1361 (2008), [0709.2301](#).
- [383] S. Riemer-Sorensen and S. H. Hansen (2009), [0901.2569](#).
- [384] A. Boyarsky, A. Neronov, O. Ruchayskiy, and M. Shaposhnikov, Mon. Not. Roy. Astron. Soc. **370**, 213 (2006), [astro-ph/0512509](#).
- [385] A. Boyarsky, A. Neronov, O. Ruchayskiy, M. Shaposhnikov, and I. Tkachev, Phys.Rev.Lett. **97**, 261302 (2006), [astro-ph/0603660](#).
- [386] K. Abazajian and S. M. Koushiappas, Phys.Rev. **D74**, 023527 (2006), [astro-ph/0605271](#).
- [387] K. Abazajian, G. M. Fuller, and W. H. Tucker, Astrophys.J. **562**, 593 (2001), [astro-ph/0106002](#).
- [388] C. R. Watson, J. F. Beacom, H. Yuksel, and T. P. Walker, Phys.Rev. **D74**, 033009 (2006), [astro-ph/0605424](#).
- [389] H. Yuksel, J. F. Beacom, and C. R. Watson, Phys.Rev.Lett. **101**, 121301 (2008), [0706.4084](#).
- [390] A. Boyarsky, D. Malyshev, A. Neronov, and O. Ruchayskiy, Mon.Not.Roy.Astron.Soc. **387**, 1345 (2008), [0710.4922](#).
- [391] C. R. Watson, Z.-Y. Li, and N. K. Polley, JCAP **1203**, 018 (2012), [1111.4217](#).
- [392] S. Tremaine and J. E. Gunn, Phys. Rev. Lett. **42**, 407 (1979).
- [393] A. Boyarsky, O. Ruchayskiy, and D. Iakubovskiy (2008), [0808.3902](#).
- [394] D. Gorbunov, A. Khmelnitsky, and V. Rubakov, JCAP **0810**, 041 (2008), [0808.3910](#).
- [395] K. A. Olive and M. S. Turner, Phys.Rev. **D25**, 213 (1982).
- [396] A. D. Dolgov and S. H. Hansen, Astropart. Phys. **16**, 339 (2002), [hep-ph/0009083](#).
- [397] M. Viel and M. G. Haehnelt, Mon.Not.Roy.Astron.Soc. **365**, 231 (2006), [astro-ph/0508177](#).
- [398] A. Boyarsky, J. Nevalainen, and O. Ruchayskiy (2006), [astro-ph/0610961](#).

- [399] K. N. Abazajian, M. Markevitch, S. M. Koushiappas, and R. C. Hickox (2006), [astro-ph/0611144](#).
- [400] S. Riemer-Sorensen, S. H. Hansen, and K. Pedersen, *Astrophys.J.* **644**, L33 (2006), [astro-ph/0603661](#).
- [401] M. Viel, J. Lesgourgues, M. G. Haehnelt, S. Matarrese, and A. Riotto, *Phys. Rev. Lett.* **97**, 071301 (2006), [astro-ph/0605706](#).
- [402] U. Seljak, A. Makarov, P. McDonald, and H. Trac, *Phys. Rev. Lett.* **97**, 191303 (2006), [astro-ph/0602430](#).
- [403] P. Colin, O. Valenzuela, and V. Avila-Reese, *Astrophys.J.* **673**, 203 (2008), [0709.4027](#).
- [404] G. Belanger, A. Pukhov, and G. Servant, *JCAP* **0801**, 009 (2008), [0706.0526](#).
- [405] A. Boyarsky, J. Lesgourgues, O. Ruchayskiy, and M. Viel, *JCAP* **0905**, 012 (2009), [0812.0010](#).
- [406] A. Boyarsky, J. Lesgourgues, O. Ruchayskiy, and M. Viel, *Phys. Rev. Lett.* **102**, 201304 (2009), [0812.3256](#).
- [407] M. Loewenstein, A. Kusenko, and P. L. Biermann, *Astrophys.J.* **700**, 426 (2009), [0812.2710](#).
- [408] A. Kusenko, *Phys.Rept.* **481**, 1 (2009), [0906.2968](#).
- [409] J. den Herder, A. Boyarsky, O. Ruchayskiy, K. Abazajian, C. Frenk, et al. (2009), [0906.1788](#).
- [410] K. N. Abazajian (2009), [0903.2040](#).
- [411] J. Wu, C.-M. Ho, and D. Boyanovsky, *Phys.Rev.* **D80**, 103511 (2009), [0902.4278](#).
- [412] D. Boyanovsky and J. Wu, *Phys.Rev.* **D83**, 043524 (2011), [1008.0992](#).
- [413] D. Boyanovsky, *Phys.Rev.* **D83**, 103504 (2011), [1011.2217](#).
- [414] R. M. Dunstan, K. N. Abazajian, E. Polisensky, and M. Ricotti (2011), [1109.6291](#).
- [415] M. Nemevsek, G. Senjanovic, and Y. Zhang, *JCAP* **1207**, 006 (2012), [1205.0844](#).
- [416] A. Boyarsky, O. Ruchayskiy, and M. Markevitch (2006), [astro-ph/0611168](#).
- [417] A. Boyarsky, A. Neronov, O. Ruchayskiy, and M. Shaposhnikov, *Phys. Rev.* **D74**, 103506 (2006), [astro-ph/0603368](#).
- [418] S. Riemer-Sorensen, K. Pedersen, S. H. Hansen, and H. Dahle (2006), [astro-ph/0610034](#).
- [419] A. Boyarsky, O. Ruchayskiy, D. Iakubovskiy, M. G. Walker, S. Riemer-Sorensen, et al., *Mon.Not.Roy.Astron.Soc.* **407**, 1188 (2010), [1001.0644](#).
- [420] H. de Vega and N. Sanchez, *Mon.Not.Roy.Astron.Soc.* **404**, 885 (2010), [0901.0922](#).

- [421] C. Destri, H. de Vega, and N. Sanchez, *New Astronomy* **22**, **39** (2013), 1204.3090.
- [422] A. Boyarsky, A. Neronov, O. Ruchayskiy, and I. Tkachev, *Phys.Rev.Lett.* **104**, 191301 (2010), 0911.3396.
- [423] O. R. A. Boyarsky and M. Shaposhnikov, Contribution to Open Symposium - European Strategy Preparatory Group, Krakow, Poland, September 2012, <https://indico.cern.ch/contributionDisplay.py?contribId=127&confId=175067> (2012).
- [424] A. Boyarsky, D. Iakubovskiy, and O. Ruchayskiy, *Phys.Dark Univ.* **1**, 136 (2012).
- [425] C. Weniger, *JCAP* **1208**, 007 (2012), 1204.2797.
- [426] L. Bergstrom, *Phys.Rev.* **D86**, 103514 (2012), 1208.6082.
- [427] S. Dodelson and L. M. Widrow, *Phys. Rev. Lett.* **72**, 17 (1994), hep-ph/9303287.
- [428] T. Asaka, M. Shaposhnikov, and A. Kusenko, *Phys. Lett.* **B638**, 401 (2006), hep-ph/0602150.
- [429] F. Bezrukov, H. Hettmansperger, and M. Lindner, *Phys.Rev.* **D81**, 085032 (2010), 0912.4415.
- [430] F. Bezrukov, A. Kartavtsev, and M. Lindner (2012), 1204.5477.
- [431] P. Di Bari, P. Lipari, and M. Lusignoli, *Int.J.Mod.Phys.* **A15**, 2289 (2000), hep-ph/9907548.
- [432] T. Asaka, M. Laine, and M. Shaposhnikov, *JHEP* **0701**, 091 (2007), hep-ph/0612182.
- [433] V. Klimov, *Sov.Phys.JETP* **55**, 199 (1982).
- [434] V. Klimov, *Sov.J.Nucl.Phys.* **33**, 934 (1981).
- [435] H. A. Weldon, *Phys.Rev.* **D26**, 2789 (1982).
- [436] L. Wolfenstein, *Phys. Rev.* **D17**, 2369 (1978).
- [437] S. P. Mikheev and A. Y. Smirnov, *Sov. J. Nucl. Phys.* **42**, 913 (1985).
- [438] X.-D. Shi and G. M. Fuller, *Phys. Rev. Lett.* **82**, 2832 (1999), astro-ph/9810076.
- [439] S. Das and K. Sigurdson, *Phys.Rev.* **D85**, 063510 (2012), 1012.4458.
- [440] R. J. Scherrer and M. S. Turner, *Phys.Rev.* **D31**, 681 (1985).
- [441] M. Shaposhnikov and I. Tkachev, *Phys. Lett.* **B639**, 414 (2006), hep-ph/0604236.
- [442] A. Anisimov, Y. Bartocci, and F. L. Bezrukov (2008), 0809.1097.
- [443] F. Bezrukov and D. Gorbunov, *JHEP* **1005**, 010 (2010), 0912.0390.
- [444] F. Bezrukov, D. Gorbunov, and M. Shaposhnikov, *JCAP* **0906**, 029 (2009), 0812.3622.

- [445] K. Petraki and A. Kusenko, Phys.Rev. **D77**, 065014 (2008), 0711.4646.
- [446] D. Gorbunov and A. Panin, Phys.Lett. **B700**, 157 (2011), 1009.2448.
- [447] J. Bond, G. Efstathiou, and J. Silk, Phys.Rev.Lett. **45**, 1980 (1980).
- [448] A. J. Benson, A. Farahi, S. Cole, L. A. Moustakas, A. Jenkins, et al. (2012), 1209.3018.
- [449] J. Sommer-Larsen, P. Naselsky, I. Novikov, and M. Gotz, Mon.Not.Roy.Astron.Soc. **352**, 299 (2004), astro-ph/0309329.
- [450] B. W. O’Shea and M. L. Norman, Astrophys.J. **648**, 31 (2006), astro-ph/0602319.
- [451] P. Bode, J. P. Ostriker, and N. Turok, Astrophys. J. **556**, 93 (2001), astro-ph/0010389.
- [452] S. H. Hansen, J. Lesgourgues, S. Pastor, and J. Silk, Mon. Not. Roy. Astron. Soc. **333**, 544 (2002), astro-ph/0106108.
- [453] M. Viel, J. Lesgourgues, M. G. Haehnelt, S. Matarrese, and A. Riotto, Phys. Rev. **D71**, 063534 (2005), astro-ph/0501562.
- [454] M. Viel, G. D. Becker, J. S. Bolton, M. G. Haehnelt, M. Rauch, et al., Phys.Rev.Lett. **100**, 041304 (2008), 0709.0131.
- [455] R. K. de Naray, G. D. Martinez, J. S. Bullock, and M. Kaplinghat (2009), 0912.3518.
- [456] F. Villaescusa-Navarro and N. Dalal, JCAP **1103**, 024 (2011), 1010.3008.
- [457] A. Schneider, R. E. Smith, A. V. Maccio, and B. Moore (2011), 1112.0330.
- [458] V. Lora, A. Just, F. Sanchez-Salcedo, and E. Grebel, Astrophys.J. **757**, 87 (2012), 1207.5681.
- [459] T. Asaka, S. Blanchet, and M. Shaposhnikov, Phys. Lett. **B631**, 151 (2005), hep-ph/0503065.
- [460] T. Asaka and M. Shaposhnikov, Phys. Lett. **B620**, 17 (2005), hep-ph/0505013.
- [461] M. Shaposhnikov, hep-th/0708.3550 (2007), 0708.3550.
- [462] M. Shaposhnikov and D. Zenhausern, Phys. Lett. **B671**, 187 (2009), 0809.3395.
- [463] M. Shaposhnikov and D. Zenhausern, Phys. Lett. **B671**, 162 (2009), 0809.3406.
- [464] N. Sahu and U. A. Yajnik, Phys.Lett. **B635**, 11 (2006), hep-ph/0509285.
- [465] A. Boyarsky, A. Neronov, O. Ruchayskiy, and M. Shaposhnikov, JETP Lett. **83**, 133 (2006), hep-ph/0601098.
- [466] D. Gorbunov and M. Shaposhnikov, PoS **KAON**, 047 (2008).
- [467] F. Bezrukov, J.Phys.Conf.Ser. **110**, 082002 (2008), 0710.2501.
- [468] F. L. Bezrukov and M. Shaposhnikov, Phys. Lett. **B659**, 703 (2008), 0710.3755.

- [469] J. Garcia-Bellido, D. G. Figueroa, and J. Rubio, Phys. Rev. **D79**, 063531 (2009), 0812.4624.
- [470] M. Shaposhnikov, JHEP **08**, 008 (2008), 0804.4542.
- [471] V. Gorkavenko and S. Vilchynskiy, Eur.Phys.J. **C70**, 1091 (2010), 0907.4484.
- [472] T. Asaka and H. Ishida, Phys.Lett. **B692**, 105 (2010), 1004.5491.
- [473] J. Garcia-Bellido, J. Rubio, M. Shaposhnikov, and D. Zenhausern, Phys.Rev. **D84**, 123504 (2011), 1107.2163.
- [474] F. Bezrukov, D. Gorbunov, and M. Shaposhnikov, JCAP **1110**, 001 (2011), 1106.5019.
- [475] V. M. Gorkavenko, I. Rudenok, and S. I. Vilchynskiy (2012), 1201.0003.
- [476] K. Allison (2012), 1210.6852.
- [477] A. Boyarsky, J. Frohlich, and O. Ruchayskiy, Phys.Rev.Lett. **108**, 031301 (2012), 1109.3350.